

การตัดแปรทางเคมีของแป้งมันสำปะหลังเพื่อสมบัติความต้านแรงดึงของแผ่นพอลิเอทิลีนย่อยสลายได้



นางสาวโปรดปราน ทาเขียว

วิทยานิพนธ์นี้เป็นส่วนหนึ่งของการศึกษาตามหลักสูตรปริญญาวิทยาศาสตรบัณฑิต  
สาขาวิชาปิโตรเคมีและวิทยาศาสตร์พอลิเมอร์ หลักสูตรปิโตรเคมีและวิทยาศาสตร์พอลิเมอร์  
คณะวิทยาศาสตร์ จุฬาลงกรณ์มหาวิทยาลัย

ปีการศึกษา 2543

ISBN 974-346-595-2

ลิขสิทธิ์ของจุฬาลงกรณ์มหาวิทยาลัย

CHEMICAL MODIFICATION OF CASSAVA STARCH FOR TENSILE PROPERTIES OF  
DEGRADABLE POLYETHYLENE SHEETS



Ms. Prodepran Thakeow

A Thesis Submitted in Partial Fulfillment of the Requirement  
For the Degree of Master of Science in Petrochemistry and Polymer Science  
Program of Petrochemistry and Polymer Science

Faculty of Science

Chulaongkorn University

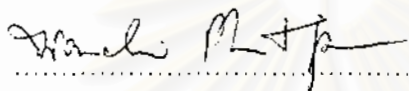
Academic Year 2000

ISBN 974-346-595-2

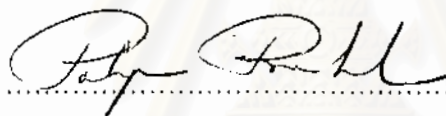
Thesis Title           CHEMICAL MODIFICATION OF CASSAVA STARCH FOR TENSILE  
                                  PROPERTIES OF DEGRADABLE POLYETHYLENE SHEETS  
By                         Ms. Prodepran Thakeow  
Program                 Petrochemistry and Polymer Science  
Thesis Advisor         Professor Suda Kiatkamjornwong, Ph.D.  
Thesis Co-advisor     Mr. Manit Sonsuk, M.S.

---

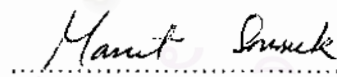
Accepted by the Faculty of Science, Chulalongkorn University in Partial Fulfillment  
of the Requirements for the Master's Degree

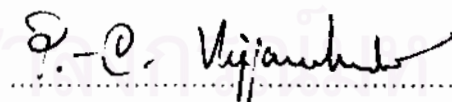
..... Dean of Faculty of Science  
(Associate Professor Wanchai Phothisiphichitr, Ph.D.)

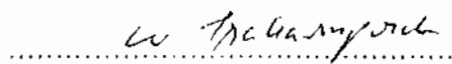
THESIS COMMITTEE

..... Chairman  
(Professor Pattarapan Prasassarakich, Ph.D.)

..... Thesis Advisor  
(Professor Suda Kiatkamjornwong, Ph.D.)

..... Thesis Co-advisor  
(Mr. Manit Sonsuk, M.S.)

..... Member  
(Assistant Professor Pin-Chawee Vejjanukroh, Ph.D.)

..... Member  
(Associate Professor Wimonrat Trakarnpruk, Ph.D.)

โปรดปราน ทาเชียว : การตัดแปรทางเคมีของแป้งมันสำปะหลังเพื่อสมบัติความต้านแรงดึงของแผ่นพอลิเอทิลีนย่อยสลายได้. (CHEMICAL MODIFICATION OF CASSAVA STARCH FOR TENSILE PROPERTIES OF DEGRADABLE POLYETHYLENE SHEETS) อ. ที่ปรึกษา : ศาสตราจารย์ ดร. สุดา เกียรติกำจรวงศ์, อ. ที่ปรึกษาร่วม : นายมานิตย์ ช้อนสุข, 130 หน้า. ISBN 946-346-595-2.

ได้เตรียมกราฟต์โคพอลิเมอร์ของกรดอะคริลิกและแป้งมันสำปะหลังโดยการฉายรังสีแกมมาพร้อมกันด้วย  $^{60}\text{Co}$  และทำการตัดแปรสมบัติทางเคมีของกราฟต์โคพอลิเมอร์ที่เตรียมได้ซึ่งมีสมบัติชอบน้ำให้มีสมบัติไม่ชอบน้ำ จากนั้นนำไปผสมกับพลาสติกพอลิเอทิลีน เพื่อศึกษาสมบัติทางกายภาพและเชิงกลต่อไป ทำการเตรียมกราฟต์โคพอลิเมอร์โดยรังสีแกมมาด้วยการใช้อัตราการเปล่งรังสี  $2 \text{ kgy h}^{-1}$  ปริมาณรังสี  $10 \text{ kGy}$  และอัตราส่วนของกรดอะคริลิกต่อแป้งมันสำปะหลังเป็น 1:1 พบว่ากราฟต์โคพอลิเมอร์ที่ได้มีปริมาณไฮโดรฟิลิซิตีร้อยละ 2.7 แอด-ออนร้อยละ 24.9 การเปลี่ยนเป็นพอลิเมอร์ทั้งหมดร้อยละ 40 ประสิทธิภาพในการเกิดกราฟติงร้อยละ 90 และสัดส่วนในการเกิดกราฟติงร้อยละ 33.2

เมื่อทำการตัดแปรทางเคมีของกราฟต์โคพอลิเมอร์ด้วยวิธีเอสเทอร์ฟิเคชันและอีเทอร์ฟิเคชัน โดยใช้พอลิเอทิลีนไกลคอล 4000 และ โพรพิลีนออกไซด์ ตามลำดับ พบว่ามีปริมาณพอลิเอทิลีนไกลคอล 4000 และ หมู่ไฮดรอกซีโพรพิลเท่ากับร้อยละ 15.2 และ 1.30 ตามลำดับ ซึ่งทำการวิเคราะห์โดยใช้ฟูเรียร์ทรานส์ฟอร์มอินฟราเรดสเปกโทรสโคปี  $^{13}\text{C}$ -NMR และ  $^1\text{H}$ -NMR สเปกโทรเมทรี และอัลตราไวโอเลตสเปกโทรสโคปี นำแป้งตัดแปรที่เตรียมได้มาผสมกับพลาสติกพอลิเอทิลีนความหนาแน่นต่ำในปริมาณต่างๆ โดยใช้เครื่องทูโรลมิลล์และนำมาทดสอบสมบัติความต้านแรงดึง ความแข็ง ความร้อน การย่อยสลายโดยการฝังดิน การดูดซึมน้ำ จากการทดลองพบว่า ค่าความต้านแรงดึงของพลาสติกพอลิเอทิลีนความหนาแน่นต่ำผสมแป้งตัดแปรมีค่าลดลงเมื่อเทียบกับพลาสติกพอลิเอทิลีนความหนาแน่นต่ำ แต่มีแนวโน้มเพิ่มขึ้นเมื่อปริมาณของแป้งตัดแปรในพลาสติกผสมเพิ่มขึ้น แป้งตัดแปรสามารถเพิ่มความแข็งให้กับแผ่นพลาสติกผสมได้ แต่ลดความต้านทานการสลายตัวด้วยความร้อนของพลาสติกพอลิเอทิลีนความหนาแน่นต่ำจาก  $350^\circ\text{C}$  เป็น  $300^\circ\text{C}$  ของพลาสติกผสม การย่อยสลายของพลาสติกผสมโดยการฝังดินนั้นเกิดขึ้นได้อย่างช้าๆ สอดคล้องกับสมบัติการดูดซึมน้ำของแผ่นพลาสติกผสมซึ่งมีค่าน้อยกว่า 2.5%

ภาควิชา .....  
สาขาวิชา ..... ปิโตรเคมีและวิทยาศาสตร์พอลิเมอร์ .....  
ปีการศึกษา .2543.....

ลายมือชื่อนิสิต .....  
ลายมือชื่ออาจารย์ที่ปรึกษา .....  
ลายมือชื่ออาจารย์ที่ปรึกษาร่วม .....

# # 4072319223 : MAJOR PETROCHEMISTRY AND POLYMER SCIENCE

KEY WORD: irradiation / graft copolymerization / starch / degradable polyethylene

Ms. Prodepran Thakeow : CHEMICAL MODIFICATION OF CASSAVA STARCH FOR TENSILE PROPERTIES OF DEGRADABLE POLYETHYLENE SHEETS. THESIS ADVISOR : Professor Suda Kiatkamjornwong, Ph.D., THESIS CO-ADVISOR : Mr. Manit Sonsuk, M.S., 130 pp. ISBN 946-346-595-2.

Cassava starch-*g*-poly(acrylic acid) copolymers were prepared by a simultaneous irradiation technique of  $\gamma$ -rays irradiation from a  $^{60}\text{Co}$  source. The graft copolymers obtained were later modified their chemical properties from hydrophilicity to hydrophobicity, and were mixed with LDPE. The physical and mechanical properties of the blends were studied. The mixture of acrylic acid and gelatinized starch (ratio 1:1) was irradiated with  $\gamma$ -rays of a dose rate of  $2 \text{ kGy h}^{-1}$  to obtain dose of  $10 \text{ kGy}$ . The resulting graft copolymer contained 2.7% homopolymer, 24.9% add-on, 40% conversion, 90% grafting efficiency, and 33.2% grafting ratio.

The chemical modifications were carried out by esterification and etherification with poly(ethylene glycol) 4000 and propylene oxide, respectively. The amounts of the poly(ethylene glycol) 4000 and the hydroxypropyl group on the modified starch were found to be 15.25 and 1.30%, respectively. Fourier transform infrared spectroscopy,  $^{13}\text{C}$ -NMR and  $^1\text{H}$ -NMR spectrometry, and ultraviolet spectroscopy were used to confirm the reaction and to determine the amounts of the hydroxypropyl group. This modified starch was mixed with LDPE at various proportions in a two-roll mill. Mechanical and hardness properties, thermal property, degradation in soil, and water absorption were investigated as a function of blend composition. It was found that the tensile strength of LDPE composite sheets slightly decreased, but they showed a positive tendency to increase with the increasing amount of the modified cassava starch. The hardness was increased with increasing amount of the modified cassava starch, but the resistance to thermal degradation was decreased from  $350^\circ\text{C}$  of LDPE to  $300^\circ\text{C}$  of blends. The degradation of plastic sheets in a soil burial test took place slowly, in relevant with the low value water absorption which less than 2.5%.

Department .....	Student's signature .....
Field of study ..Petrochemistry and polymer science	Advisor's signature .....
Academic year ..2000.....	Co-advisor's signature .....

## ACKNOWLEDGEMENTS

The author would like to take this opportunity to express her gratitude to her advisor, Professor Suda Kiatkamjornwong, Ph.D., and co-advisor, Mr. Manit Sonsuk, M.S., for their advice, assistance, and encouragement through out the course of this thesis. The auther is very grateful to her advisor who graciously gave her time to read, correct, and comment on the details of this thesis. The auther would also like to thank her thesis committee: Professor Pattarapan Prasassarakich, Ph.D., Assistant Professor Pin-Chawee Vejjanukroh, Ph.D., and Associate Professor Wimonrat Trakarnpruk, Ph.D., for their comments and suggestions. She would like to thank Mrs. Jindarom Chavajareernpun for her kind help in the radiation technique. Appreciations are also expressed to the Graduate School of Chulalongkorn University for the partial financial support, the Office of Atomic Energy for Peace, the Department of Imaging and Printing Technology, Faculty of Science for providing the facilities in laboratory, equipment, and the necessary chemicals; to the Scientific and Technology Research Equipment Center, the National Metal and Materials Technology, Rubber Research Institute of Thailand, and the Department of Chemistry, Faculty of Science, King Mongkut Institute of Technology of Latkrabang for providing the scientific instruments.

She would like to thank Ms. Wanida Chantong for her help and support, Ms. Duangkamol Tantiwat (Thai Peroxide Co., Ltd.) for providing field test space and assistance during the soil burial test; and to her friends whose names are not mentioned here for their assistance and encouragement.

Last but not certainly the least, she would like to extend her gratefulness to her mother, father, and sister for their tireless assistance, encouragement, and endless love.

# CONTENTS

	PAGE
ABSTRACT (in Thai) .....	iv
ABSTRACT (in English) .....	v
ACKNOWLEDGEMENTS .....	vi
CONTENTS .....	vii
LIST OF TABLES .....	xi
LIST OF FIGURES .....	xiv
ABBREVIATIONS .....	xvii
CHAPTER 1 : INTRODUCTION .....	1
1.1 Introduction .....	1
1.2 Objectives .....	3
1.3 Expected Benefits Obtained for the Development of the Research ...	3
1.4 Scope of the Investigation .....	4
1.5 Contents of the Thesis .....	5
CHAPTER 2 : THEORY AND LITERATURE REVIEW .....	6
2.1 Starch .....	6
2.1.1 Chemistry of Starch .....	6
2.1.2 Chemical Structure .....	6
2.1.3 Starch Modification .....	8
2.2 Terminology and Definition .....	15
2.2.1 Gelatinization of Starch .....	15
2.2.2 Percentage of Homopolymer .....	15
2.2.3 Percentage of Add-on .....	16
2.2.4 Percentage of Conversion.....	16
2.2.5 Percentage of Grafting Efficiency.....	16
2.2.6 Percentage of Grafting Ratio .....	16
2.2.7 G Value .....	16
2.3 Literature Survey .....	17

## CONTENTS(continued)

	PAGE
CHAPTER 3 : EXPERIMENT .....	25
3.1 Chemicals, Equipment, and Glassware .....	25
3.2 Preparation Scheme .....	29
3.3 Procedure .....	30
3.3.1 Graft Copolymerization .....	30
3.3.1.1 Gelatinization of Cassava Starch .....	30
3.3.1.2 Grafting of Acrylid Acid onto Gelatinized Starch by Simultaneous Irradiation .....	30
3.3.1.3 Effects of the Total Dose (kGy) and the Dose Rate (kGy h <sup>-1</sup> ) on Graft Copolymerization .....	30
3.3.1.4 Effects of the Acrylic Acid-to-Starch Ratio on Graft Copolymerization .....	31
3.3.1.5 Homopolymer Extraction .....	32
3.3.1.6 Hydrolysis of Starch and Side-Chain Recovery.....	32
3.3.1.7 Characterization Graft Copolymer .....	32
3.3.2 Esterification of Starch-g-poly(acrylic acid) .....	33
3.3.2.1 Acid Hydrolysis for Side-Chain Recovery .....	33
3.3.3 Etherification of Esterified Starch-g-polyacrylate .....	33
3.3.3.1 Spectrophotometric Determination of the Hydroxypropyl Group in the Modified Starch .....	34
3.3.4 Compounding of Plastic Materials (Blend Prepatation) .....	35
3.3.5 Compression Moulding .....	36
3.3.6 Mechanical Properties Test .....	36
3.3.7 Hardness Measurement .....	36
3.3.8 Soil Burial Test .....	36
3.3.9 Water Absorption Test .....	37
3.3.10 Morphology Property Test .....	37
3.3.11 Thermal Property Test .....	37
3.3.12 Contact Angle Measurement .....	37

## CONTENTS(continued)

	PAGE
CHAPTER 4 : RESULTS AND DISCUSSION .....	38
4.1 Proof of Grafting by Fourier Transform Infrared Spectroscopy .....	38
4.2 Graft Copolymerization of Grating of Acrylic Acid onto Gelatinized Starch by Simultaneous Irradiation .....	45
4.2.1 Effects of the Total Dose and the Dose Rate on Graft Copolymerization .....	45
4.2.1.1 Relationship between Total Dose and Dose Rate and % Homopolymer .....	46
4.2.1.2 Relationship between Total Dose and Dose Rate and % Add-on .....	48
4.2.1.3 Relationship between Total Dose and Dose Rate and % Conversion .....	49
4.2.1.4 Relationship between Total Dose and Dose Rate and % Grafting Efficiency .....	50
4.2.1.5 Relationship between Total Dose and Dose Rate and % Grafting Ratio .....	51
4.2.2 Effects of the Acrylic Acid-to-Starch Ratio on Graft Copolymerization at the Dose Rate of 2 kGy h <sup>-1</sup> and the Total Dose of 10 and 12 kGy .....	52
4.2.2.1 Relationship between the Acrylic Acid-to- Starch Ratio on Graft Copolymerization at the Dose Rate of 2 kGy h <sup>-1</sup> and the Total Dose of 10 and 12 kGy (a) homopolymer .....	53
4.2.2.2 Relationship between the Acrylic Acid-to- Starch Ratio on Graft Copolymerization at the Dose Rate of 2 kGy h <sup>-1</sup> and the Total Dose of 10 and 12 kGy (b) add-on .....	54

## CONTENTS(continued)

	PAGE
4.2.2.3 Relationship between the Acrylic Acid-to-Starch Ratio on Graft Copolymerization at the Dose Rate of 2 kGy h <sup>-1</sup> and the Total Dose of 10 and 12 kGy (c) conversion .....	55
4.2.2.4 Relationship between the Acrylic Acid-to-Starch Ratio on Graft Copolymerization at the Dose Rate of 2 kGy h <sup>-1</sup> and the Total Dose of 10 and 12 kGy (d) grafting efficiency .....	56
4.2.2.5 Relationship between the Acrylic Acid-to-Starch Ratio on Graft Copolymerization at the Dose Rate of 2 kGy h <sup>-1</sup> and the Total Dose of 10 and 12 kGy (e) grafting ration .....	57
4.3 Esterification of Starch-g-poly(acrylic acid) .....	58
4.3.1 Characterization of Esterified Starch-g-polyacrylate .....	59
4.3.1.1 Characterization of Esterified Starch-g-polyacrylate by Fourier Transform Infrared Spectroscopy .....	59
4.3.1.2 Characterization of Esterified Starch-g-polyacrylate by <sup>13</sup> C-NMR and <sup>1</sup> H-NMR Spectrometry .....	59
4.3.2 Determination of Poly(ethylene glycol) 4000 on Esterified Starch-g-polyacrylate .....	62
4.4 Etherification of Esterified Starch-g-polyacrylate .....	70
4.4.1 Characterization of Modified Starch by <sup>13</sup> C-NMR and <sup>1</sup> H-NMR Spectrometry .....	70

## CONTENTS(continued)

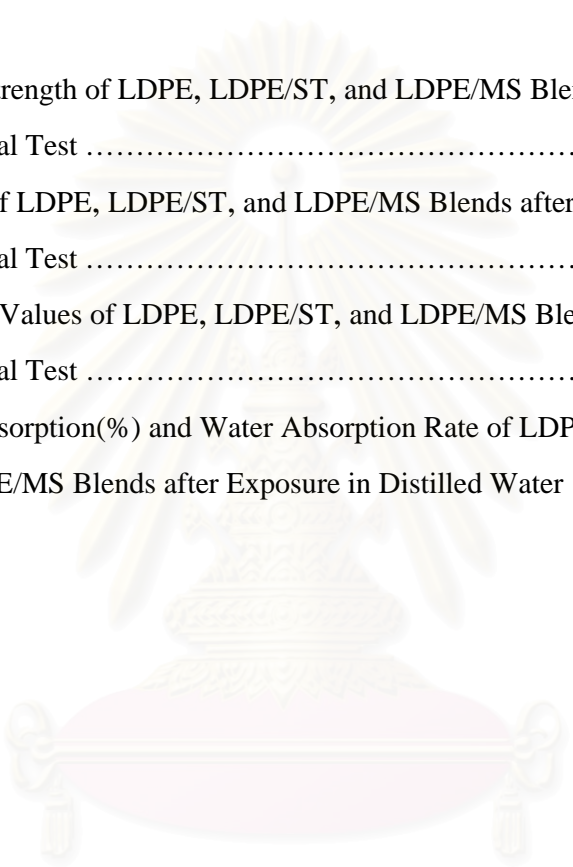
	PAGE
4.4.2 Spectrophotometric Determination of Hydroxypropyl Group on the Modified Starch .....	73
4.2.3 Overall Reaction Scheme .....	76
4.5 Contact Angle Measurement .....	77
4.6 Plastic Compounding and Characterization .....	78
4.6.1 Effect of Starch and Modified Starch Contents on Mechanical Properties of Low Density Polyethylene Composite Sheets .....	78
4.6.2 Blend Morphology of the Samples .....	82
4.6.3 Failure Morphology of the Samples .....	84
4.6.4 Hardness Measurement .....	88
4.6.5 Thermal Property Analysis .....	90
4.7 Soil Burial Test .....	100
4.7.1 Mechanical Property Measurement .....	101
4.7.2 Hardness Measurement .....	105
4.7.3 Surface Morphology of the Samples .....	108
4.8 Water Absorption Test .....	112
CHAPTER 5 : CONCLUSIONS AND SUGGESTION .....	116
Conclusions .....	116
Suggestion and Future Work .....	119
REFERENCES .....	120
APPENDIX A : Radiation Dosimetry .....	125
VITA .....	130

## LIST OF TABLES

TABLES	PAGE
3.1 Physical Properties of Low Density Polyethylene .....	27
3.2 Typical Properties of Ethylene-bis-Stearamide (ARMOWAX EBS SF) .....	27
3.3 Composition of Starch- and Modified Starch-LDPE Sheets .....	35
4.1 Fourier Transform Infrared Vibrations and Assignments for Cassava Starch, Poly(acrylic acid), Cassava Starch-g-Poly(acrylic acid) before and after Homopolymer Extraction with Methanol and Cassava Starch-g-Poly (acrylic acid) after Acid Hydrolysis of Starch with Glacial Acetic Acid .....	39
4.2 Effects of Total Dose and Dose Rate on the Graft Copolymerization .....	45
4.3 Effects of Acrylic Acid-to-starch Ratio on the Graft Copolymerization at the Dose Rate of $2 \text{ kGy h}^{-1}$ and the Total Dose of 10 and 12 kGy .....	52
4.4 Characterization of Cassava Starch-g-Poly(acrylic acid) for Esterification ..	58
4.5 Peak Assignment of $^{13}\text{C}$ -NMR Spectra of Starch-g-Poly(acrylic acid) and Esterified Starch-g-Polyacrylate .....	60
4.6 Peak Assignment of $^1\text{H}$ -NMR Spectra of Starch-g-Poly(acrylic acid) and Esterified Starch-g-Polyacrylate .....	61
4.7 Peak Assignment of $^{13}\text{C}$ - and $^1\text{H}$ -NMR Spectra of the Modified Starch .....	70
4.8 Calibration Data for Determination of the Hydroxypropyl Equivalent Groups .....	74
4.9 Experimental Data for Determination of the Hydroxypropyl Equivalent Groups .....	75
4.10 Contact Angle Measurement .....	77
4.11 Tensile Strength and % Strain of LDPE, LDPE/ST, and LDPE/MS Blends at Various Compositions .....	78
4.12 Contact Angle Measurement of Starch, Modified Starch, EBS wax, LDPE, Starch/EBS wax and Modified Starch/EBS wax .....	88
4.13 Decomposition Temperature and the Percentage of Weight Loss of Starch, Modified Starch, and LDPE/MS blends at Various Contents .....	100
4.14 Hardness Values of LDPE, LDPE/ST, and LDPE/MS Blends at Various Compositions .....	101

## LIST OF TABLES (continued)

<b>TABLES</b>	<b>PAGE</b>
4.14 Tensile Strength of LDPE, LDPE/ST, and LDPE/MS Blends after Soil Burial Test .....	101
4.13 %Strain of LDPE, LDPE/ST, and LDPE/MS Blends after Soil Burial Test .....	101
4.15 Hardness Values of LDPE, LDPE/ST, and LDPE/MS Blends after Soil Burial Test .....	106
4.16 Water Absorption(%) and Water Absorption Rate of LDPE, LDPE/ST, and LDPE/MS Blends after Exposure in Distilled Water .....	113


  
 สถาบันวิทยบริการ  
 จุฬาลงกรณ์มหาวิทยาลัย

## LIST OF FIGURES

FIGURES	PAGE
1.1 Degradation of starch-filled plastics .....	2
2.1 Schematic structure of amylose and amylopectin .....	7
3.1 Overall schematic experiment process .....	29
4.1 Fourier transform infrared spectrum of cassava starch .....	40
4.2 Fourier transform infrared spectrum of poly(acrylic acid) .....	41
4.3 Fourier transform infrared spectrum of cassava starch-g-poly(acrylic acid) before homopolymer extraction .....	42
4.4 Fourier transform infrared spectrum of cassava starch-g-poly(acrylic acid) after homopolymer extraction .....	43
4.5 Fourier transform infrared spectrum of cassava starch-g-poly(acrylic acid) after acid hydrolysis .....	44
4.6 Effects of the total dose and the dose rate on %homopolymer .....	47
4.7 Effects of the total dose and the dose rate on %add-on .....	48
4.8 Effects of the total dose and the dose rate on %conversion .....	49
4.9 Effects of the total dose and the dose rate on %grafting efficiency .....	50
4.10 Effects of the total dose and the dose rate on %grafting ratio .....	51
4.11 Effects of acrylic acid-to-starch ratio on the graft copolymerization at the dose rate of $12 \text{ kGy h}^{-1}$ and the total dose of 10 kGy and 12 kGy in terms of %homopolymer .....	53
4.12 Effects of acrylic acid-to-starch ratio on the graft copolymerization at the dose rate of $12 \text{ kGy h}^{-1}$ and the total dose of 10 kGy and 12 kGy in terms of %add-on .....	54
4.13 Effects of acrylic acid-to-starch ratio on the graft copolymerization at the dose rate of $12 \text{ kGy h}^{-1}$ and the total dose of 10 kGy and 12 kGy in terms of %conversion .....	55
4.14 Effects of acrylic acid-to-starch ratio on the graft copolymerization at the dose rate of $12 \text{ kGy h}^{-1}$ and the total dose of 10 kGy and 12 kGy in terms of %grafting efficiency .....	56

## LIST OF FIGURES (continued)

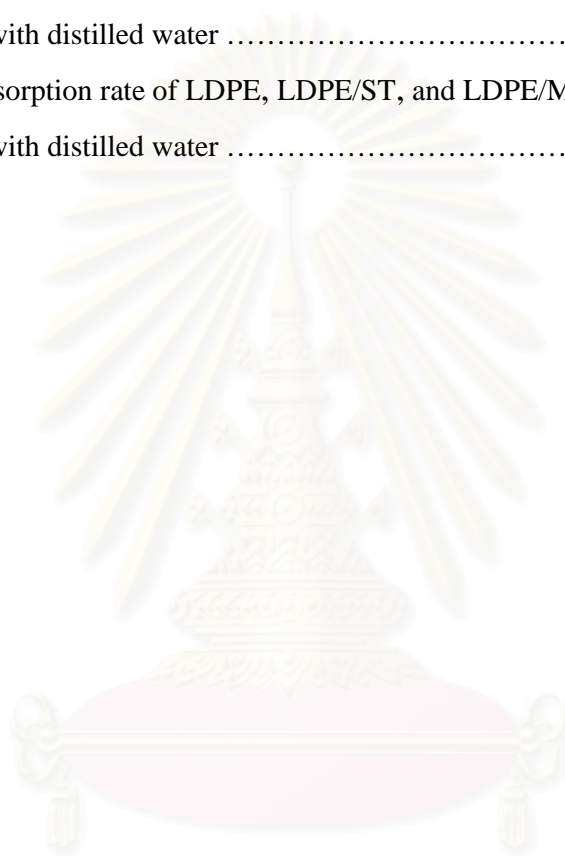
FIGURES	PAGE
4.15 Effects of acrylic acid-to-starch ratio on the graft copolymerization at the dose rate of 12 kGy h <sup>-1</sup> and the total dose of 10 kGy and 12 kGy in terms of %grafting ratio .....	57
4.16 Fourier transform infrared spectrum of esterified starch-g-poly(acrylic acid) .....	63
4.17 Fourier transform infrared spectrum of standard polystyrene film .....	64
4.18 <sup>13</sup> C-NMR spectrum of starch-g-poly(acrylic acid) .....	65
4.19 <sup>13</sup> C-NMR spectrum of starch-g-polyacrylate .....	66.
4.20 <sup>1</sup> H-NMR spectrum of cassava starch .....	67
4.21 <sup>1</sup> H-NMR spectrum of the side chain of starch-g-poly(acrylic acid) .....	68
4.22 <sup>1</sup> H-NMR spectrum of the side chain of esterified starch-g-polyacrylate .....	68
4.23 <sup>13</sup> C-NMR spectrum of the modified starch .....	71
4.24 <sup>1</sup> H-NMR spectrum of the modified starch.....	72
4.25 Calibration curve for the determination of the hydroxypropyl equivalent group .....	74
4.26 Tensile strength of LDPE, LDPE/ST, and LDPE/MS blends at various contents .....	80
4.27 Relative tensile strength of LDPE, LDPE/ST, and LDPE/MS blends at various contents .....	80
4.28 Percentage strain of LDPE, LDPE/ST, and LDPE/MS blends at various contents .....	81
4.29 Relative percentage strain of LDPE, LDPE/ST, and LDPE/MS blends at various contents .....	81
4.30 SEM micrograph of the fractured LDPE .....	82
4.31 SEM micrograph of the fractured LDPE/ST10 .....	83
4.32 SEM micrograph of the fractured LDPE/MS10 .....	83
4.33 SEM micrographs of the failed surface (after the tensile test) of LDPE .....	85
4.34 SEM micrographs of the failed surface (after the tensile test) of LDPE/ST10 .....	86
4.35 SEM micrographs of the failed surface (after the tensile test) of LDPE/MS10 .....	87

## LIST OF FIGURES (continued)

<b>FIGURES</b>	<b>PAGE</b>
4.36 Hardness values of LDPE, LDPE/ST, and LDPE/MS blends at various contents .....	89
4.37 Relative hardness values of LDPE, LDPE/ST, and LDPE/MS blends at various contents .....	89
4.38 TG and DTG thermograms of cassava starch .....	91
4.39 TG and DTG thermograms of cassava starch-g-poly(acrylic acid) .....	92
4.40 TG and DTG thermograms of esterified starch-g-polyacrylate .....	93
4.41 TG and DTG thermograms of modified starch .....	94
4.42 TG and DTG thermograms of LDPE .....	95
4.43 TG and DTG thermograms of LDPE/MS1 blend .....	96
4.44 TG and DTG thermograms of LDPE/MS5 blend .....	97
4.45 TG and DTG thermograms of LDPE/MS10 blend .....	98
4.46 TG and DTG thermograms of LDPE/MS20 blend .....	99
4.47 Tensile strength of LDPE, LDPE/ST, and LDPE/MS blends after soil burial test .....	103
4.48 Percentage strain of LDPE, LDPE/ST, and LDPE/MS blends after soil burial test .....	104
4.49 Initiation of biodegradation in hydrocarbon polymers .....	105
4.50 Hardness measurement of LDPE, LDPE/ST, and LDPE/MS blends after soil burial test .....	107
4.51 SEM micrograph of the control LDPE sheet .....	109
4.52 SEM micrograph of the LDPE sheet at 2-month soil burial test.....	109
4.53 SEM micrograph of the control LDPE/ST20 sheet .....	110
4.54 SEM micrograph of the the LDPE/ST20 sheet at 2-month soil burial test....	110
4.55 SEM micrograph of the control LDPE/MS20 sheet .....	111
4.56 SEM micrograph of the the LDPE/MS20 sheet at 2-month soil burial test....	111

**LIST OF FIGURES (continued)**

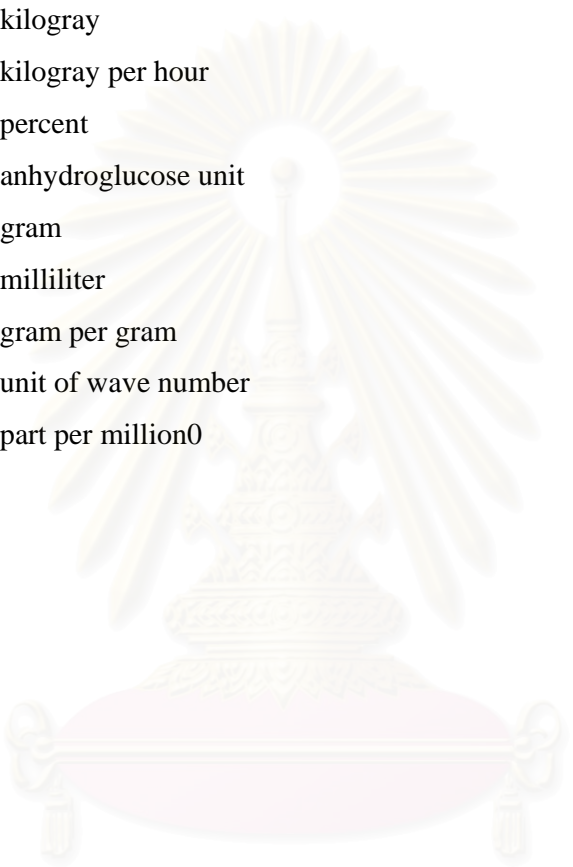
<b>FIGURES</b>	<b>PAGE</b>
4.57 Water absorption of LDPE, LDPE/ST, and LDPE/MS blends after contact with distilled water .....	114
4.58 Water absorption rate of LDPE, LDPE/ST, and LDPE/MS blends after contact with distilled water .....	115



สถาบันวิทยบริการ  
จุฬาลงกรณ์มหาวิทยาลัย

**LIST OF ABBREVIATIONS**

$^{60}\text{Co}$	cobalt-60
$\gamma$ -ray	gamma ray
kGy	kilogray
kGy h <sup>-1</sup>	kilogray per hour
%	percent
AGU	anhydroglucose unit
g	gram
ml	milliliter
g g <sup>-1</sup>	gram per gram
cm <sup>-1</sup>	unit of wave number
ppm	part per million



สถาบันวิทยบริการ  
จุฬาลงกรณ์มหาวิทยาลัย

# CHAPTER 1

## INTRODUCTION

### 1.1 Introduction

Over the past half-century, synthetic plastics have become the major new material for everyday life. Much of this growth has taken place at the expense of more traditional materials, such as steel, aluminium, paper and glass. Synthetic polymers, such as polystyrene (PS), polypropylene (PP), and polyethylene (PE), are widely used for food packaging or food service items, the biomedical field, and agriculture. Because they are easily-produced, convenient, cheap, long-lasting, and so on. The use of plastics in packaging is growing at the rate about 25 per cent per annum [1]. It is almost inevitable that they will continue to play an essential part in the distribution of food and other perishable commodities in spite of the threaten concern about their resistance to biodegradation. This situation leads to the growing problem of pollution. Although these inert polymers can be degraded by the natural surrounding, but the degradation process takes very long time. Therefore, there has been an increasing interest in the development of biodegradation polymers, such as:

- (a) synthesis of biodegradable polymers such as poly(3-hydroxy butyrate) or PHB and poly(3-hydroxy valerate) or PHV [2],
- (b) incorporation of natural product such as starch into polymers [3].

Polyethylene is one of the most dominant packaging materials, bringing with the real problems in the disposal of one-trip packaging. There are many attempts trying to make polyethylene easily degraded. The popular method is the use of starch as the natural filler in polyethylene. When exposure to a soil environment, the starch component is consumed by microorganism, leading to increased porosity, void formation, and the loss of integrity of plastics matrix. The plastic matrix will be broken down in to smaller particles. The view of this process is shown in Figure 1.1.

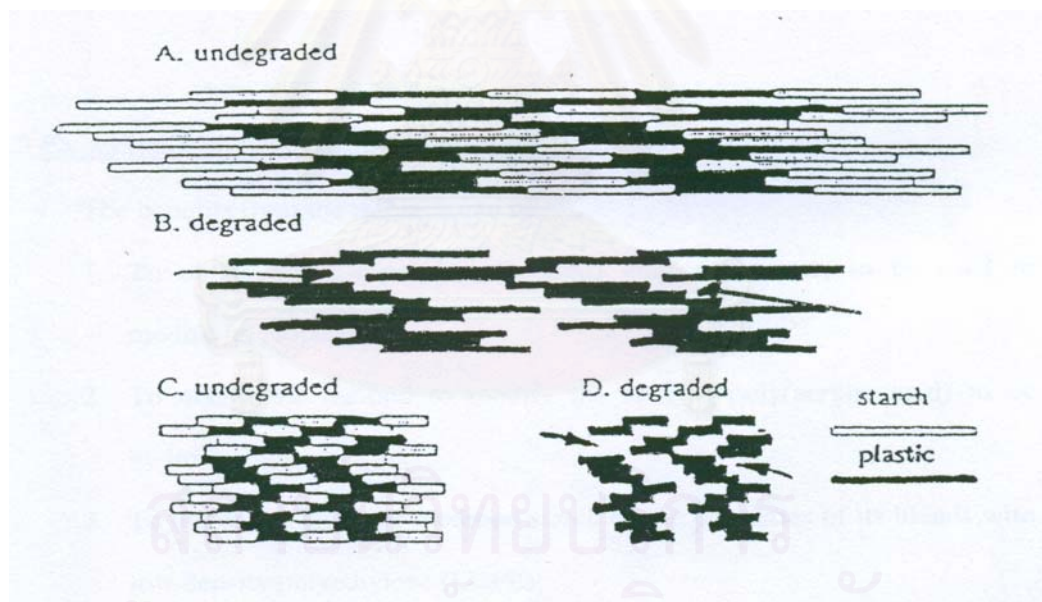


**Figure 1.1** Degradation of starch-filled plastics

## **1.2 Objectives**

The objectives of this research are following:

1. To determine a suitable condition for the synthesis of starch-g-poly(acrylic acid) graft copolymers by a simultaneous irradiation method.
2. To modify the obtained starch-g-poly(acrylic acid) to have hydrophobic property by esterification with poly(ethylene glycol) 4000 and etherification with propylene oxide.
3. To study the effect of the modified starch on the properties of its blends with low density polyethylene (LDPE).
4. To study the degradation of the modified starch/LDPE blends by soil burial test.

## **1.3 Expected Benefits Obtained from of the Research**

The benefits from the research can be

1. To obtain starch-g-poly(acrylic acid) graft copolymer, to be used to modify its property.
2. To obtain the method to modify the starch-g-poly(acrylic acid) to be hydrophobicity.
3. To obtain the effect of modified starch on the properties of its blends with low density polyethylene (LDPE).
4. To obtain the degradability of the modified starch/LDPE blends in soil.

## **1.4 Scope of Investigation**

In this research, the necessary procedures are as follows:

1. Literature survey and in-depth study of this research work.
2. Preparing the graft copolymers of starch-g-poly(acrylic acid) via gamma irradiation by a simultaneous irradiation technique with the variation of the following parameters: total dose (kGy), dose rate (kGy h<sup>-1</sup>), and acrylic acid-to-starch ratio to obtain the suitable and appropriate reaction conditions.
3. Extracting the homopolymer (poly(acrylic acid)) of the crude product.
4. Hydrolyzing the graft copolymers by acid hydrolysis method.
5. Characterizing the graft copolymer in the terms of:
  - a) %homopolymer
  - b) %add-on
  - c) %conversion
  - d) %grafting efficiency
  - e) %grafting ratio.
6. Esterifying the obtained graft copolymer with poly(ethylene glycol) 4000.
7. Etherifying the product from (6) with propylene oxide.
8. Compounding the plastic materials using a two-roll mill machine and making the plastic sheets with a compression moulding machine.
9. Studying the plastic sheet properties as follows:
  - a) Tensile strength and %strain test
  - b) Blend and failure morphology test
  - c) Hardness measurement

- d) Thermal property measurement
- e) Degradation in soil burial test
- f) Water absorption test.

10. Summarizing the results and preparing the report.

### **1.5 Content of the Thesis**

The content of this thesis comprises of five chapters. Chapter 1 involves an introduction of the present research, which gives reasons and objectives of the work. Details of the subsequently theoretical consideration and literature reviews are explained in Chapter 2 for those who want to understand the history and trends of the part investigated. Chapter 3 involves the procedure of grafting acrylic acid onto cassava starch by a simultaneous irradiation technique, modifying the graft copolymer with poly(ethylene glycol) 4000 and propylene oxide, and compounding the plastic materials for studying their properties. The results and discussions are described in Chapter 4, the graft copolymers were characterized in the terms of %homopolymer, %add-on, %conversion, %grafting efficiency, and %grafting ratio. Fourier transform infrared spectroscopy, nuclear magnetic resonance spectrometry, and ultraviolet spectroscopy were used for following the change of the obtained product in each step. Tensile strength, %strain, morphology, hardness, thermal property, degradation in soil, and water absorption were studied in order to evaluate the properties of LDPE composite sheets. The conclusion and suggestion of this work are given in Chapter 5.

## CHAPTER 2

### THEORY AND LITERATURE REVIEW

#### 2.1 Starch

Starch or polysaccharides presents a link with the energy of the sun, which is partially captured during photosynthesis. Starch is a biological material and naturally occurs in a wide variety of plants and agricultural crop. The size of starch, ranging from about 3 to 100  $\mu\text{m}$ , depends on the type of crops. For cassava starch, its granular size ranges from 5 to 35  $\mu\text{m}$  [4].

##### 2.1.1 The Chemistry of Starch

Starch is a high polymer composed of repeating 1,4- $\alpha$ -D-glucopyranosyl units. These monomers, called anhydroglucose unit (AGU), are joined together with  $\alpha$ -glucosidic linkage. This bond is acetal, stable under alkaline conditions and hydrolyzed under acid conditions. The hydroxyl groups can react to form ethers and can be oxidized to aldehyde, ketone, and carbonyl groups.

Although starch is a hydrophilic polymer, it is not all soluble in water. This property is influenced by the nature of monomer units, by the type of glucosidic linkage and by the presence or absence of hydrogen bonding between adjacent polysaccharide chains.

##### 2.1.2 Chemical Structure

Most starches are composed of two structurally different polysaccharides, the linear amylose and the branch amylopectin (Figure 2.1). Their relative amounts, structures and molecular masses are determined by means of genetic and environmental control, and therefore wide variation occurs among plants.

### 2.1.2.1 Amylose

Amylose is the linear component, produced by 1,4- $\alpha$ -D-glucosidic linkage. It is a minor component, typically ranging from 20% to 30%. Its molecular weight is about 0.2-2 millions. For cassava starch, the amylose content is about 16.5-22%.

### 2.1.2.2 Amylopectin

Amylopectin is the branched component which is composed of short 1,4- $\alpha$ -linked chains connected to each other by an  $\alpha$ (1,6) glucosidic linkage. The molecular mass of amylopectin is about 100-400 millions, but the average chain length is only 20-30 glucose units.

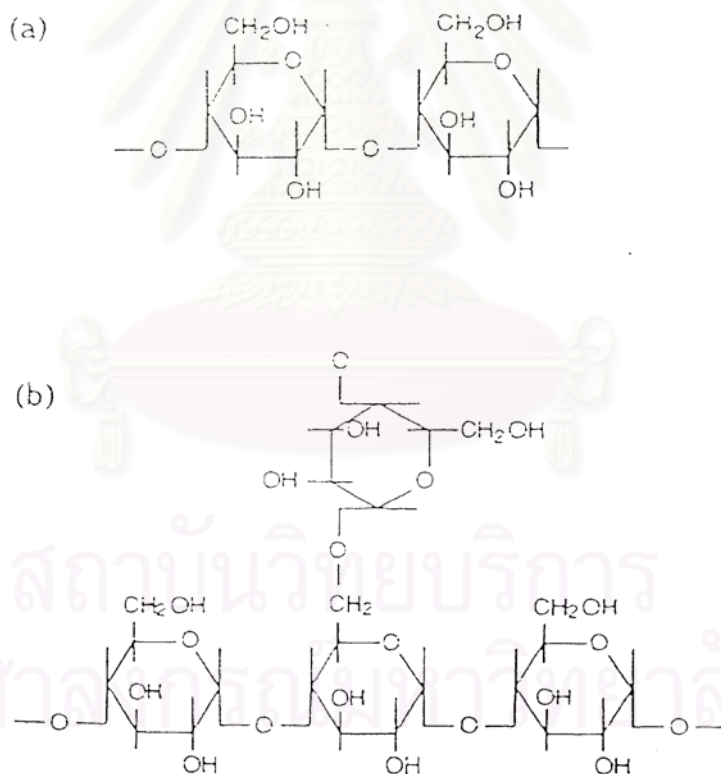


**Figure 2.1** Schematic structures of (a) amylose and (b) amylopectin  
(G, glucopyranose)

### 2.1.3 Starch Modification

The characteristics of starch can be modified by chemical treatment to enhance or repress its intrinsic properties or to impart new ones. Graft copolymerization method and the derivatization of the glucosidic hydroxyl groups have gained importance in chemical modification of starches.

#### 2.1.3.1 Graft copolymerization

Most graft copolymers are formed by free radical graft copolymerizations, a free radical produced on starch reacts with vinyl monomer. A number of initiating methods have been used to prepare graft copolymers, and these may be divided into two broad categories:

##### i) Chemical Methods [5]

There are several methods of chemical initiation, but the most widely used method is the reaction of starch with ceric salts, such as ceric ammonium nitrate dissolved in dilute nitric acid. Pretreatment of starch with ozone-oxygen mixtures has also been used.

##### ii) Radiation Methods [6]

Starch free radicals have been produced to initiate graft copolymerization by interaction with electromagnetic radical. The most popular technique is initiation by means of gamma-ray irradiation, which offers certain advantages over chemical methods. Radiation methods for preparation of graft copolymers are often easier to handle than most conventional chemical methods.

When high-energy radiation interacts with matter its intensity decreases, primarily because of scattering and energy absorption by some irradiated molecules. Three major processes are operative, photoelectric effect, Compton scattering, and production of electron pairs.

For gamma rays from Co-60, the predominant effect in organic material is Compton scattering. In the Compton effect the incident gamma ray interacts with an orbital electron ejecting the electron from its orbital and producing another photon of low energy. Both the electron and photon subsequently interact with the material or surrounding giving rise to essentially two processes, one of

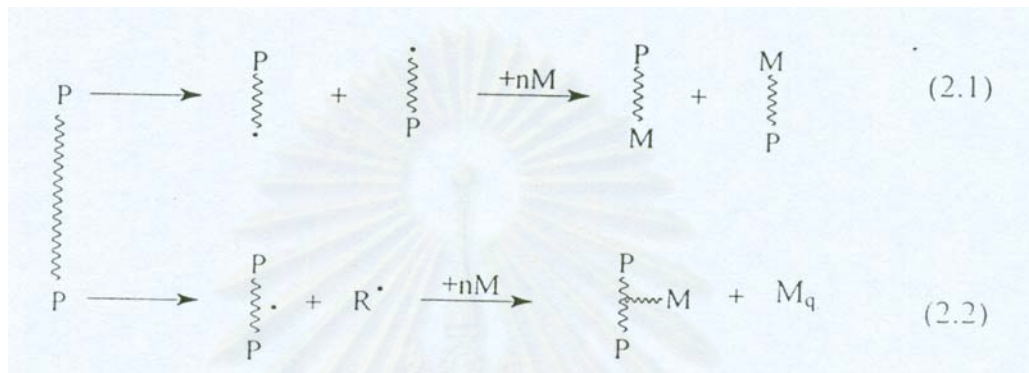
ionization and the other of excitation. In the case of ionization, the Compton electron transfers sufficient energy to the orbital electron of another atom to overcome the force binding it to the nucleus. The electron is therefore ejected, leaving behind a positive ion. If the energy is insufficient to cause ejection of an electron, the energy level of the atom is raised and the atom is said to be in an excited state. The ions and excited molecules are very reactive; they either react with other materials present in the system or decompose into radicals and atoms or molecules. The free radical produced upon irradiation of polymeric systems may be used to initiate graft copolymerization.

There are many different methods of radiation grafting such as direct or mutual irradiation of a polymer in the presence of a monomer and in the absence of air, preirradiation of a polymer in air to yield peroxy groups and the subsequent contact with a monomer in the absence of air. Preirradiation of a polymer in a vacuo yields trapped radicals followed by heating in the presence of another monomer. In the absence of air, irradiation of two polymeric substrates is in intimate contact. In the absence and presence of air, polymer lattice swollen with monomer are irradiated.

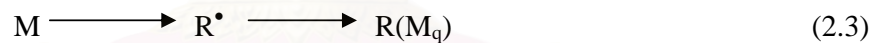
In this thesis, only the direct grafting method is considered. The direct or mutual irradiation is the simplest grafting method, involving the irradiation of a polymeric substrate in the presence of a monomer and in the absence of oxygen. Graft copolymerization of the monomer to the polymer is then initiated through the free radicals generated in the latter.

A number of important factors must be considered, however, before applying the direct radiation method to a given polymer-monomer system. Ionizing radiation as such is unselective. One must consider not only the effect of irradiation on the polymeric substrate, but also the effect on the monomer, the solvent, or any other substance present in the system. Together with the radiation sensitivity of the polymer-monomer combination one must also consider the effect of the radiation on the actual polymeric substrate. In general, polymer either degrade or

crosslink under irradiation. If the polymer degrades then irradiation in the presence of a monomer will lead predominantly to block-type copolymer; if the polymer crosslinks, graft structures will result. This may be represented schematically as follow:



Here  $\text{P} \cdot$  and  $\cdot \text{P}$  represent polymeric free radicals derived from  $\text{P} \text{---} \text{P}$ , and  $\text{R} \cdot$  represents a low molecular weight radical or hydrogen atom. The homopolymer ( $\text{M}_q$ ) arises from initiation by small radicals  $\text{R} \cdot$  and also by radiolysis of the monomer  $\text{M}$ .



#### *Kinetic Features of Radical Grafting*

For the simplest case of polymer swollen by or immersed in a monomer, the polymer is completely insoluble in the monomer. If one assumes that the graft copolymerization occurs by a radical chain process, then, the overall reaction scheme can be divided into three main stems: initiation, propagation, and termination. This may be represented as follows.

Initiation:



$$r = kI \quad (2.5)$$

Addition of the first monomer to initial radical:



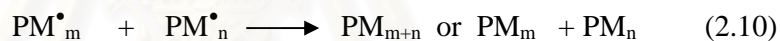
$$r_i = k_i[P^\bullet][M] \quad (2.7)$$

Propagation:



$$r_p = k_p[M_n^\bullet][M] \quad (2.9)$$

Termination by two growing radicals:



$$\begin{aligned} r_t &= 2 k_t[PM_m^\bullet][PM_n^\bullet] \\ &\approx 2 k_t[PM_n^\bullet]^2 \end{aligned} \quad (2.11)$$

If one makes the normal assumption that the length of the polymer chains is long, then the reaction (2.6) can be neglected with respect to the reaction (2.8), and one obtains the following relation for the rate of graft copolymerization.

$$r_p = k_p[PM_n^\bullet][M] \quad (2.12)$$

Introducing the conventional steady-state assumption that the rate of change of the radical concentration is small compared to its rates of formation and disappearance, then

$$k_i[P^\bullet][M] = 2 k_t[PM_n^\bullet]^2 \quad (2.13)$$

i.e. ,

$$r_i = 2k_i[PM_n^*]^2 \quad (2.14)$$

$$[PM_n^*] = (r_i/2k_t)^{1/2} \quad (2.15)$$

On combining equation 2.12 and 2.15, one obtains for the rate of graft copolymerization:

$$r_p = k_p[M] (r_i/2k_t)^{1/2} \quad (2.16)$$

Where

I = intensity of radiation

P = backbone polymer

P<sup>\*</sup> = polymer radical

PM<sub>m</sub>, PM<sub>n</sub>, P<sub>m/n</sub> = graft copolymer

M = grafting monomer

r = rate of initiation of polymer radicals

r<sub>i</sub> = rate of initiation of graft reaction

r<sub>p</sub>, r<sub>t</sub> = rate of propagation and termination, respectively

K = rate constant for initiation of polymer radicals

k<sub>i</sub> = rate constant for initiation of graft reaction

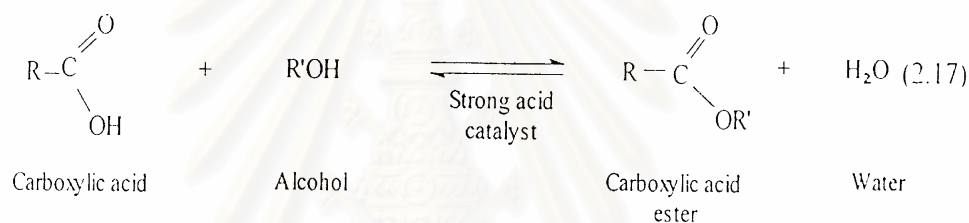
r<sub>p</sub>, r<sub>t</sub> = propagation and termination rate constant, respectively

In practice, however, the situation is not quite as straightforward as this, because of the number of specific features resulting from the special reaction condition also prevailing in most grafting systems. The gel effect, chain transfer, phase separation, and diffusion effects are, but a few of the many factors, which can seriously affect the reaction kinetics.

### 2.1.3.2 Esterification of carboxylic acid group [7, 8]

The formation of a carboxylic acid ester (usually called simply an ester) can be prepared by treatment of a carboxylic acid with an alcohol in the presence of an acid catalyst. The acids most commonly used are sulfuric acid, hydrochloric acid as a gas bubble in the reaction medium and *p*-toluenesulfonic acid. The conversion of carboxylic acid and alcohol to an ester is given the special name **Fischer esterification** after the German chemist Emil Fischer (1852-1919).

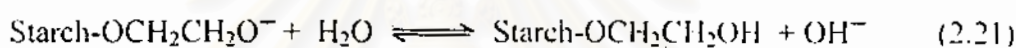
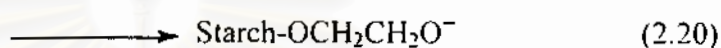
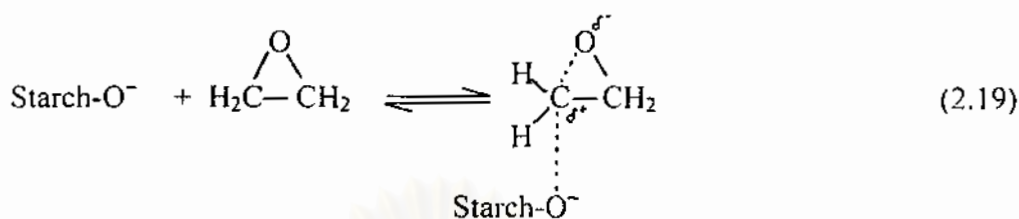
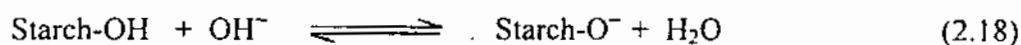
The general reaction equation is presented as follow:



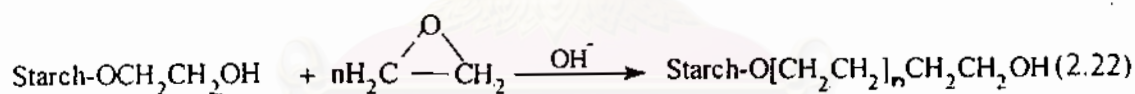
Fischer esterification is a reversible reaction, and generally appreciable concentration of both the carboxylic acid and ester are present at equilibrium. Therefore, to obtain a good yield of ester, it is necessary to force the reaction to completion either by removing the water as it is formed or using excess of the reactants. The equilibrium is frequently shifted to product using an alcohol as both a solvent and a reactant.

### 2.1.3.3 Starch Etherification [9]

Starch molecule can be etherified at the reactive hydroxyl group in the presence of alkaline catalyst. There are three principal methods for the etherification, the ring opening of epoxides, the nucleophilic displacement of aliphatic halogens or sulfate groups (the Williamson synthesis), and the Michael-type addition. The most widely known method is ring opening of epoxides. This procedure proceeds by the attack of polysaccharide anion to epoxides. The most common of epoxide used is ethylene oxide. The reaction mechanism is shown below:



At high degree of substitution, some polyoxyethyl groups are formed.



If starch reacts with propylene oxide, two different starch ethers may result depending on whether the nucleophilic attack takes place at the primary or at the secondary carbon atom.



The major and usually the only product is that resulting from a nucleophilic attack at the least-hindered (primary) carbon.

## **2.2 Terminology and Definition**

In order to make several points in the thesis clear, some specific terms must be clarified.

### **2.2.1 Gelatinization of Starch**

Gelatinization of starch occurs either by chemical or thermal treatment. In this thesis, the latter is considered.

When starch granules are heated continuously, they absorb water, increase many folds in size, and gelatinize. Consequently, the initially thin and opaque, and finally transparent. As a result of cooking, starch forms a continuous system, referred to as starch cook or starch paste. In a starch cook or paste, there is a mixture of hydrates; swollen granules and granule particles, held together by a typical maize of associative forces. The temperature at which this drastic change occurs is usually termed the gelatinization or, more correctly, the pasting temperature of starch. More exactly, the gelatinization temperature is recorded as a temperature range in which the starch granules loss their birefringence when observed under the microscope. The gelatinization temperature is a characteristic property of starch. For cassava starch, it ranges about 60-85 °C

### **2.2.2 Percentage of Homopolymer**

Homopolymer is the ungrafted polymer, in this case, poly(Acrylic acid). Homopolymer formed can be obtained by subtracting the weight before and after soxhlet extraction of graft copolymer and homopolymer with methanol. The different weight is poly(Acrylic acid) which is soluble in methanol.

$$\% \text{ homopolymer} = \frac{(\text{Weight before extraction} - \text{Weight after extraction}) \times 100}{\text{Weight before extraction}} \quad (2.25)$$

### 2.2.3 Percentage of Add-on

The percentage of add-on is the percent of the grafted polymer in the graft copolymer, determined as follows:

$$\% \text{add-on} = \frac{\text{Weight of Polymer Grafted} \times 100}{\text{Initial Weight of Graft copolymer}} \quad (2.26)$$

### 2.2.4 Percentage of Conversion

The conversion of monomer is the change of monomer charged to polymer, which comprises homopolymer and graft copolymer. In this research, the conversion of acrylic acid monomer is polymerized into the form of poly(Acrylic acid) and grafted poly(Acrylic acid)(Starch-g-poly(Acrylic acid)). This parameter can be calculated by:

$$\% \text{conversion} = \frac{\text{Weight of Polymer formed} \times 100}{\text{Weight of Monomer charged}} \quad (2.27)$$

### 2.2.5 Percentage of Grafting Efficiency

This term is used to describe graft copolymerization reactions and defined as the percentage of the total synthetic polymer formed that has been grafted on starch. High grafting efficiency would afford mainly a physical mixture of grafted starch and a small amount of homopolymer. It can be calculated as follows:

$$\% \text{grafting efficiency} = \frac{\text{Weight of Polymer grafted} \times 100}{\text{Weight of Homopolymer} + \text{Weight of Polymer grafted}} \quad (2.28)$$

### 2.2.6 Percentage of Grafting Ratio

This term is defined as the percentage ratio between grafted polymer and starch. After doing acid hydrolysis, it can be calculated as follows:

$$\% \text{ grafting ratio} = \frac{\text{Weight of Grafted polymer} \times 100}{\text{Weight of Substrate (Starch)}} \quad (2.29)$$

### 2.2.6 G Values

G values are the term used to measure the chemical yields or free radical yield from high-energy radiation. A G value is the number of molecules formed or reacted per 100 e.V. of energy absorbed per gram. The G value of an irradiated system is sometimes markedly altered by the presence of another species.

## 2.3 Literature Survey

Nai-Hong and Micheal William [10] prepared a new hydrogel(HG) from polyglycol and an organic acid without crosslinking. They used this new material as a filler for a commercial grade of linear low density polyethylene(LLDPE). The blend of 1%HG and LLDPE was carried out by using a Brabender mixer. After characterization by DSC they found that the two polymers were phase-separated in the blend, with  $T_m$  of the LLDPE and various HG transitions almost unchanged. Moreover, the tensile testing of solid-state specimens showed that the tensile strength and modulus of the blend were also superior to those of the LLDPE, the former by 20% and E by 40%. Despite a major improvement in these measures of strength in solids, no changes were observed in the dominant crystal structure, and ductility was also unchanged at 14% strain to break.

Reyes et al. [11] investigated the grafting of acrylic acid(AA) to starch with gamma-preirradiated starch and aqueous solution of acrylic acid. The rate of grafting increased initially with time, then decreased, and approached zero when the

percentage grafting reached a maximum value. At a given radiation dose, the rate of grafting was proportional to the first power of the concentration of the irradiated starch and the 1.5 power of the initial concentration of acrylic acid. Solvent effects on degree of grafting, molecular weight, and number of grafted branches were evaluated. Higher degrees of grafting were achieved with electron-irradiated starch at radiation doses lower than those used with gamma rays.

Zaharan et al. [12] grafted acrylic and methacrylic acid to rayon and cotton using the irradiation technique with  $^{60}\text{Co}$   $\gamma$ -rays. They found that the rate of grafting increased with increasing temperature and monomer concentration, as did the final degree of grafting. The amount and rate of grafting also increased with the total irradiation dose, but they tended to level off at higher doses, in agreement with the leveling off of the radical content reported previously. Methacrylic acid grafted more and faster than acrylic acid to both rayon and cotton. Methacrylic acid grafted more with rayon than cotton, but acrylic acid gave somewhat similar yields with both fibers. The water absorbancy of the grafted fibers depended strongly on their posttreatment. Decrystallizing with 70% zinc chloride or with hot sodium hydroxide developed supersorbency. The two treatments in succession gave the highest value. Methacrylic acid, which brought about less sorbency could be readily and practically achieved by the method described.

Gulten et al. [13] grafted acrylic acid(AA) to cellulose using ceric ammonium nitrate(CAN) as an initiator in aqueous nitric acid solution at 30, 50, 70, and 90°C during reaction periods of 30 to 180 minutes. About 45% of the AA was polymerized at 90°C after 180 minutes. The grafted polymer and homopolymer were isolated by acetone from the reaction mixture, dried, and subjected to soxhlet extraction with dioxane to separate the homopolymer, poly(acrylic acid) , from the graft copolymer. The water absorption capacities and grafting value of grafted cellulose were also determined. The maximum grafting yield was obtained at 30°C. It was also observed that poly(acrylic acid)-grafted cellulose produced at 30°C had the highest water

retention capacity. The time dependence of AA conversion allowed a calculation of first-order reaction rate constants. These rate constants were then used to determine apparent activation energy.

Athawale et al. [14] graft-polymerized methacrylic acid(MA) onto starch using  $Ce^{4+}$  initiator in aqueous medium. The dependence of grafting on the reaction variables, such as monomer and initiator concentrations, and time and temperatures, was studied in detail. Acid hydrolysis and infrared (IR) spectroscopy were used for the confirmation of graft copolymer formation. Further, representative graft copolymer was characterized by x-ray diffraction(XRD), thermogravimetric analysis(TGA), and differential scanning calorimetry(DSC).

Goni et al. [15] carried out the study on the graft copolymerization of methyl acrylate, ethyl acrylate and n-butyl methacrylate on the linear fraction of starch(amylose), initiated by ceric ammonium nitrate. The results were compared with those obtained previously for methyl methacrylate and butyl acrylate. They obtained the following maximum grafting efficiency = 99% for poly(methyl acrylate), percent grafting = 338% for poly(ethyl methacrylate) and percent total conversion = 97% for poly(n-butyl methacrylate).

Mingzhu et al. [16] carried out a study of ceric ammonium nitrate(CAN) initiated graft copolymerization of metha acrylate(MA) onto potato starch. The variables affecting the graft were investigated. The optimum condition for the copolymerization was obtained; they were the concentrations of MA, CAN and nitric acid( $HNO_3$ ) ( $1.08$ ,  $5.0 \times 10^{-3}$ , and  $8.1 \times 10^{-2}$  mol/L, respectively). The reaction temperature was ca.  $50^\circ C$  and the reaction time was 2 hours. The molecular weight of grafted poly(methyl acrylate) had been determined. On the basis of experimental results, the mechanism of grafting had been explored, a new kinetic equation of the grafted copolymerization was consequently established.

Iyer et al. [17] prepared superabsorbant polymers using acrylonitrile grafted to corn starch employing low levels of gamma ray radiation as an initiator. Various grafting parameters were studied at these two dosages. Absorbancy values for the final products were reported. Use of the above superabsorbant as a dessiccant were evaluated. The product was used in a final application where dispersions of low viscosity and high water absorbance are desired.

Hallden and Wesslen [18] prepared a graft copolymer containing poly(ethylene oxide) side chains attached to a polyethylene backbone by coupling of poly(ethylene-*co*-acrylic acid) (PEAA) and poly(ethylene oxide) monomethyl ethers (MPEO) by esterification in *o*-xylene at 140°C. The MPEO side chains had molecular weights of 750-5000. The chemical composition of the graft copolymers was analyzed by NMR and FT-IR spectroscopy. The weight fraction of the MEPO grafts in graft copolymers was found to be around 0.4. The graft copolymers exhibited a phase-separated morphology with the backbone and the MPEO grafts forming separated crystalline phases. The MPEO phase had a melting point temperature of 8-25°C, lower than the corresponding MPEO homopolymers, as determined by DSC. The melting point of the crystalline phase formed by the PEAA main chains was close to that of the pure PEAA. Crystallinity was also determined by x-ray diffraction.

Kiatkamjornwong et al. [19] prepared the degradable polyethylene film by blending with 0-20%w/w of cassava starch, 0-2%w/w of soya oil and 0-0.1%w/w of ferric stearate. The dispersing agent used was Epolene wax. The oxidative degradation of the film was measured by outdoor weathering testing in comparison with indoor testing, and soil burial testing for six month. Biodegradation was determined by measurements of the populations of *Aspergillus niger* and *Penicillium pinophilum* fungi. All degradation processes were followed by monitoring chemical and physical changes of the samples by infrared spectroscopy, average molecular weights by viscosity method, and tensile properties. They found that the concentrations of the carbonyl groups were high in iron stearate starch-filled PE film, and there were high populations of *Aspergillus niger* and *Penicillium pinophilum*

fungi on the samples. For indoor-outdoor exposure test, the iron-stearate starch-filled PE films lost their physical properties after two months of outdoor exposure, while the films kept indoor remained unchanged for longer than 6 months. For soil burial test it took a long time than that outdoor test to degrade.

Goheen and Wool [20] produced the binary polymer films containing different percentages of corn starch and low-density polyethylene(LDPE), which were exposed to soils over a period of 8 months and monitored for starch removal and chemical changes of the matrix using FTIR spectroscopy. A standard curve using the area of C-O stretch band and empirical second-degree polynomial to fit the data made it possible to calculate the starch concentration over a wide range(0-46% by mass). Starch removal was found to proceed rapidly during the first 40 days and to near completion in very high starch blends(52% and 67% by weight). Starch removal was slower, consisting of mostly surface removal in 29% starch blends. Weight loss data supported spectroscopic data showing similar gross features. Weight loss and spectroscopic data were consistent with percolation theory and suggested that starch removal continued past 240 days. Degradation rate in different soil containing different amounts of organic matter were approximately the same after the period of a few weeks. IR analysis did not show significant chemical change in the polyethylene matrix after 240 days. However, the matrix did show evidence of swelling, an increase in surface area, and removal of low molecular weight components.

Willet [21] studied the mechanical properties of composites of granular starch and LDPE as functions of starch volume fraction  $\phi$ , granule size, and presence of compatibilizer. Property-volume fraction relationships were interested using various theories of composite properties. The dependence of elongation ( $E \approx \phi^{1/3}$ ) and tensile strength( $\sigma \approx \phi^{1/3}$ ) agree with the theoretical predictions, although the proportionality constants are less negative than theoretical values. The addition of compatibilizer(ethylene-co-acrylic acid copolymer,EAA) did not significantly affected the elongation or tensile strength, but significantly increased the composite tensile modulus. The corn starch/PE moduli could be described by the Kerner or Halpin-Tsou equations. Analysis of the composite moduli data using the Halpin-Tsou

equations. Analysis of the composite moduli data using the Halpin-Tsou equations allowed the estimation of the moduli of granular starch. The value obtained, 15 GPa, is considerably greater than most unfilled synthetic polymers of importance, but significantly lower than the modulus of cellulose. It is also greater than a previously reported value of 2.7 GPa.

Thiebaud et al. [22] prepared starch cotanoates OCST1.8 and OCST 2.7 with degree of substitution(d.s.) of 1.8 and 2.7, respectively, and dodecanoate DODST 2.7 (d.s.=2.7) by esterification of native starch with fatty acid chlorides. Their analyzes, including elemental analysis, FTIR, contact angle, DSC, and TGA measurements confirmed the esterification reaction of starch and the degree of substitution. The ester group was found to act like an internal plasticizer, with increases in the number and the size of fatty acyl chain grafted onto starch. These starch esters were mixed with low-density polyethylene(LDPE) at various portions in a Haake Rheo-mixer. Water and moisture absorption, thermal and mechanical properties and biodegradation were investigated as a function of blend composition. The DODST2.7/LDPE blends showed the general better thermal stability and higher elongation, but lower tensile strength and water absorption, than did corresponding OCST/LDPE blends. The addition of starch esters to LDPE led to a very slow rate of biodegradation of these blends.

Arvanitoyannis et al. [23] studied the mechanical properties and gas/water permeabilities of extrudates of LDPE, wheat starch and ethylene acrylic acid(EAA) or polycaprolactone(PCL) after their conditioning at various relative humidities. Satisfactory agreement was found between the experimental values, pertaining the mechanical properties, and estimates obtained by applying several semi-empirical equations. The presence of starch contents (>30%) or PCL had an adverse effect on the mechanical properties of LDPE/starch blends, whereas EAA acted as a compatibilizer by increasing the percentage elongation of the blends. Gas permeability and water vapor transmission rate increased proportionally to the starch/PCL content in the blend. Several theoretical and semi-empirical calculations

were also applied for gas permeabilities and possible interpretations were provided for the occasionally observed deviations between the experimental and theoretical values.

Sagar and Merrill [24] examined the properties of starch esters for their possible application as environmentally degradable thermoplastics. The rheological, thermal, and mechanical properties of a series of fatty-acid esters of the high-amylose starch (as well as the effects of adding plasticizer on some selected properties) were evaluated. The ester group, which acts like an internal plasticizer makes these starch-based materials more processable and more ductile. However, their properties and cost, compared to commodity thermoplastics lead us to believe that their commercial applications are likely to be limited.

Aburto et al. [25] prepared and studied a series of starch and amylose ester with different degrees of substitution and side-chain length. The esters were prepared by acylation of the polysaccharide with the appropriate acid chlorides, such as octanoic, dodecanoic, and octadecanoic. The degrees of substitution were 0.54, 1.8, and 2.7, respectively. After preparation, the resulting esters were characterized by elemental analysis,  $^1\text{H}$  nuclear magnetic resonance ( $^1\text{H-NMR}$ ), Fourier transform infrared spectroscopy (FT-IR), differential scanning (DSC), thermogravimetric analysis (TGA), and water uptake measurements. Their mechanical properties and, in particular, the tensile strength and elongation at break depend on the side-chain length and on the degree of substitution. The extent of their biodegradability, after exposure to activated sludge, was assessed by weight loss measurement and scanning electron microscopy (SEM). It was found that these new materials are biodegradable, and the biodegradation rate decreases with increasing degree of esterification.

Kang et al. [26] modified starch into a more hydrophobic material by an introduction of a cholesterol unit, and the different starch-composition high-density polyethylene (HDPE) film were prepared with an addition of either native starch or

modified starch to compare the physical properties. The addition of either native starch or modified starch resulted in decreased crystallinities in all the different composited films containing starch. Interestingly, HDPE-blown films containing



สถาบันวิทยบริการ  
จุฬาลงกรณ์มหาวิทยาลัย

## CHATER III

### EXPERIMENT

#### 3.1 Chemicals, Equipment, and Glassware

##### 3.1.1 Chemicals

Tapioca starch was kindly supplied from Thai Wah Public Company Limited. It was the super high-grade flour, which contained 13.5% of moisture. Its properties also consisted of a pH value of 4.00-7.00, pulp of 0.20 ml. max., 0.20% ash and viscosity of 550 B.U..

Acrylic acid, AA, was provided by Thai Mitsui Chemical Company Limited and was used without further purification. The purity of this monomer is 99.5 min. percent by weight.

Maleic acid, purum >98%(HPLC)

Fluka, Buchs, Switzerland

Acetic acid glacial  $\approx$ 100% min. assay 99.8%

BDH, Poole, England

Perchloric acid 65%, Analysis grade min. assay 64%

Carlo Erba, Milan, Italy

Hydrochloric acid 37%, RPE

Carlo Erba, Milan, Italy

Poly(ethylene glycol) 4000, Lab grade

Fluka, Buchs, Switzerland

*p*-Toluene sulfonic acid, Analysis grade

Fluka, Buchs, Switzerland

Methanol, Analysis grade

Merck, Darmstadt, Germany

Propylene oxide, purum>99%

Fluka, Buchs, Switzerland

Sodium hydroxide anhydrous pallet, Analysis grade min. assay 98%

Carlo Erba, Milan, Italy

Isopropanol alcohol, Analysis grade min. assay 99.9%

Carlo Erba, Milan, Italy

Sulfuric acid 96%, Analysis grade

Carlo Erba, Milan, Italy

Ninhydrin crystal, Analysis grade

Merck, Darmstadt, Germany

Propylene glycol, Analysis grade

Merck, Darmstadt, Germany

Sodium bisulfite, Analysis grade

Merck, Darmstadt, Germany

Acetone and methanol, Commercial grade

Arsom Co., Ltd., Bangkok, Thailand

Polyethylene (LDPE) ST1018

Liack Seng Trading Co., Ltd., Bangkok, Thailand

Physical properties of the material are listed in Table 3.1.

Ethylene-bis-stearamide (EBS wax)

Supplied from Chemmin Corporation Ltd., Bangkok, Thailand

Properties of EBS wax are presented in Table 3.2.

**Table 3.1** Physical Properties of Linear Low Density Polyethylene

Property	Unit	Test Method	Value
Melt Index(2.16 kg/190°C)	g/10 min.	ASTM D1238	30.00
Density	g/cm <sup>3</sup>	ASTM D1505	0.916
Tensile Strength at Yield	N/mm <sup>2</sup>	ASTM D638	9.0
Tensile Strength at Break	N/mm <sup>2</sup>	ASTM D628	7
Ultimate Elongation	%	ASTM D638	300
Vicat Softening	°C	ASTM D1525	83

Remark: 1. The values presented on the above table are typical laboratory averages.

2. All grades meet F.D.A. requirements as listed in food additives regulation 21 CFR 177.1520 for use in direct contact foods.

**Table 3.2** Typical Properties of Ethylene-bis-Stearamide (ARMOWAX EBS SF)

Parameter	Property
Acid Value	6.0 max
Amine Value	3.0 max
Color Gardner	3 max
Water Content (%)	0.20 max
Ash (%)	0.10 max
Melting Point (°C)	141.5-145.0
Volatile Matter (%)	0.5 max
Particle Size	
200 mesh pass	85 min
Average Particle Size (µm)	45
Odor	Slight fatty odor
Appearance	Fine powder

Remark: Armowax is a registered trade mark of Lion Akzo Co. Ltd., used by Palmaminde under licence.

### 3.1.2 Equipment and Glassware

4-necked reactor, water bath circulator, stirrer, mechanical stirrer, aluminium tubes, hot plate and magnetic stirrer, heating mantle, analytical balance, centrifugator, grinder, Soxhlet extraction glassware and other general laboratory glassware and equipment

Cobalt-60 Irradiator (Gammabeam 650 Unit, Serial No. 18R)

Nordian International Inc., Canada

Two-roll Mill Compounding Machine, Model LRM 110

Lab Tech Engineer Co., Ltd., Thailand

Crushing Machine

Bosco Engineering Co., Ltd., Thailand

Compression Moulding Machine, Model LP20

Lab Tech Engineer Co., Ltd., Thailand

Fourier Transform Infrared Spectrophotometer, Model 1760

Perkin Elmer, USA.

UV-VIS-NIR Scanning Spectrophotometer, Model UV-3101PC

Shimadzu, Japan

Tensile Testing Machine, Model 1011 Serial No. 1353

Instron, USA.

Hardness Tester, Model 716

Instrument & MFG Co., USA.

Scanning Electron Microscopy, JSM-6400

JEOL, Japan

Nuclear Magnetic Resonance Spectrometer, Model DPX-300

Bruker, Switzerland

Thermal Gravimetry Analyzer, Model TGA 7

Perkin Elmer, USA.

### 3.2 Preparation Scheme

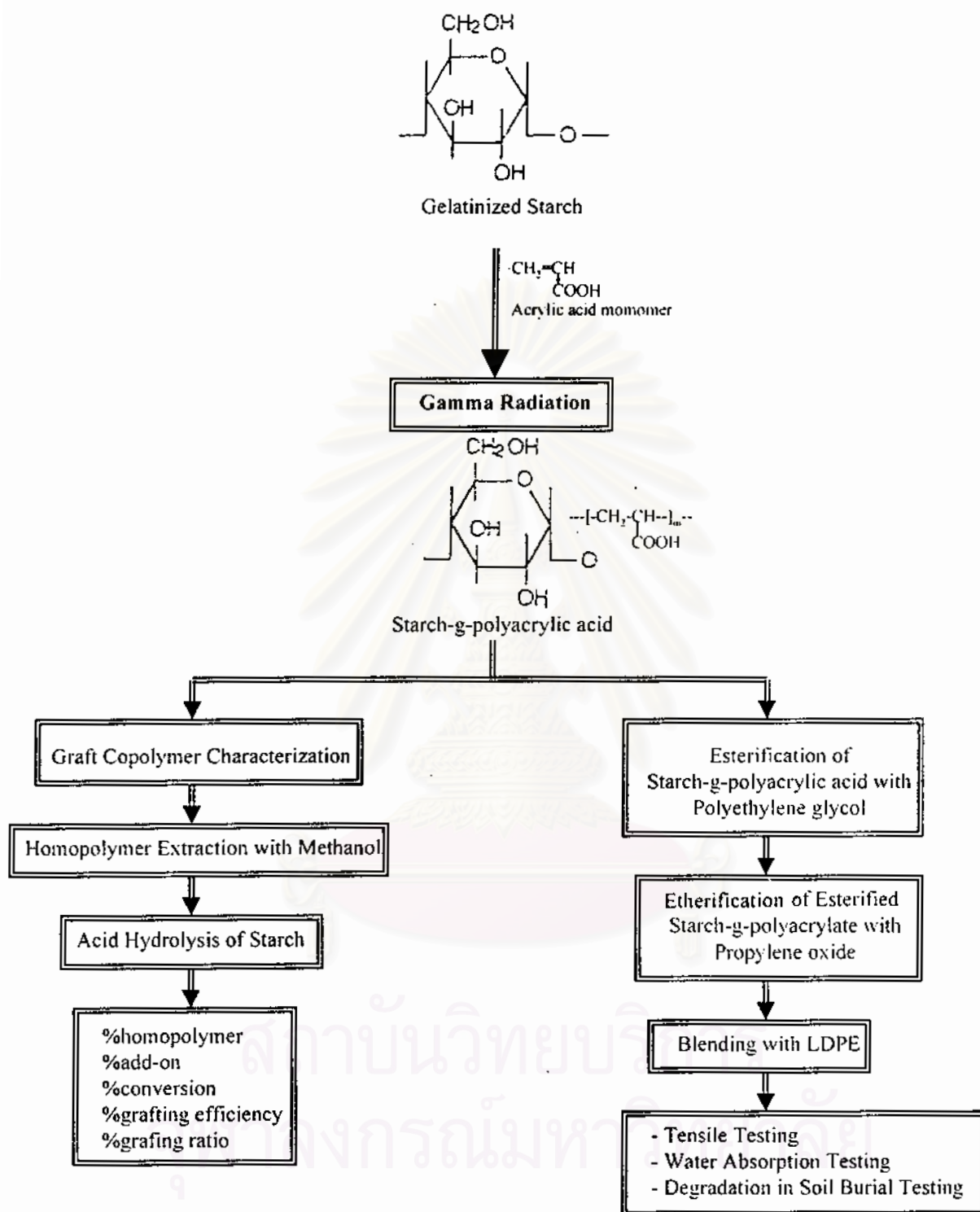


Figure 3.1 Overall schematic experimental process

### 3.3 Procedure

#### 3.3.1 Graft copolymerization

##### 3.3.1.1 Gelatinization of Cassava Starch

The amount of 20 g of cassava starch was dissolved in 400 ml of distilled water, taken into the reactor and kept stirring at 400 rpm for 1 hour. The system temperature was maintained at around  $85 \pm 3$  °C. After this treatment, the paste-like slurry was formed, and it was then cooled to room temperature. The gelatinization and cooling processes were carried out in the atmosphere of nitrogen in order to get rid the entrapped oxygen in the gelled starch.

##### 3.3.1.2 Grafting of Acrylic Acid onto Gelatinized Cassava Starch by Simultaneous Irradiation Technique

Acrylic acid, 20 g, and 2% (w w<sup>-1</sup>) of maleic acid were dissolved in 50 ml of distilled water. The mixture was then added into the gelatinized starch. The gelatinized starch-acrylic acid mixture was stirred at 400 rpm for 45 minutes. Bubbling of nitrogen gas through the mixture was continued for the duration of mixing. After the desired mixing time had elapsed, the mixture was transferred to an aluminium tube and was purged with nitrogen gas for 5 minutes. The tube was tightly closed with a lid and paraffin film and then irradiated by gamma-ray irradiator.

##### 3.3.1.3 Effect of Total Dose(kGy) and Dose Rate(kGy/hr) on Graft Copolymerization

There were 3 values of dose rate used in this section, which were 2, 5, and 12 kGyhr. Each dose rate was given to obtain the total dose of 2, 4, 6, 8, 10, and 12 kGy. These dose rates and total doses were used to irradiate the gelatinized starch-acrylic acid mixture as described in Section 3.3.1.2.

After the irradiation, the irradiated product was dispersed in acetone in order to remove an unreacted acrylic acid monomer. The mixture was continuously stirred for 20 minutes and was left overnight. After that, it was

centrifuged to separate an insoluble poly(acrylic acid), a homopolymer, and the starch-g-poly(acrylic acid), graft copolymer. The precipitants were washed with 2 portions of acetone and were then dried in a vacuum oven at 65 °C for 24 hours.

The dried sample was inspected with an FT-IR spectrophotometer (Perkin Elmer, Model 1760) and was consequently measured for %homopolymer, %add-on, %conversion, %grafting efficiency, and %grafting ratio. The higher %add-on and the lower %homopolymer indicate the appropriate total dose and dose rate for studying the effect of acrylic acid/starch ratios on graft copolymerization in the next section.

#### 3.3.1.4 Effect of Acrylic acid/Starch Ratios on Graft Copolymerization

Various amounts of acrylic acid (2% of maleic acid) solution were added to the gelatinized starch to obtain the acrylic acid/starch ratios of 0.5:1, 1:1, 1.5:1, 2.0:1, and 5.0:1. The experimental procedure was carried out as described in Section 3.3.1.2, and the optimum total dose and dose rate were obtained from Section 3.3.1.3. The dried sample was also characterized as mentioned in Section 3.3.1.3 to determine the optimum ratio of acrylic acid/starch for further chemical modification.

#### 3.3.1.5 Homopolymer Extraction with Methanol

The exact weight of dried homopolymer and graft copolymer (in a dried powder form, 5.0 g) was subjected to extraction with methanol in a Soxhlet apparatus for 24 hours to separate homopolymer of poly(acrylic acid). The extracted product was dried in a vacuum oven at 65 °C for 24 hours. After that it was weighed to determine the amount of homopolymer by subtracting the weight before and after extraction. All products were detected with FT-IR spectrophotometry.

### 3.3.1.6 Hydrolysis of Starch and Side-chain Recovery

The graft copolymer (1.0 g) was accurately weighed and added to 100-ml glacial acetic acid, which was heated to 90-100°C. The sample was stirred for 1 hour. After that, 2 ml of 65% perchloric acid was added dropwise, and the mixture was allowed to continuously stir for 2 minutes. The reaction mixture was immediately poured into cold acetone to precipitate the acrylic acid polymer side chain. The acetone-insoluble polymer was filtered, washed with cold acetone until neutral, and then it was dried in a vacuum oven at 50°C for 24 hours.

### 3.3.1.7 Characterization of Graft Copolymer

#### 3.3.1.7.1 Determination of Percentage Homopolymer

The weights obtained from Section 3.3.1.5 were the weight before and after Soxhlet extraction, which were used for the following calculation. The difference between these two weights was the amount of poly(acrylic acid) polymerized as a by-product.

#### 3.3.1.7.2 Determination of Percentage Add-on

The weights of the side chain polymer and graft copolymer obtained from Section 3.3.1.6 were used to compute the percentage add-on for starch.

#### 3.3.1.7.3 Determination of Percentage Conversion

The experimental procedures described in Sections 3.3.1.5 through 3.3.1.6 were carried out. The weight of grafted polymer along with homopolymer was regarded as the total conversion of acrylic acid monomer.

#### 3.3.1.7.4 Determination of Percentage Grafting Efficiency

The percentage of grafting efficiency was calculated by comparing the weight of grafted polymer to the total weight of grafted and ungrafted polymers obtained from the experimental procedures in Section 3.3.1.5 and 3.3.1.6.

#### 3.3.1.7.5 Determination of Percentage Grafting Ratio

The experimental procedures in Section 3.3.1.6 gave the weights of polymer in the graft copolymer, and the substrate (starch), which were regarded as the percentage grafting ratio.

### **3.3.2 Esterification of Starch-g-polyacrylic acid**

Starch-g-polyacrylic acid (30.0 g) and poly(ethylene glycol) 4000 (PEG 4000, 41.75 g) were allowed to react under nitrogen atmosphere at 70°C in methanol (300 ml) in the presence of p-toluene sulfonic acid (6.67 g) for 8 hours. The reaction was carried out in a 5-necked glass flask equipped with a stirrer, thermometer, nitrogen gas inlet, condenser and column packed with molecular sieve. The starch-g-poly(acrylic acid) was first dispersed in methanol, and then the catalyst, and the PEG 4000 were added respectively. After the time of reaction had elapsed, the reaction mixture was left cool. The mixture was filtered on a suction filter, washed with methanol, and dried at 50°C in a vacuum oven for 24 hours.

#### 3.3.2.1 Acid Hydrolysis for Side-chain Recovery

The accurate weight (1.00g) of esterified starch-g-polyacrylate was added in to 100 ml of 1 N hydrochloric acid. The mixture was stirred and refluxed for 6 hours. The insoluble polymer was filtered, washed with distilled water until neutral, and dried in a vacuum oven.

### **3.3.3 Etherification of Esterified Starch-g-polyacrylate**

A suspension comprising 50 g of the obtained esterified starch-g-polyacrylate from Section 3.3.2, 1.5 g of sodium hydroxide, 4 g of distilled water, 100 g of iso-propanol, and 50 ml of propylene oxide was agitated in a closed vessel at 50°C for 48 hours. After that, the suspension was neutralized with acetic acid and filtered on a suction filter. The product was washed with an excess amount of methanol and dried at 50°C in a vacuum oven for 24 hours. This product was later called the modified starch.

### 3.3.3.1 Spectrophotometric Determination of the Hydroxypropyl Group in the Modified Starch

#### 3.3.3.1.1 Preparation of Calibration Curve

Propylene glycol, 10 ml, was transferred to a 100-ml volumetric flask, diluted with distilled water to a volume of 100 ml. The volumes of 0.0, 0.10, 0.15, 0.20, 0.25 and 0.30 ml of standard solution were transferred to each 100-ml volumetric flask and diluted to the desired volume with distilled water. The solutions for a preparation of calibration curve contained 0.00, 1.04, 1.56, 2.08, 2.60 and 3.12 mg of propylene glycol, respectively. Each solution of 0.5 ml was pipetted to 12.5-ml graduated test tubes. The 4 ml of 83% sulfuric acid was added dropwise to each flask. The solution was mixed well, and placed in a boiling water bath for exactly 3 minutes. After that the tubes were transferred to an ice bath until chilled. A portion of 0.3 ml of 3% ninhydrin in a 5% aqueous sodium bisulfite solution was carefully allowed to run down the wall of the test tubes. The mixtures were immediately shaken well and placed in a 25°C water bath for 100 minutes. After that the volume in each tube was adjusted to 12.5 ml with 83% sulfuric acid and mixed by inverting the tubes several times. They were transferred to a cell and the absorbance at 590 nm was measured. The amount of hydroxypropyl group can be determined by applying the factor 0.7763 to convert micrograms of the glycol to hydroxypropyl group equivalent.

#### 3.3.3.1.2 Measurement of Hydroxypropyl Group Equivalent in the Modified Starch

The accurate weight (0.10 g) of modified starch was put into a 50-ml conical flask. The 25.00 ml. of 1 N sulfuric acid was added. The sample of esterified starch-g-polyacrylate was prepared in the same manner. The flasks were then immersed in a boiling water bath for 1 hour and left cool. Each solution was filtered and the content was diluted to 100 ml with distilled water. A portion of 0.50 ml of each solution was pipetted into 12.5-ml graduated test tube, the experiments were carried out in the same manner for the preparation of a calibration curve.

### 3.3.4 Compounding of Plastic Materials (Blend Preparation)

The low density polyethylene (LDPE) and modified starch was blended in a two-roll mill, of which front roll and back roll temperatures were set at 165 and 175 °C, respectively. The modified starch was dried in a vacuum oven at 50 °C for 24 hours prior to mixing. The LDPE were poured on the rolls and preheated for 5 minutes. The rolls were allowed to rotate while the plastic was melted. The required quantity of the modified starch and EBS wax were hand mixed in a plastic beaker and gradually added into the molten plastic. The blending time was 20 minutes. While blending a brass scrapping knife and a wood scrapper were used for manual mixing in order to increase good homogeneity in all directions. After the compounding, the LDPE/modified starch sheet was removed from the two-roll mill. The composition of each formula was shown in Table 3.3. Sample codes used in this section were selected to explain the meaning:

LDPE : Low density polyethylene contained only 2 g of EBS wax

LDPE/ST1 : LDPE contained starch 1 g and EBS wax 2 g

LDPE/MS1 : LDPE contained modified starch 1 g and EBS wax 2 g.

**Table 3.3** Composition of Starch- and Modified Starch Polyethylene (LDPE) Sheets

Formula	Sample Code	LDPE (g)	Starch (g) (ST)	Modified Starch (g) (MS)	EBS Wax (g)
1	LDPE	100	-	-	2
2	LDPE/ST1	100	1	-	2
3	LDPE/ST5	100	5	-	2
4	LDPE/ST10	100	10	-	2
5	LDPE/ST20	100	20	-	2
6	LDPE/MS1	100	-	1	2
7	LDPE/MS5	100	-	5	2
8	LDPE/MS10	100	-	10	2
9	LDPE/MS20	100	-	20	2

### **3.3.5 Compression Molding**

The obtained modified starch-LDPE sheet was cut into small chips by a crushing machine. Before placing the chips in the mould (150 x 150 x 2.5 mm), it was preheated for 5 minutes. The chips were then placed in a mould and preheated for 5 minutes. The temperature used in this process was set at 170°C. The time for compression was 5 minutes with the pressure of 6895 kN/m<sup>2</sup>. After the time had elapsed, the compressed sheet was removed to the cooling part and cool for 5 minutes with a constant pressure of 6895 kN/m<sup>2</sup>.

### **3.3.6 Mechanical Properties Test**

The sheets obtained from Section 3.3.5 were then cut to fit the standard test method for mechanical properties, tensile strength and elongation, of plastic according to ASTM D638-96 [28]. The test was performed on an Instron mechanical tester (Model 1011). The crosshead speed of 500 mm/min was used. Five specimens were tested for each blend.

### **3.3.7 Hardness Measurement**

The hardness of material was measured using a hardness tester (Model 716). The plastic sheets were pressed for 15 seconds with a weight of 5 kg (Shore D). The median values were used for analysis.

### **3.3.8 Soil Burial Test**

The soil burial test is an outdoor experiment, which provides a realistic environment with seasonal changes, less control of soil wetness and temperature, and in the presence of macro-organisms. The test was carried out from July through September 2000 for 3 months. The plastic sheets were buried at a depth of 7-9 inches, staked of for further ease in relocating samples. After the plastic sheets were removed, their surfaces were then wiped with water. They were then dried at 50°C for 24 hours in a vacuum oven and kept in dark before tensile testing.

### **3.3.9 Water Absorption Test**

The water absorption test was measured using a plastic sheet of 25 x 25 x 25mm dimension according to ASTM D570-98 [29]. The test specimens were first dried in a vacuum oven for 24 hours at 50°C, cooled in a desiccator, and immediately weighed. The conditioned specimens were entirely immersed in a container of distilled water. At a regular time interval, each sample was removed from the water tank, dried by wiping with cloth, and subsequently weighed to determine the water uptake. The samples were placed back in water after each measurement. The water absorption was calculated as the weight difference between the substantially saturated weight and the dry weight.

### **3.3.10 Morphology Property Analysis**

A JSM-6400 scanning electron microscope (SEM, JEOL) was used to observe the morphology of the blends. The polymer blends were fractured in liquid nitrogen and the fractured surfaces were sputter coated with a thin layer of gold before observation.

### **3.3.11 Thermal Property Analysis**

Thermalgravimetry analysis was performed on Perkin Elmer Thermogravimetric analyzer (TGA 7). The sample was heated with a heating rate of 20 °C/min in a nitrogen atmosphere up to 500 and 700 °C. Prior to thermal analysis, the samples were dried in a vacuum oven at 65°C for 24 hours.

### **3.3.12 Contact Angle Measurement**

The contact angle between the water droplets and polymer films of esterified starch-g-polyacrylate, etherified modified starch, EBS wax, and LDPE were measured using the contact angle goniometer (FACE, Japan). The values were later used to calculate for the work of adhesion.

## CHAPTER 4

### RESULTS AND DISCUSSION

#### **4.1 Proof of Grafting by Fourier Transform Infrared Spectroscopy**

In order to prove the graft copolymerization of acrylic acid monomer onto the starch backbone, the mixture of gelatinized starch and acrylic acid monomer after irradiation polymerization was characterized by Fourier transform infrared (FT-IR) spectroscopy, which could be used to demonstrate the changes in graft copolymerization. The Fourier transform infrared spectra of cassava starch, poly(acrylic acid) , the cassava starch-g-poly(acrylic acid) before and after homopolymer extraction with methanol, and starch-g-poly(acrylic acid) after acid hydrolysis of starch with glacial acetic acid are shown in Figures 4.1 through 4.5, respectively. The Fourier transformed infrared vibrations and assignments of spectrum are shown in Table 4.1.

The infrared spectrum of cassava starch in Figure 4.1 manifests the characteristic peak of C-O stretching (C-O-C and C-O-H) at  $1000-1100\text{ cm}^{-1}$ . After grafting of starch with acrylic acid monomer, the three distinguished peaks can be observed, which attributed to the presence of the carboxylic acid group (Figure 4.3) in the graft copolymer. The spectrum in Figure 4.5 is the spectrum of starch-g-poly(acrylic acid) after hydrolysis of starch with perchloric method, resembled the spectrum of poly(acrylic acid) (Figure 4.2). It can be seen that the characteristic peak of starch was drastically decreased and there was a slightly decrease in the peak area of the stretching peak of the O-H group at  $3450\text{ cm}^{-1}$ .

**Table 4.1** Fourier Transform Infrared Vibrations and Assignment for Cassava Starch, Poly(acrylic acid), the Cassava Starch-g-poly(acrylic acid) before and after homopolymer extraction with methanol and Starch-g-poly(acrylic acid) after acid hydrolysis of starch with glacial acetic acid (perchloric method)

Frequency (cm <sup>-1</sup> )	Major IR bands of Components Assignments and Remarks
<b>Starch</b>	
3435(s,br)	O-H Stretching
2933(m)	C-H Stretching
1648(w-m)	O-H Bending
1460(m)	CH <sub>2</sub> Bending
1422,1369(m)	C-H Bending
1019(s,br)	C-O Stretching (C-O-C and C-O-H)
<b>Poly(acrylic acid)</b>	
3100(br)	O-H Stretching of Carboxylic acid
2950(s)	C-H Stretching
1700(s)	C=O Stretching of Carboxylic acid
1450,1425(m)	C-H Bending
1300,1150(m)	C-O Stretching of Carboxylic acid
<b>Starch-g-poly(acrylic acid)(additional peaks)</b>	
3425(w,br)	O-H Stretching of Carboxylic acid
1727(s)	C=O Stretching of Carboxylic acid
1244(m)	C-O Stretching of Carboxylic acid
<b>Grafted poly(acrylic acid)</b>	
3425(br)	O-H Stretching of Carboxylic acid
2963(m)	C-H Stretching
1723(s)	C=O Stretching of Carboxylic acid
1454,1412(m)	C-H Bending
1243, 1168(m)	C-O Stretching

w = weak, m = medium, s = strong, br = broad

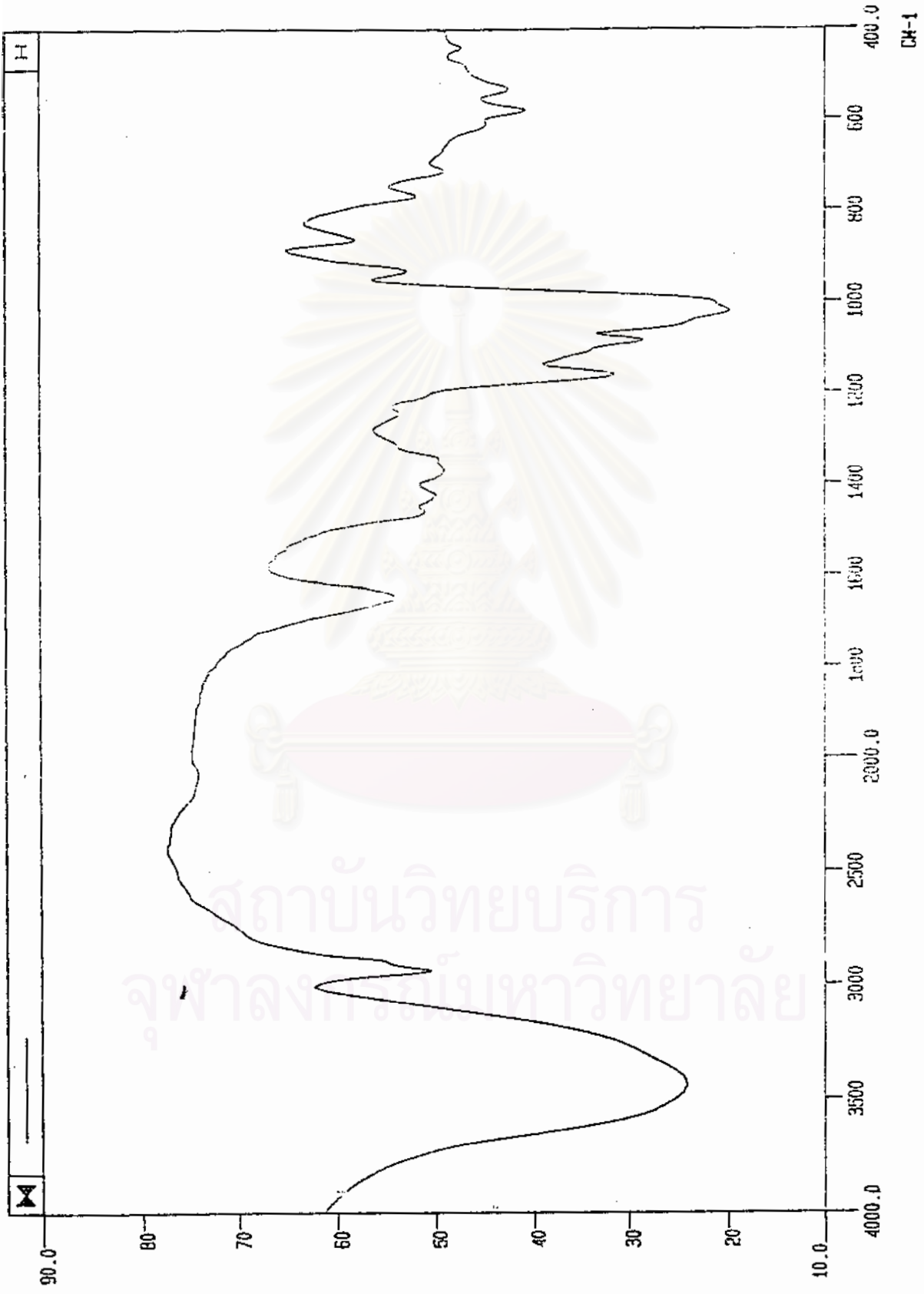


Figure 4.1 Fourier transform infrared spectrum of cassava starch

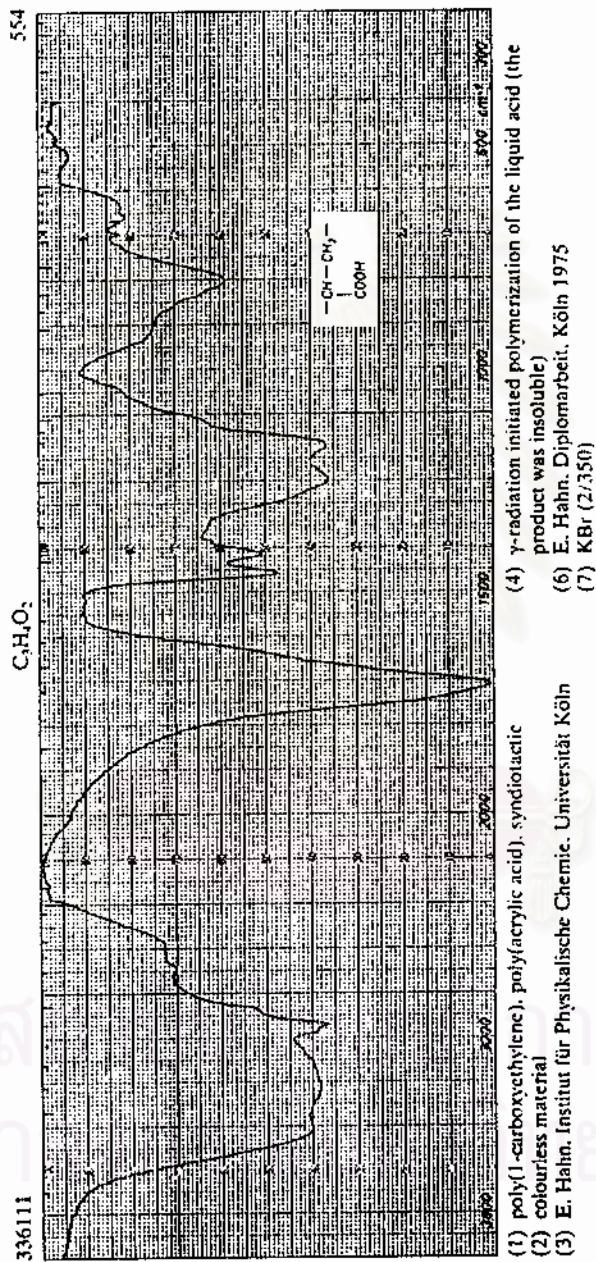


Figure 4.2 Fourier transform infrared spectrum of poly(acrylic acid)



Figure 4.3 Fourier transform infrared spectrum of cassava starch-g-poly(acrylic acid) before homopolymer extraction



**Figure 4.4** Fourier transform infrared spectrum of cassava starch-g-poly(acrylic acid) after homopolymer extraction



Figure 4.5 Fourier transform infrared spectrum of cassava starch-g-poly(acrylic acid) after acid hydrolysis

## **4.2 Graft Copolymerization of Acrylic Acid onto Cassava Starch by Simultaneous Technique**

### **4.2.1 Effects of the Total Dose and the Dose Rate on Graft Copolymerization**

After the gelatinized cassava starch and acrylic acid had been irradiated under the gamma ray irradiator, the obtained product was then characterized by extracting the homopolymer with methanol in a Soxhlet extractor and subsequently splitting the anhydroglucose unit by Dennenberg and Abbott's method. The characterization of graft copolymer is presented in the terms of %homopolymer, %add-on, %conversion, %grafting efficiency, and %grafting ratio as shown in Table 4.2

**Table 4.2** Effects of the Total Dose and the Dose Rate on the Graft Copolymerization

<b>Dose Rate</b>	<b>Total Dose</b>	<b>HM(%)</b>	<b>AO(%)</b>	<b>CV(%)</b>	<b>GE(%)</b>	<b>GR(%)</b>
2	2	4.8±0.2	8.8±0.4	14.1±0.8	63.7±0.2	9.6±0.2
	4	4.3±0.2	10.1±0.4	15.5±0.6	69.2±0.6	11.2±0.2
	6	5.4±0.3	13.3±0.4	18.4±0.6	69.8±0.5	15.3±0.4
	8	2.2±0.1	15.8±0.2	21.4±0.5	87.8±0.4	18.8±0.6
	10	5.7±0.2	21.8±0.9	36.2±1.0	78.3±0.3	27.9±1.0
	12	5.6±0.3	34.7±0.8	58.8±0.7	85.5±0.7	53.2±1.5
5	2	9.8±0.3	1.8±0.2	12.9±1.2	14.5±0.8	1.9±0.1
	4	9.2±0.3	3.4±0.2	14.25±0.8	25.4±1.7	3.6±0.2
	6	7.1±0.4	6.2±0.4	15.34±1.1	44.8±1.8	6.6±0.2
	8	6.2±0.5	10.7±0.6	19.3±1.3	62.0±0.8	12.0±0.8
	10	1.8±0.1	19.5±0.5	25.13±0.9	91.5±0.9	24.2±0.7
	12	4.7±0.2	22.5±0.8	29.1±1.3	82.1±1.0	33.5±1.0

**HM** = homopolymer, **AO** = add-on, **CV** = conversion, **GE** = grafting efficiency, **GR** = grafting ratio

**Total Dose Unit:** kGy

**Dose Rate Unit:** kGy h<sup>-1</sup>

**Table 4.2** Effect of Total Dose and Dose Rate on Graft Copolymerization(Continued)

Dose Rate	Total Dose	HM(%)	AO(%)	CV(%)	GE(%)	GR(%)
12	2	9.1±0.5	1.3±0.2	11.1±0.8	11.6±0.8	1.3±0.1
	4	10.6±0.8	1.4±0.1	13.2±0.6	10.2±0.3	1.4±0.2
	6	13.2±0.4	2.4±0.3	17.8±0.5	13.3±0.9	2.4±0.3
	8	7.6±0.4	9.0±0.8	18.7±0.7	52.2±1.5	9.9±0.8
	10	7.9±0.3	10.1±0.6	20.2±1.2	53.9±2.0	11.2±1.2
	12	8.0±0.4	13.0±0.3	24.0±0.9	58.4±1.6	15.0±1.0

**HM** = homopolymer, **AO** = add-on, **CV** = conversion, **GE** = grafting efficiency, **GR** = grafting ratio

**Total Dose Unit:** kGy

**Dose Rate Unit:** kGy h<sup>-1</sup>

#### 4.2.1.1 Relationship between Total Dose and Dose Rate and %homopolymer

A direct grafting method is the radiation of a polymeric substrate in the presence of a monomer. It should bear in mind that the ionizing radiation is unselective, therefore not only the effect of radiation on polymeric substrate but also the effect on the monomer, the solvent, or any substance is presence in the system. So the homopolymer could be produced. The production of homopolymer may arise from initiation by small radicals and also radiolysis of monomer and the continuous phase.

From Table 4.2 and Figure 4.6, it was found that at a dose rate of 2 kGy h<sup>-1</sup>, the percentage of homopolymer varied from 2.1 to 5.6% depending on the total dose. The lowest homopolymer formation occurred at the total dose of 8 kGy and the homopolymer content increased at total dose higher than 8 kGy. At the dose rate of 5 kGy h<sup>-1</sup>, the range of the percentage of homopolymer is 1.8-9.8%. The lowest

percentage of homopolymer was obtained at the total dose of 10 kGy. At the dose rate of 12 kGy h<sup>-1</sup>, the percentage of homopolymer increased from 7.6 to 13.2%. The highest value is found at the total dose of 6 kGy.

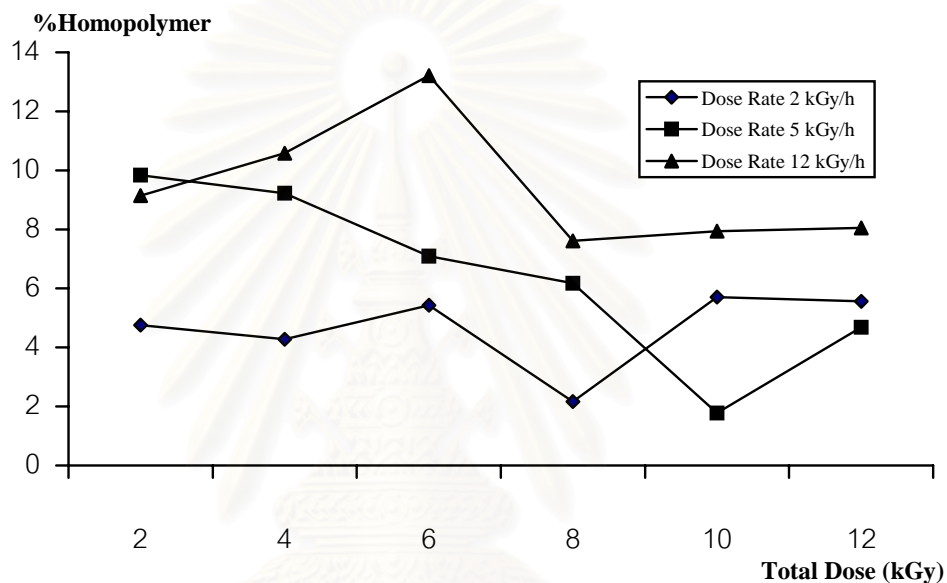


**Figure 4.6** Effects of the total dose and the dose rate on %homopolymer

It can be observed that the higher the dose rate, the more homopolymer was polymerized. This result may be explained as that at the higher dose rate the numbers of radicals were produced in a larger amount than those at the lower ones. Therefore, a great number of growing chains are generated and consequently they will be rapidly terminated.

#### 4.2.1.2 Effects of the Total Dose and the Dose Rate on %add-on

The effects of the dose rate and the total dose on %add-on are tabulated in Table 4.2 and illustrated in Figure 4.7. It can be seen that the highest %add-on was obtained at the dose rate of 2 kGy h<sup>-1</sup>. The percentage of add-on at this dose rate varied from 8.8 to 34.7, the highest value was at the total dose of 12 kGy. At the dose rate 5 kGy h<sup>-1</sup>, the percentage of add-on was in the range of 1.8-22.5. The percentage of add-on ranging from 1.3 to 13.0 was obtained at dose rate of 12 kGy h<sup>-1</sup>. It can be concluded that at the same dose rate, the increasing in total dose leads to the increase in the amount of grafted polymer on the starch backbone or it can be said that the higher the total dose, the more the grafting sites on starch backbone. The contrary effect is observed when the same total dose is considered: the grafted poly(acrylic acid) on the starch backbone increases with the decrease dose rate. The reason is the same as mention in Section 4.2.1.2.

Although G values of starch substrate (10.0) and acrylic acid monomer (9.6-12.0) are not significantly different. So one anticipates that the formation of homopolymer and grafted polymer should be equal. The experimental results did not support this concept. It can be concluded that graft copolymerization took place more than homopolymerization or it can be said that there were more radicals generated on the starch backbone than on acrylic acid monomer. This phenomenon is called a protective effect, which may occur, because the G value of an irradiated system is sometimes markedly altered by the presence of another species [31].

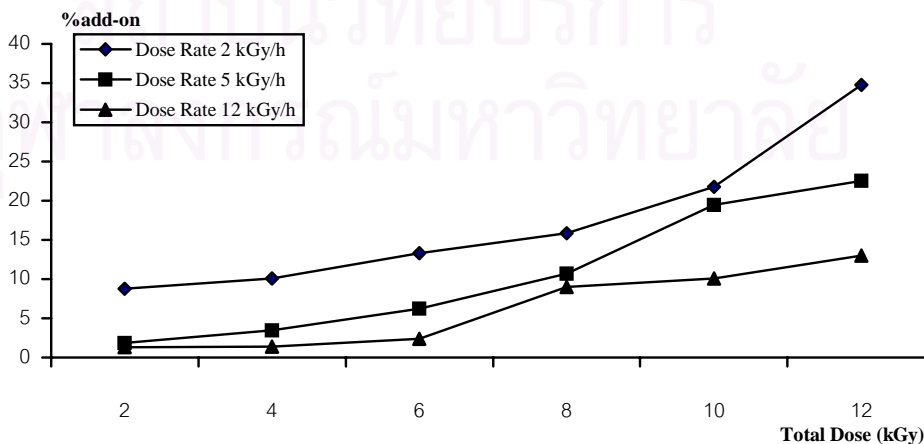


**Figure 4.7** Effects of the total dose and the dose rate on %add-on

#### 4.2.1.3 Relationship between the Total Dose and the Dose Rate on %conversion

The relationship between the total dose and the dose rate on %conversion is presented in Table 4.2 and Figure 4.8. It was found that the percentage of conversion increased with the increasing total dose and with the decreasing dose rate. Increase in the total dose enhances the formation of radicals in the reaction mixture: monomer, starch and water, which are later used to convert acrylic acid monomer to poly(acrylic acid) (homopolymer) and grafted poly(acrylic acid) (grafted polymer). When the same total dose is used the percentage of conversion decreased, when the dose rate increased. This may be presumably due to the life-time of radicals generated.

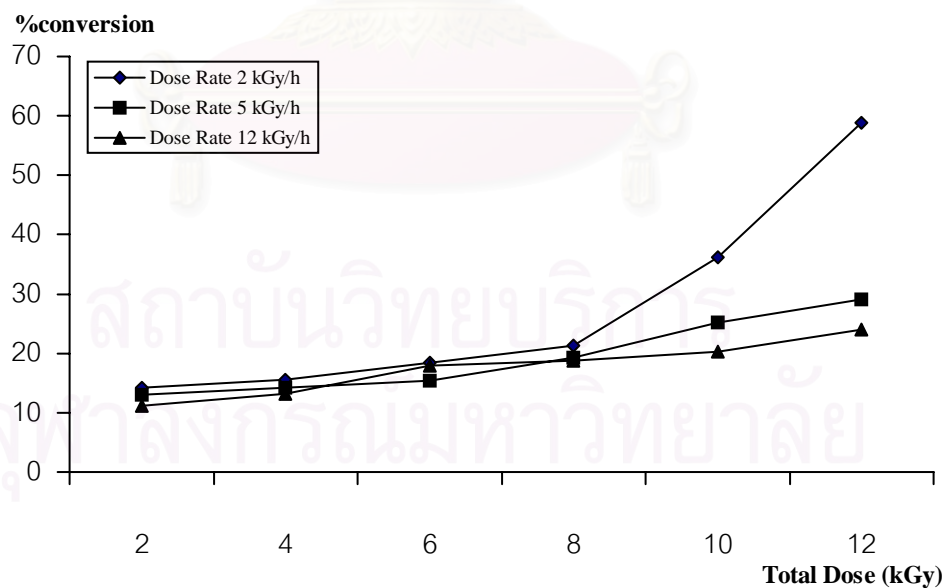


**Figure 4.8** Effects of the total dose and the dose rate on %conversion

#### 4.2.1.4 Relationship between the Total Dose and the Dose Rate on %grafting efficiency

The experimental data showing the effects of the total dose and the dose rate on percentage of grafting efficiency are given Table 4.2 and Figure 4.9. The percentage of grafting efficiency at the dose rate of 2, 5, and 12 kGy h<sup>-1</sup> were in the range of 63.7 to 87.8%, 14.5 to 91.5% and 10.8 to 58.4%, respectively. The same reason described in Section 4.2.1.2 is considered, when the total dose and dose rate increased, the grafting sites were increased, more monomer was used to form the grafted polymer. Nevertheless, small fragments of H<sup>•</sup>, OH<sup>•</sup>, and e<sub>aq</sub><sup>-</sup> still can initiate homopolymer at the expense of grafted polymer.

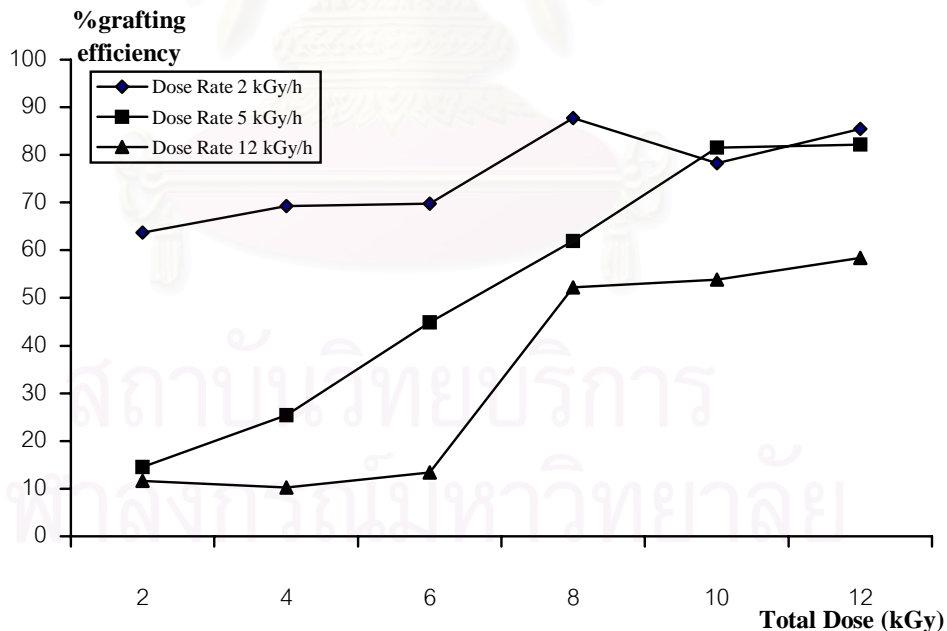


**Figure 4.9** Effects of the total dose and the dose rate on %grafting efficiency

#### 4.2.1.5 Relationship between the Total Dose and the Dose Rate on %grafting ratio

The data given in Table 4.2 and the curves Figure 4.10 present the correlation between the dose rate and the total dose on the percentage of grafting ratio. The results show that the ratio of the weights of grafted polymer to starch increases with increasing both the dose rate and the total dose. At the dose rate of 12 kGy h<sup>-1</sup>, the major composition in graft copolymer was starch and it was replaced with grafted poly(acrylic acid) when lower dose rates were utilized. The same reason mentioned in Section 4.2.1.1 is considered, that is the higher dose rate leads to the higher amount of radicals, which rapidly terminate than graft.

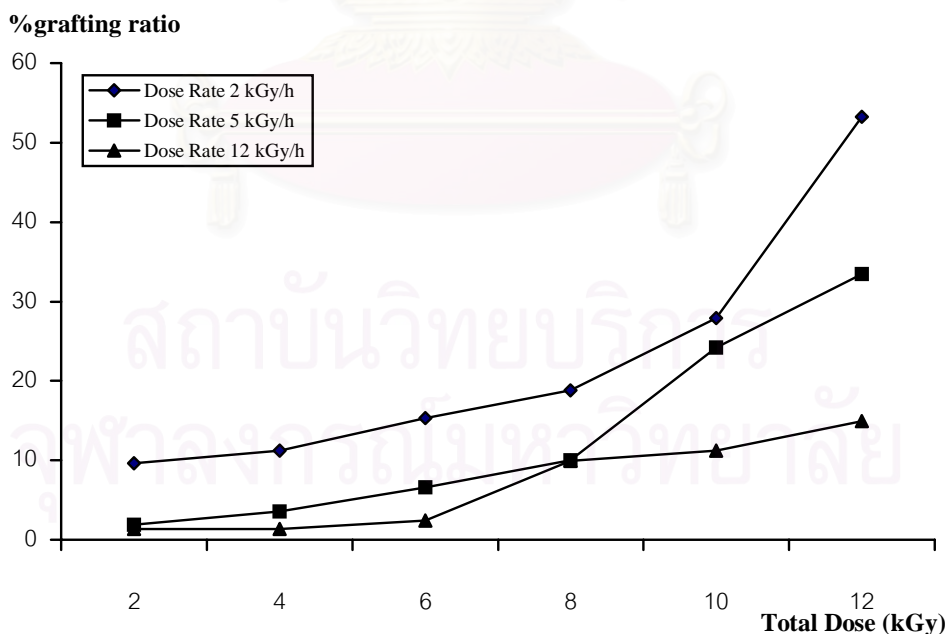


**Figure 4.10** Effects of the total dose and the dose rate on %grafting ratio

#### 4.2.2 Effect of the Acrylic acid-to-Cassava Starch Ratio on Graft Copolymerization at the Dose Rate of 2 kGy h<sup>-1</sup> and the Total Dose of 10 and 12 kGy

In this part, we studied 5 levels of acrylic acid and cassava starch ratios, which were 0.5, 1.0, 1.5, 2.0, and 5.0 g g<sup>-1</sup> at both the total dose of 10 and 12 kGy. After the radiation exposure, the reaction mixture was characterized in the terms of % homopolymer, % add-on, % conversion, % grafting efficiency, and % grafting ratio. All of these results are presented in Table 4.3

**Table 4.3** Effects of Acrylic acid-to-Cassava Starch Ratio on the Graft Copolymerization at the Dose Rate of 2 kGy h<sup>-1</sup> and the Total Dose of 10 and 12 kGy

Total Dose	Ratio	HM(%)	AO(%)	CV(%)	GE(%)	GR(%)
10	0.5	2.5±0.2	3.2±0.2	12.4±0.7	55.6±0.5	3.3±0.2
	1.0	5.7±0.4	22.0±0.8	36.9±0.4	73.4±3.3	28.1±0.8
	1.5	3.5±0.3	51.2±0.8	68.6±0.7	93.3±1.2	105.0±1.4
	2.0	3.0±0.3	61.4±1.0	86.8±0.9	95.2±1.0	159.0±0.9
	5.0	1.0±0.2	88.9±0.9	98.2±1.5	98.9±2.0	803.6±3.8
12	0.5	2.6±0.2	7.2±0.30	21.0±0.9	73.0±0.7	7.9±0.3
	1.0	5.6±0.5	34.7±0.6	58.8±1.0	85.5±1.1	53.2±0.9
	1.5	2.7±0.3	52.6±0.9	70.2±2.2	95.0±0.8	110.9±1.5
	2.0	1.3±0.1	54.4±0.9	81.5±1.7	97.6±0.9	119.1±1.2
	5.0	2.5±0.3	87.3±1.0	97.9±1.8	97.1±1.6	630.7±2.5

**HM** = homopolymer, **AO** = add-on, **CV** = conversion, **GE** = grafting efficiency, **GR** = grafting ratio

**Total Dose Unit:** kGy

**Ratio:** acrylic acid to starch ratio (g g<sup>-1</sup>)

4.2.2.1 Relationship between Acrylic Acid-to-Cassava Starch Ratio on Graft Copolymerization at the Dose Rate of 2 kGy h<sup>-1</sup> and the Total Dose of 10 and 12 kGy

a) Homopolymer

The curve illustrated in Figure 4.10 and the experimental data shown in Table 4.3 demonstrate the effect of acrylic acid-to-starch ratio on graft copolymerization at the dose rate of 2 kGy h<sup>-1</sup> and the total dose of 10 and 12 kGy in the terms of %homopolymer. At the total dose of 10 kGy, the percentage of homopolymer increased to the highest value of 5.7% at the ratio of 1.0 and they became decreased when the ratio was higher. The similar result is also found at the total dose of 12 kGy. However, at the ratio of 5.0 the percentage of homopolymer tended to increase. It can be found that the higher the total dose, the lower the homopolymer formation. Because the higher total dose leads to the more grafting sites [31].

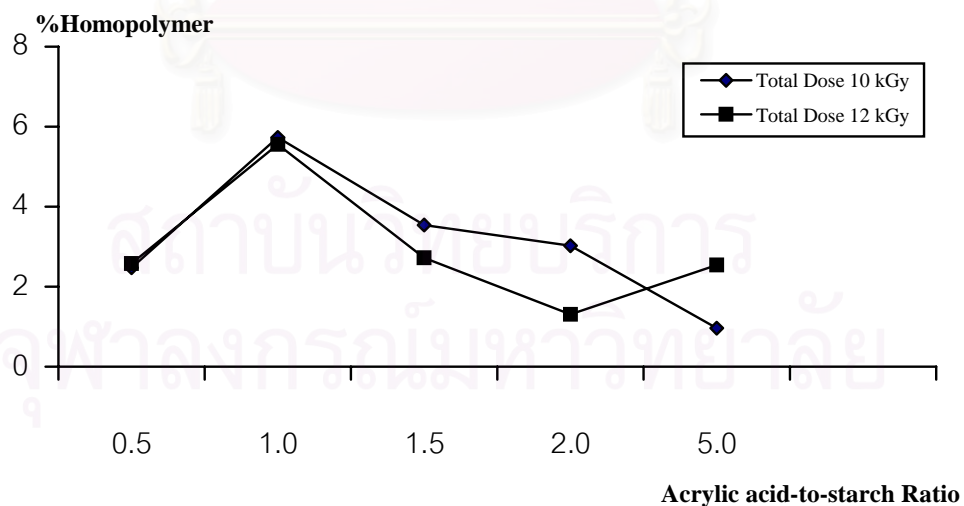


**Figure 4.11** Effect of acrylic acid-to-cassava starch ratio on the graft copolymerization at the dose rate of 2 kGy h<sup>-1</sup> and the total dose of 10 and 12 kGy in terms of %homopolymer

4.2.2.2 Relationship between Acrylic acid-to-Cassava Starch Ratio on Graft Copolymerization at the Dose Rate of 2 kGy h<sup>-1</sup> and the Total Dose of 10 and 12 kGy

b) Add-on

The percentage of add-on of acrylic acid onto gelatinized cassava starch is plotted between acrylic acid-to-starch ratio as shown in Figure 4.11. It can be seen from Table 4.3 as well as Figure 4.11 that the percentages of add-on at the total dose of 10 kGy were in the range of 3.2-88.9% and at total dose of 12 kGy its range were 7.2-86.3%. It can be concluded that the percentage of add-on increased with increasing acrylic acid monomer. This is presumably due to the fact that increased in monomer enhanced the monomer accessibility. Moreover, gel effect may occur in the viscous system, leading to graft copolymerization or increasing in the percentage of add-on.

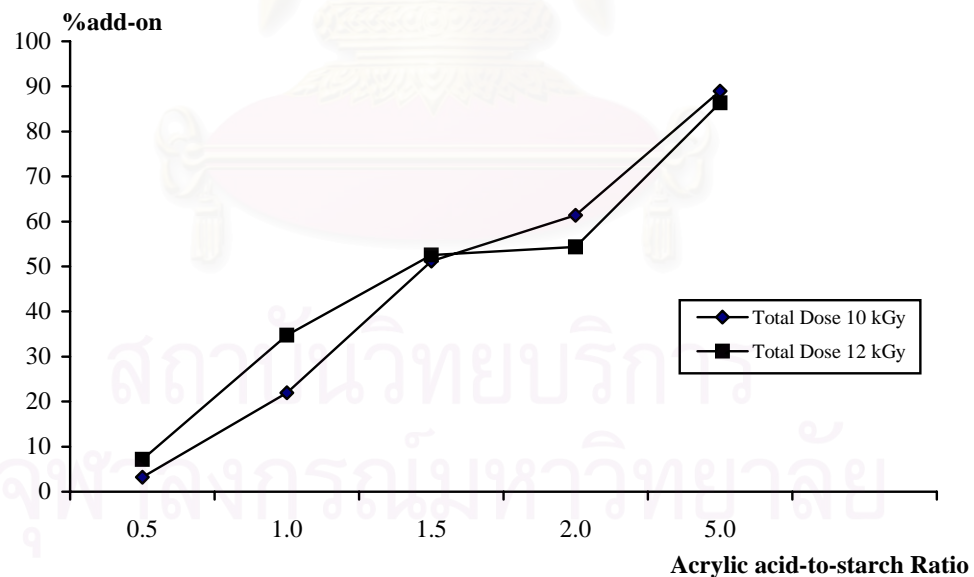


**Figure 4.12** Effect of acrylic acid-to-cassava starch ratio on the graft copolymerization at the dose rate of 2 kGy h<sup>-1</sup> and the total dose of 10 and 12 kGy in the terms of %add-on

4.2.2.3 Relationship between Acrylic acid-to-Cassava Starch Ratio on Graft Copolymerization at the Dose Rate of 2 kGy h<sup>-1</sup> and the Total Dose of 10 and 12 kGy

c) Conversion

It can be seen from Table 4.3 and Figure 4.12 that the percentage of conversion significantly increased and generally approached 100%. At higher amounts of acrylic acid (higher ratio), there were plenty of acrylic acid, which could diffuse to the active sites on the starch backbone to form graft copolymers. Under radiolysis, free radicals of acrylic acid were formed, which later generated their homopolymers. Moreover, at the higher concentration of acrylic acid monomer, gel effect may take place and accelerates graft copolymerization and also homopolymerization to give a higher conversion.

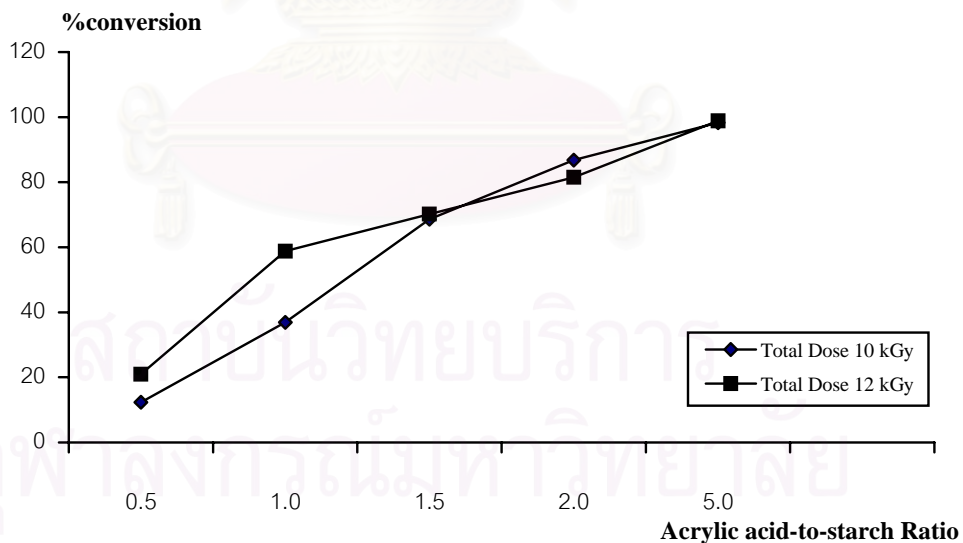


**Figure 4.13** Effect of acrylic acid-to-cassava starch ratio on the graft copolymerization at the dose rate of 2 kGy h<sup>-1</sup> and the total dose of 10 and 12 kGy in the terms of %conversion

4.2.2.4 Relationship between Acrylic acid-to-Cassava Starch Ratio on Graft Copolymerization at the Dose Rate of 2 kGy h<sup>-1</sup> and the Total Dose of 10 and 12 kGy

d) Grafting efficiency

From Table 4.3 and Figure 4.13, it can be seen that at the total dose of 10 kGy, the percentage of grafting efficiency increased from 55.6 to 98.9%, and at the total dose of 12 kGy, it increased from 73.0 to 97.6%. It can be observed that the percentage of grafting efficiency increased with increasing monomer-to-starch ratio. This result suggested that the higher concentration of acrylic acid could diffuse to reach the active sites on starch polymer. Gel effect could be the main reason to reduce the termination reaction. Therefore, %grafting efficiency was markedly increased.

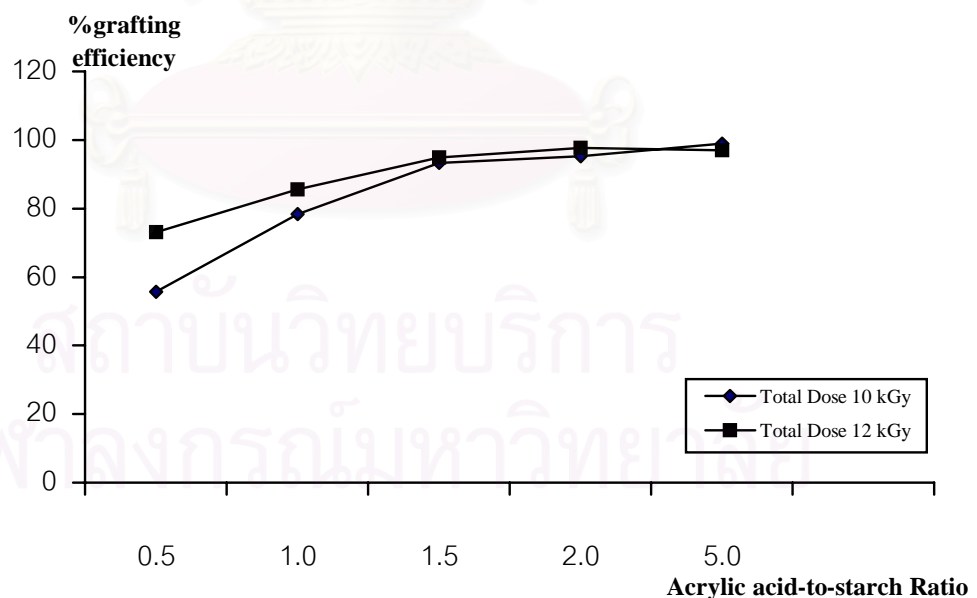


**Figure 4.14** Effect of acrylic acid-to-cassava starch ratio on the graft copolymerization at the dose rate of 2 kGy h<sup>-1</sup> and the total dose of 10 and 12 kGy in the terms of %grafting efficiency

4.2.2.5 Relationship between Acrylic acid-to-Cassava Starch Ratio on the Graft Copolymerization at the Dose Rate of 2 kGy h<sup>-1</sup> and the Total Dose of 10 and 12 kGy

e) Grafting ratio

The effect of the amount of acrylic acid-to-starch ratio on grafting ratio is shown in Table 4.5 and Figure 4.14. It indicates that the % grafted poly(acrylic acid) increases straightly when more acrylic acid is added. This is caused by the gel effect described in Section (d).

It can be seen that the increased acrylic acid-to-starch ratio leads to the increased percentage of grafting ratio. The maximum value was 803.6% when the ratio and the total dose were 5.0 g g<sup>-1</sup> and 12 kGy, respectively. That means the obtained graft copolymer contained poly(acrylic acid) 8 times of starch or the graft copolymer contained mainly poly(acrylic acid).

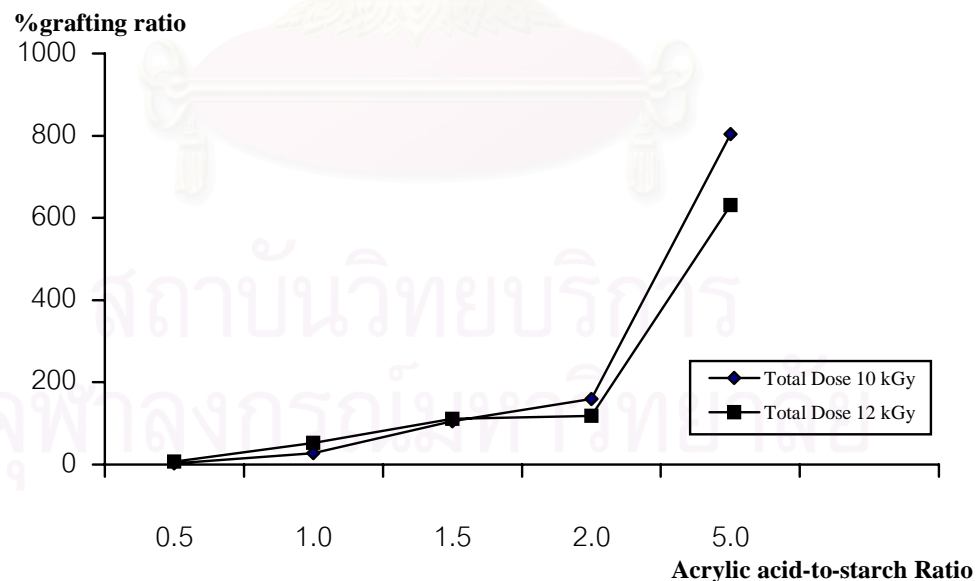


**Figure 4.15** Effect of acrylic acid-to-cassava starch ratio on the graft copolymerization at the dose rate of 2 kGy h<sup>-1</sup> and the total dose of 10 and 12 kGy in terms of % grafting ratio

### **4.3 Esterification of Starch-g-poly(acrylic acid)**

The obtained starch-g-poly(acrylic acid) is a hydrophilic graft copolymer because of the presence of carboxylic and hydroxyl groups, leading to poor adhesion with synthetic polymers. Thus, the addition of this graft copolymer to low-density polyethylene, leads to the reduction in mechanical properties. Therefore, to enhance the compatibility between two immiscible polymers, the hydrophilicity of the above mentioned functional groups should be modified. This part is the step of the carboxylic acid group modification by reacting with the hydroxyl group of poly(ethylene glycol) 4000 (PEG4000) to form the ester linkage. Starch-g-polyacrylic acid used in this section obtained from the irradiation graft copolymerization using dose rate of  $2 \text{ kGy h}^{-1}$  and the total dose of 10 kGy. The acrylic acid-to-starch ratio was 1:1. The characterization of this graft copolymer is presented in Table 4.4.

**Table 4.4** Characterization of Starch-g-poly(acrylic acid) for Esterification

<b>Characterization</b>	<b>Value</b>
%homopolymer	$2.7 \pm 0.2$
%add-on	$24.9 \pm 1.0$
%conversion	$40.0 \pm 0.8$
%grafting efficiency	$90.0 \pm 0.2$
%grafting ratio	$33.2 \pm 1.8$

Dose rate  $2 \text{ kGy h}^{-1}$ , Total dose 10 kGy, Starch-to-acrylic acid ratio = 1:1

### 4.3.1 Characterization of Esterified Starch-g-polyacrylate

After esterification, the appearance of starch-g-poly(acrylic acid) was changed from the previous characteristics, which were the rigid, non-sticky, and clearly white powder to the non-rigid, sticky, and opaque-white powder.

#### 4.3.1.1 Characterization by Fourier Transform Infrared Spectroscopy

The evidence of esterification was verified by utilizing Fourier transform infrared spectroscopy. From Figures 4.4 and 4.16 it can be stated that the carbonyl of carboxylic acid groups was converted to the carbonyl of ester groups. There is a shift of the peak at  $1727\text{ cm}^{-1}$ , which is attributed to carbonyl of the carboxylic acid, to the peak at  $1738\text{ cm}^{-1}$ , which is attributed to the carbonyl of ester group. The standardization of the FT-IR spectrophotometry was done using the polystyrene (PS) film as a standardized sample. The characteristic peak of the aromatic C=O stretching is  $1602\text{ cm}^{-1}$ , as depicted in Figure 4.17.

#### 4.3.1.2 Characterization by $^{13}\text{C}$ - and $^1\text{H}$ - NMR Spectrometry

The solid state  $^{13}\text{C}$ -NMR spectra of starch-g-poly(acrylic acid) and esterified starch-g-polyacrylate are shown in Figures 4.18 and 4.19, respectively. The peak assignments of  $^{13}\text{C}$ - NMR spectrum are listed in Table 4.5. It can be seen that there is a shift of the carbonyl carbon from 177.9 ppm to 175.6 ppm, which also indicates the conversion of carboxylic acid groups into ester groups. The  $^1\text{H}$ -NMR spectra of cassava starch, side chains of starch-g-polyacrylic acid and esterified starch-g-

polyacrylate are shown in Figures 4.20-4.22, respectively. The peak assignments of  $^1\text{H-NMR}$  spectrum are tabulated in Table 4.6. The side chains of starch-g-poly(acrylic acid) and esterified starch-g-polyacrylate were obtained by acid hydrolysis with 1 N hydrochloric acid for 6 hours. In Figures 4.21 and 4.22, it can be observed that the peaks at 5.2-5.6 ppm of equatorial protons of starch were disappeared. The chemical shift of 3.4-3.8 ppm in Figure 4.22 demonstrates the presence of poly(ethylene glycol) 4000 at the side chain of esterified starch-g-polyacrylate.

**Table 4.5** Peak Assignments of solid state  $^{13}\text{C-NMR}$  Spectra of Starch-g-poly(acrylic acid) and Esterified Starch-g-polyacrylate

Chemical Shift (ppm)	Assignments
<b>Starch-g-poly(acrylic acid)</b>	
41	Carbon of methylene group
61, 72, 82, 102	Carbon of anhydroglucose unit of starch
178	Carbon of carbonyl of poly(acrylic acid)
<b>Esterified starch-g-polyacrylate</b>	
42	Carbon of methylene group
52	Carbon of -C-O- on PEG 4000 chains
61, 72, 82, 103	Carbon of anhydroglucose unit of starch
175	Carbon of carbonyl of poly(acrylic acid)

**Remark :** Frequency 75.5 MHz

**Table 4.6** Peak Assignments of  $^1\text{H}$ -NMR Spectra of Cassava Starch, Starch-*g*-poly(acrylic acid) and Esterified Starch-*g*-polyacrylate

Chemical Shift (ppm)	Assignments
<b>Cassava starch</b>	
3.3-4.2	Protons of anhydroglucose unit of starch
4.6-4.9	Protons of water
5.2-5.6	Equatorial protons of anhydroglucose unit of starch
<b>Side chain of starch-<i>g</i>-poly(acrylic acid)</b>	
1.5	Protons of methylene groups
4.3	Protons of methyl groups, which carbon atom bonded with oxygen atom
7.2	Protons of chloroform
<b>Side chain of esterified starch-<i>g</i>-polyacrylate</b>	
1.1-2.8	Protons of methylene groups
3.4-3.8	Protons of PEG 4000
7.2-7.3	Protons of chloroform

**Remark:** Frequency 50.0 MHz

Cassava Starch in  $\text{D}_2\text{O}$

Side chain of starch-*g*-poly(acrylic acid) in  $\text{CDCl}_3$

Side chain of esterified starch-*g*-polyacrylate in  $\text{CDCl}_3$

### 4.3.2 Determination of Poly(ethylene glycol) 4000 on the Esterified Cassava Starch-g-polyacrylate by Gravimetric Method

After the esterification of cassava starch-g-poly(acrylic acid) with poly(ethylene glycol) 4000 (PEG 4000) to give the esterified cassava starch-g-polyacrylate, the amount of poly(ethylene glycol) 4000 (PEG 4000) on the cassava starch-g-polyacrylate was determined by gravimetric method of acid hydrolysis. The difference between the percentage add-on of the cassava starch-g-poly(acrylic acid) and the esterified cassava starch-g-polyacrylate after acid hydrolysis is counted as the amount of poly(ethylene glycol) 4000 (PEG 4000) on the esterified cassava starch-g-polyacrylate. The percentage add-on of the esterified cassava starch-g-polyacrylate was found  $40.1 \pm 0.8\%$ , while that of cassava starch-g-poly(acrylic acid) was  $24.9 \pm 1.0\%$ . Therefore, the amount of poly(ethylene glycol) 4000 (PEG 4000) was  $15.2 \pm 1.8\%$ .

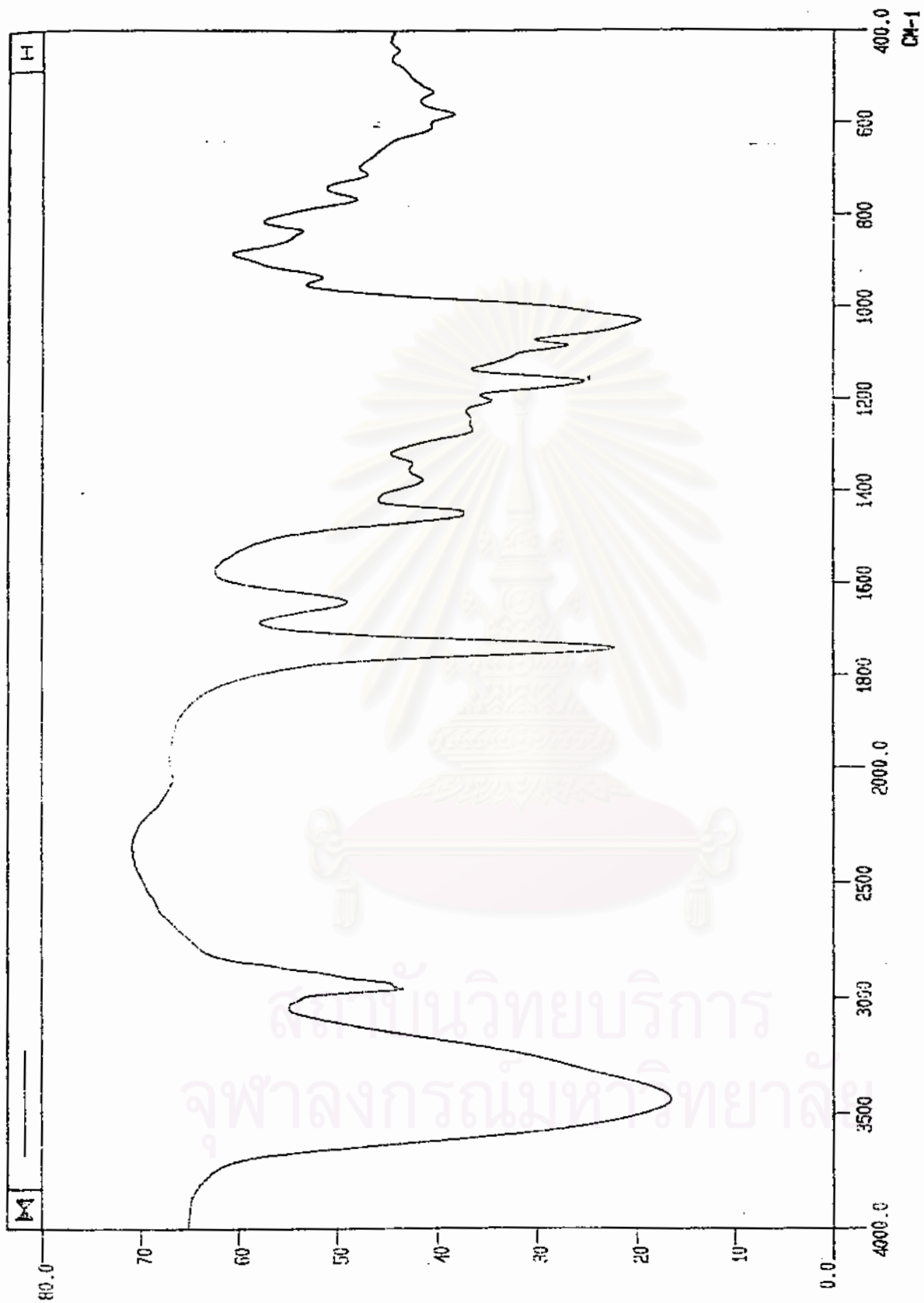


Figure 4.16 Fourier transform infrared spectrum of esterified starch-g-polyacrylate

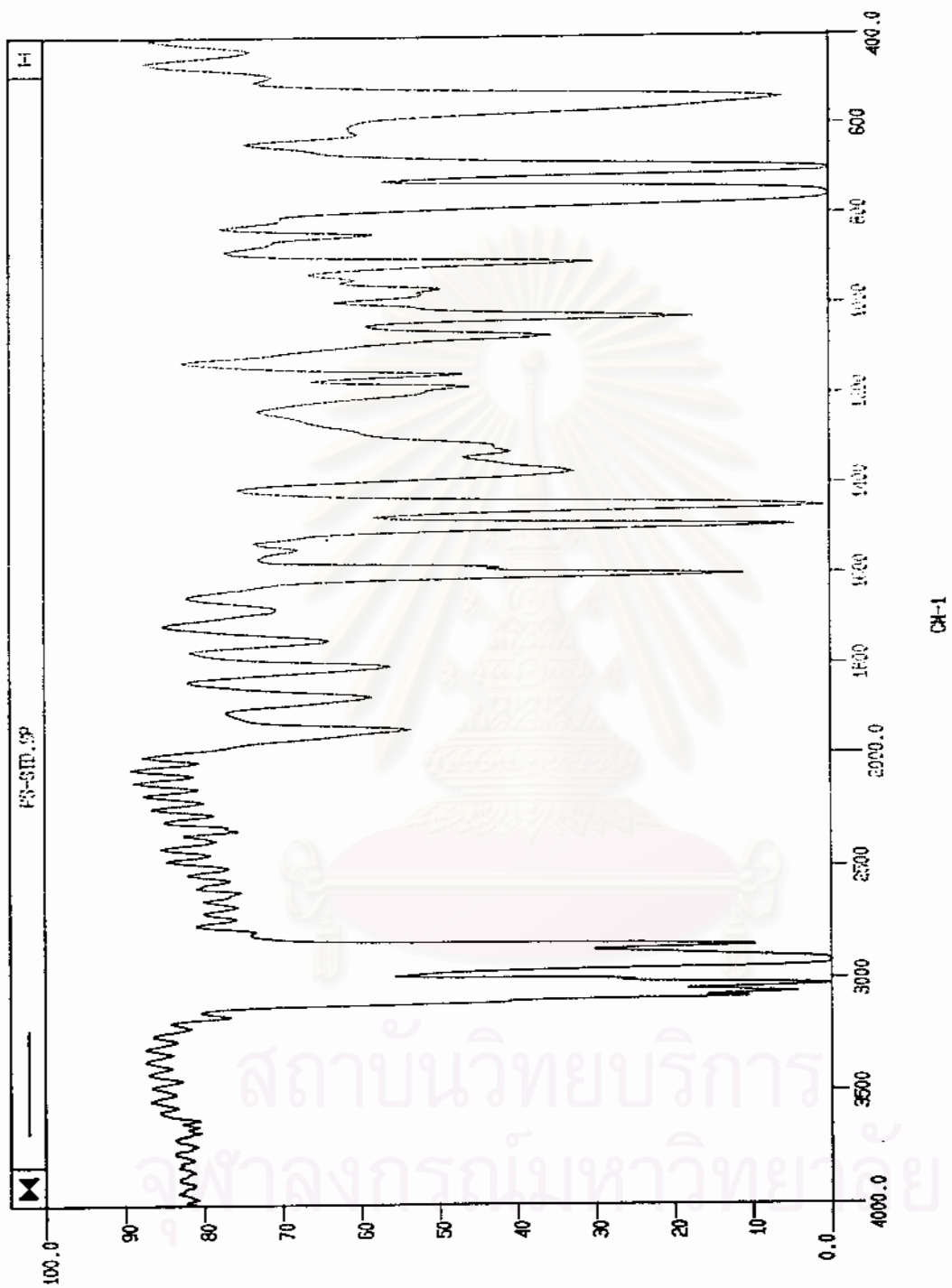


Figure 4.17 Fourier transform infrared spectrum of standard polystyrene film

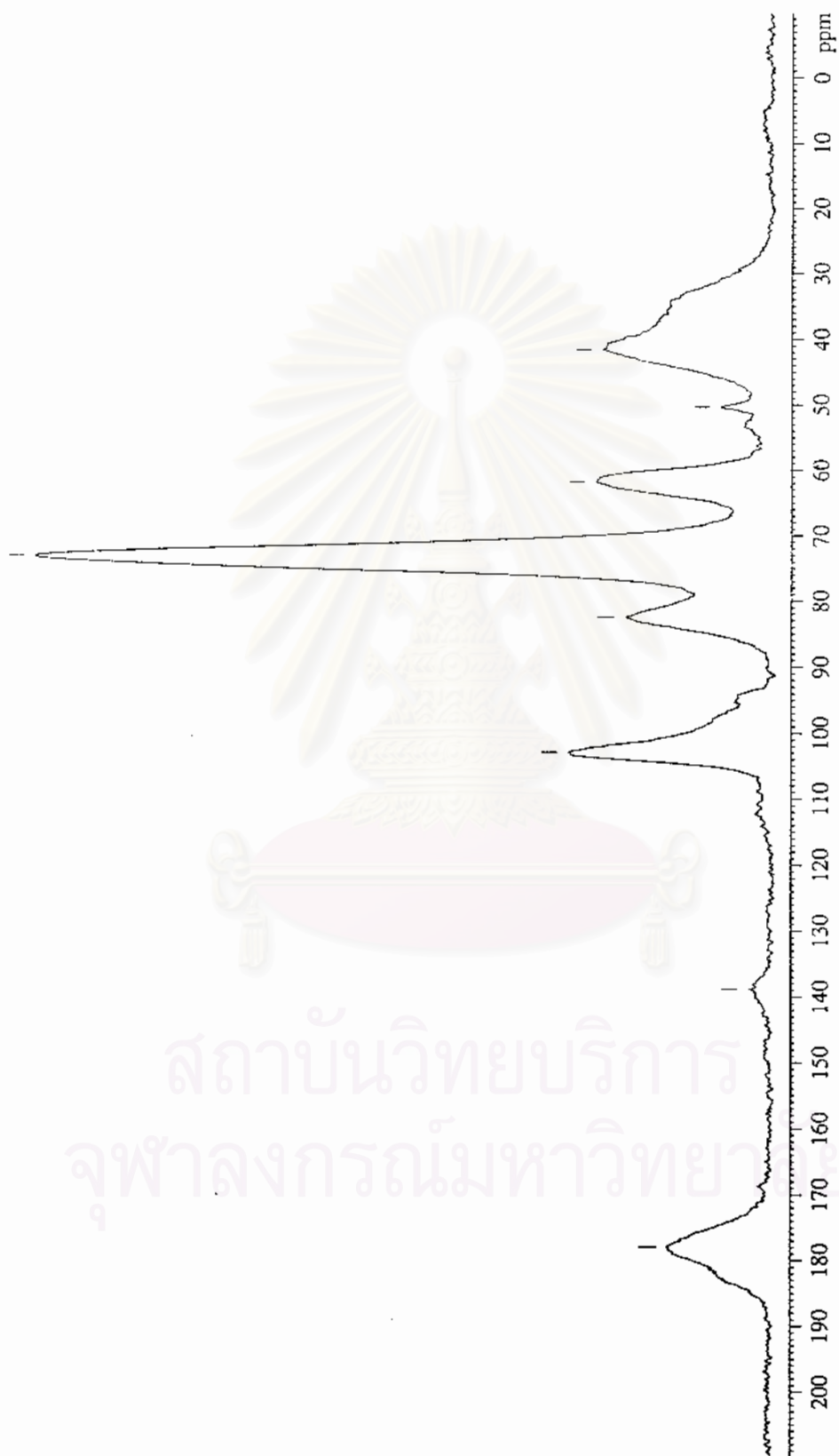


Figure 4.18  $^{13}\text{C}$ -NMR spectrum of starch-g-poly(acrylic acid)



Figure 4.19  $^{13}\text{C}$ -NMR spectrum of starch-g-polyacrylate

สถาบันวิทยบริการ  
จุฬาลงกรณ์มหาวิทยาลัย

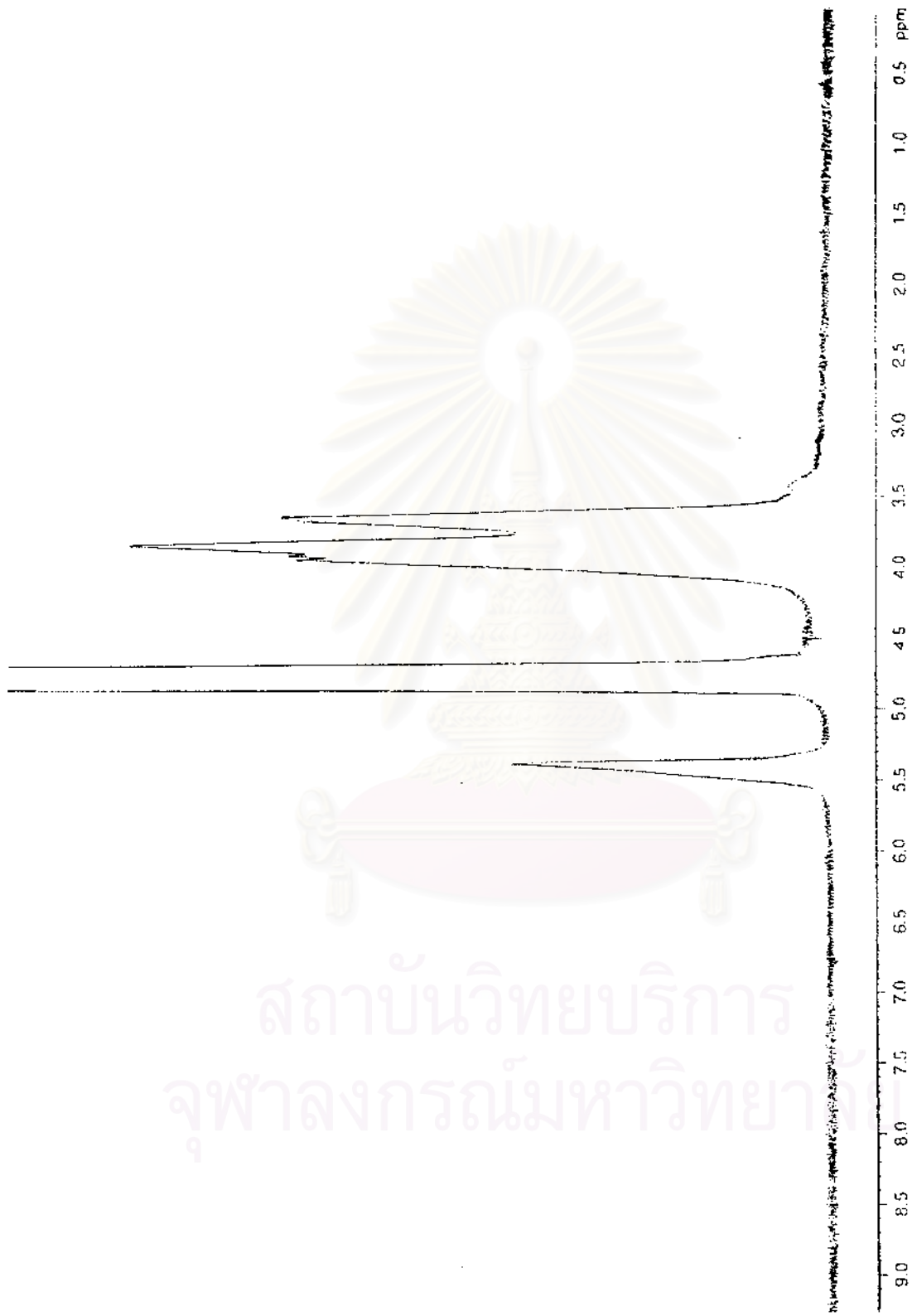


Figure 4.20  $^1\text{H-NMR}$  spectrum of cassava starch

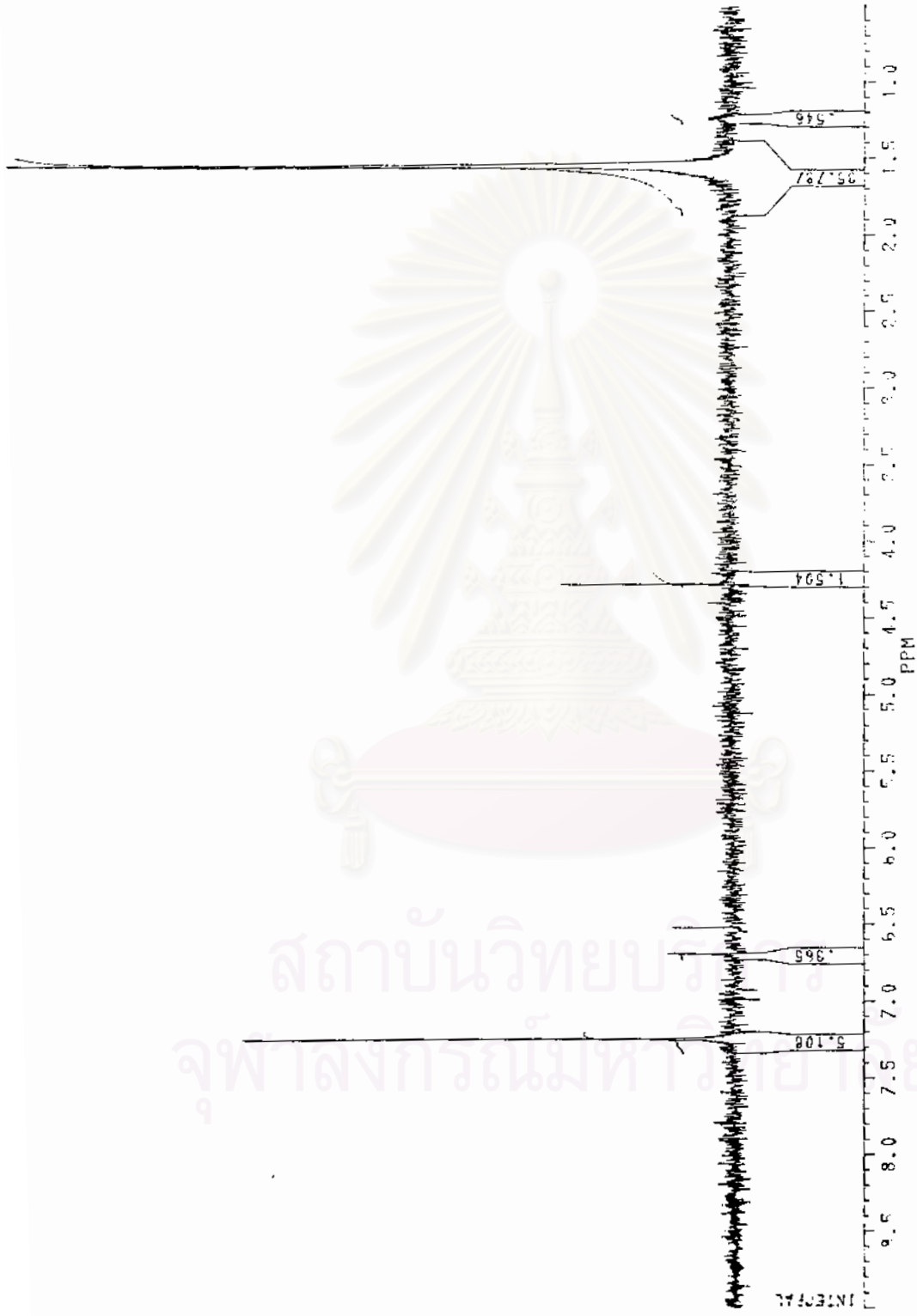
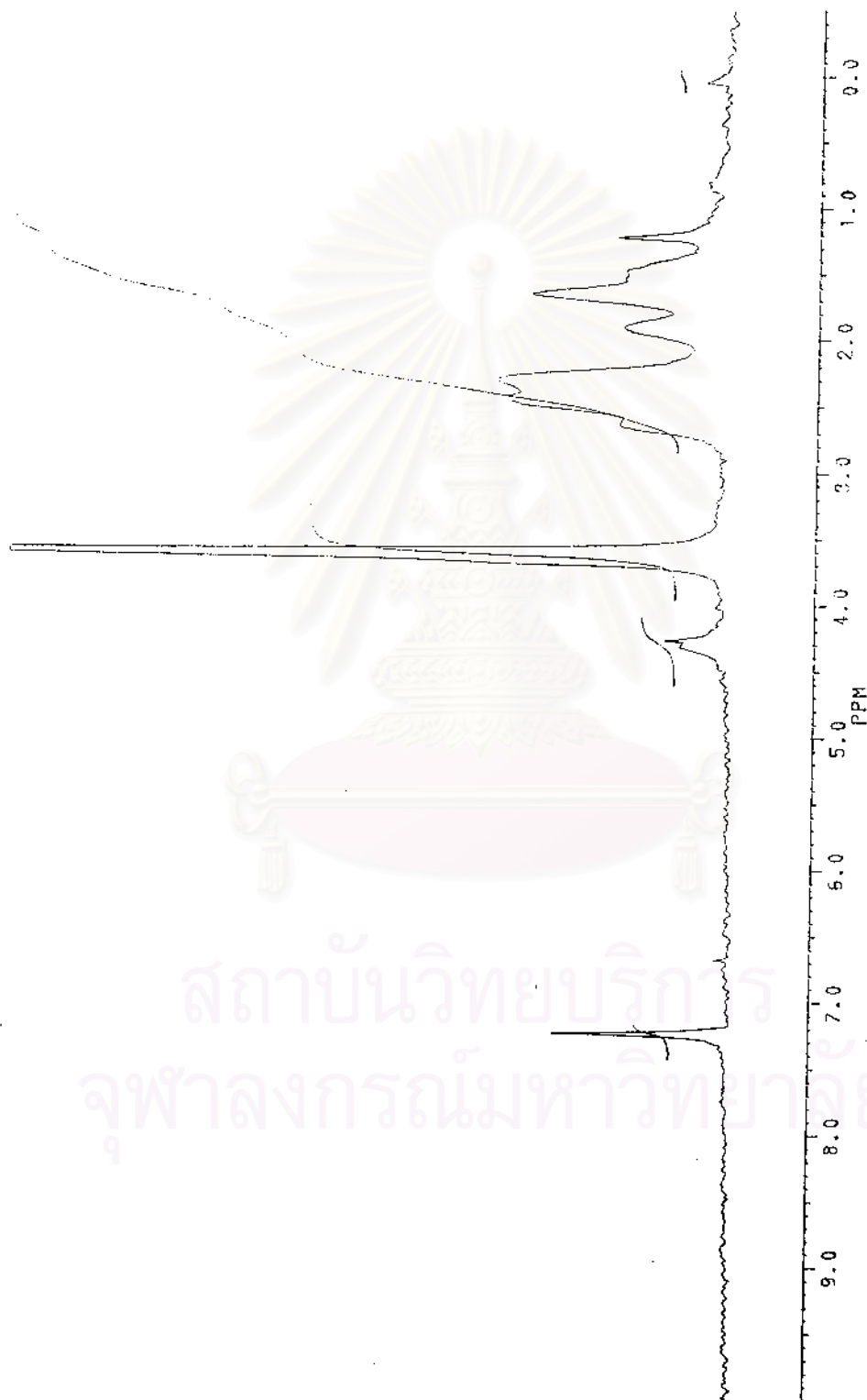


Figure 4.21 <sup>1</sup>H-NMR spectrum of the side chain of starch-g-poly(acrylic acid)



**Figure 4.22**  $^1\text{H-NMR}$  spectrum of the side chain of esterified starch-g-polyacrylate

#### **4.4 Etherification of Starch-g-polyacrylate**

The hydroxyl group on starch is etherified with propylene oxide in the presence of sodium hydroxide as a catalyst. After etherification, the white powder of esterified starch-g-polyacrylate became pale.

##### **4.4.1 Characterization of Modified Starch by $^{13}\text{C}$ - and $^1\text{H}$ -NMR Spectrometry**

The purified modified starch was analyzed by  $^{13}\text{C}$ - and  $^1\text{H}$ - NMR spectrometry.  $^{13}\text{C}$ - and  $^1\text{H}$ - NMR spectra of the modified starch are shown in Figures 4.23 and 4.24, respectively. The peak assignments are presented in Table 4.7. In Figure 4.23, the presence of the peak of chemical shift at 14-23 ppm is indicative of the presence of hydroxypropyl groups on modified starch. Furthermore, the occurrence of a distinct peak at 1.1-1.3 ppm in  $^1\text{H}$ -NMR spectrum (Figure 4.24), attributed to protons of hydroxypropyl groups on the modified starch.

**Table 4.7** Peak Assignments of  $^{13}\text{C}$ - and  $^1\text{H}$ -NMR Spectra of the Modified Starch

<b>Chemical Shift (ppm)</b>	<b>Assignments</b>
<b><math>^{13}\text{C}</math>-NMR Spectra</b>	
20	Carbon of methyl groups
42	Carbon of methylene groups
52	Carbon of -C-O- on PEG 4000 chain
61, 73, 82, 103	Carbon of anhydroglucose unit of starch
176	Carbon of carbonyl of poly(acrylic acid)

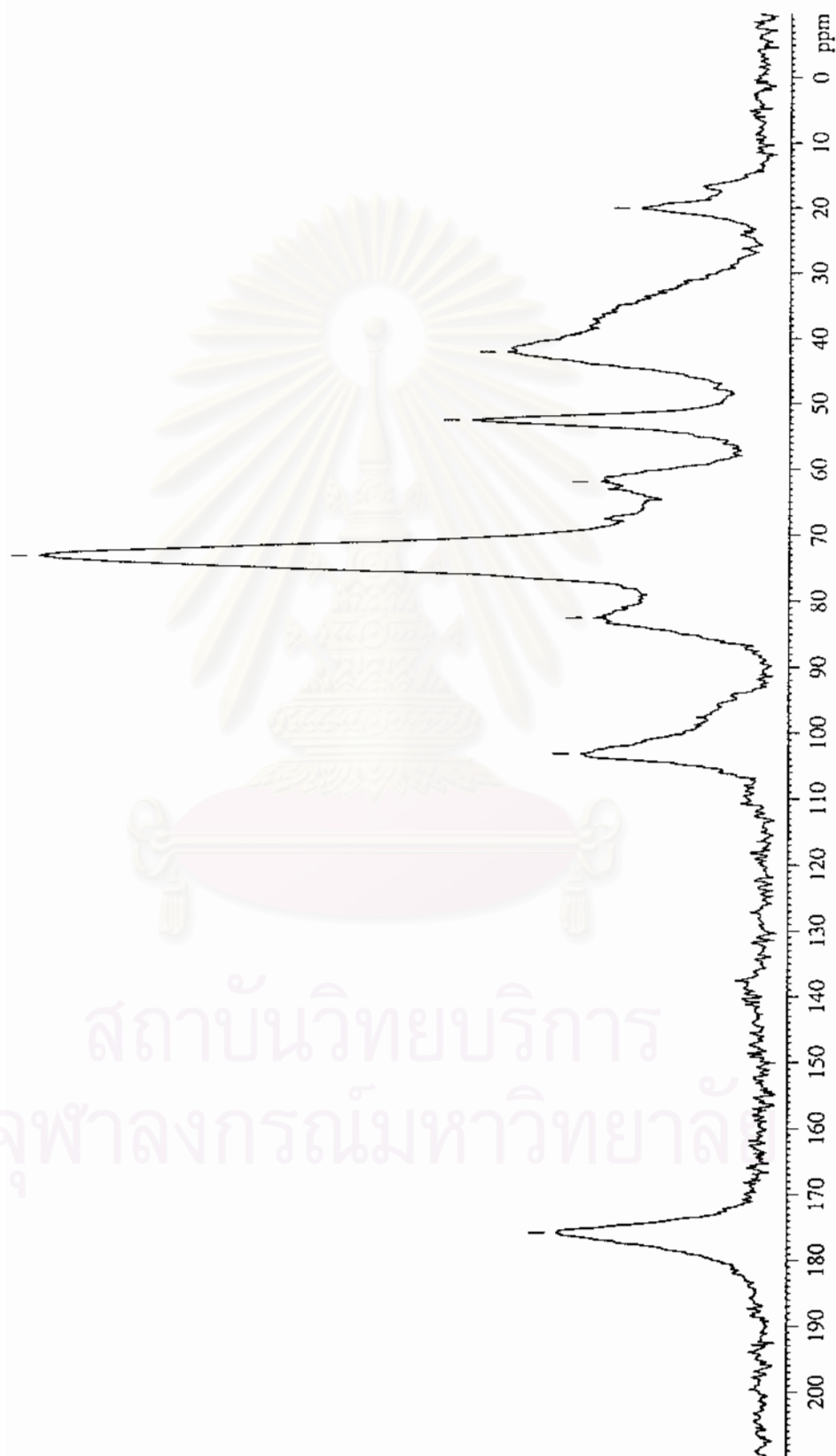


Figure 4.23  $^{13}\text{C}$ -NMR spectrum of the modified starch

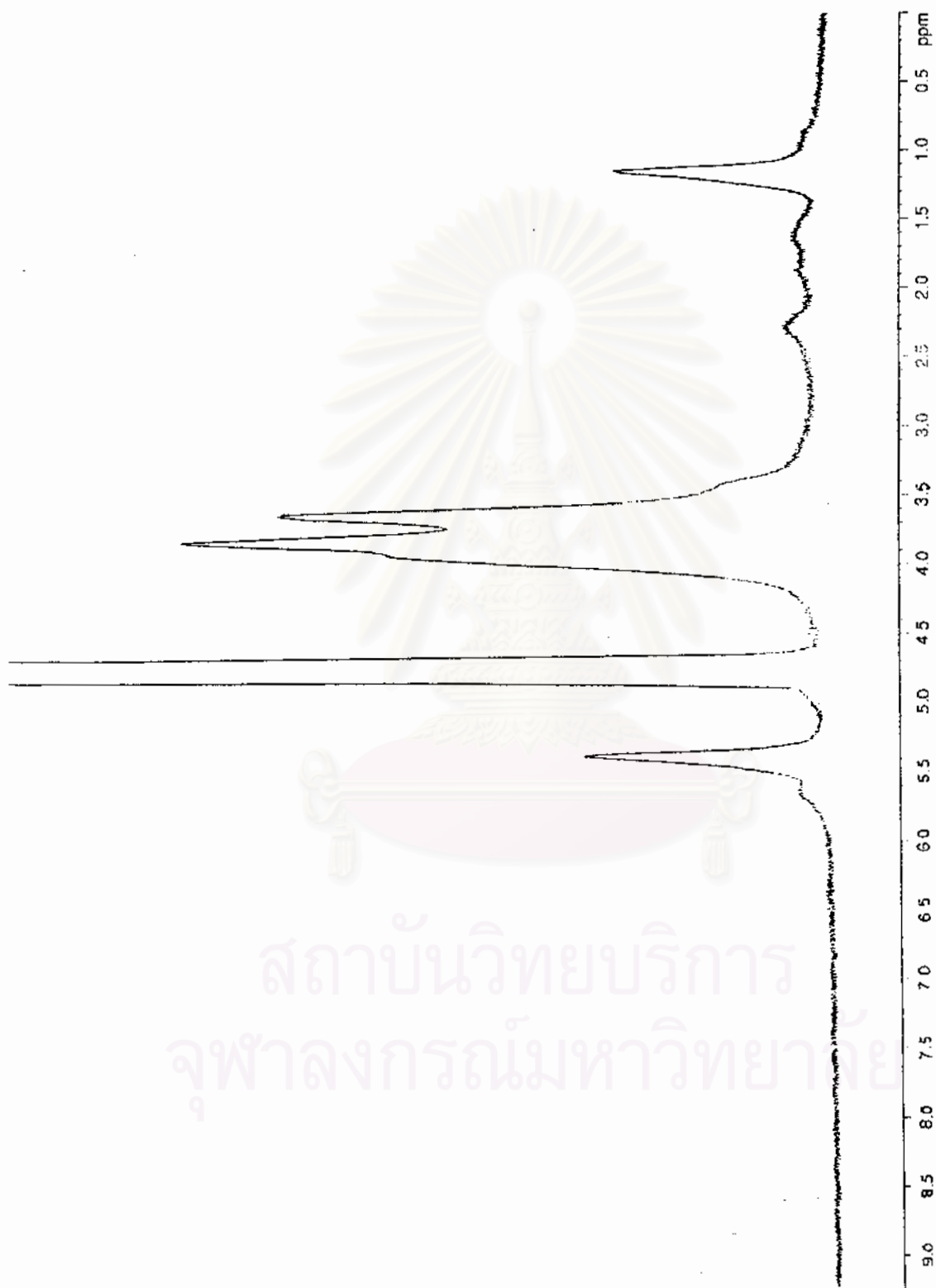


Figure 4.24 <sup>1</sup>H-NMR spectrum of the modified starch

สถาบันวิทยบริการ  
จุฬาลงกรณ์มหาวิทยาลัย

**Table 4.7** Peak Assignments of  $^{13}\text{C}$ - and  $^1\text{H}$ -NMR Spectra of the Modified Starch (Continued)

Chemical Shift (ppm)	Assignments
<b><math>^1\text{H}</math>-NMR Spectra</b>	
1.2	Protons of hydroxypropyl groups
3.6	Protons of anhydroglucose unit of starch
4.6-4.9	Protons of water
5.4	Equatorial protons of anhydroglucose unit of starch

**Remark :**  $^{13}\text{C}$ -NMR ; solid state , Frequency 75.5 MHz

$^1\text{H}$ -NMR ; solvent :  $\text{D}_2\text{O}$ , Frequency 50.0 MHz

#### 4.4.2 Spectrophotometric Determination of Hydroxypropyl Groups on the Modified Starch

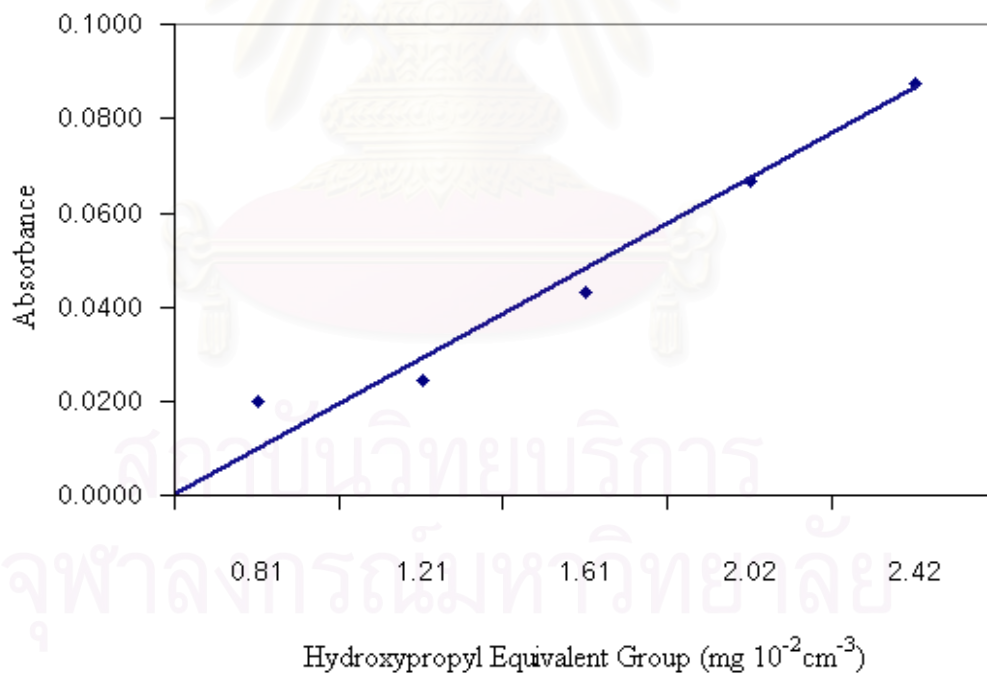
Spectrophotometric determination of the hydroxypropyl group on the modified starch was done according to Jones and Riddick method [32]. This method involves hydrolysis of the hydroxypropyl group to propylene glycol, which in turn is dehydrated to propionaldehyde and to an enolic form of allyl alcohol. These products are measured spectrophotometrically after they are reacted with ninhydrin to form a product having a purple color.

##### 4.4.2.1 Preparation of Calibration Curve

The solution of propylene glycol in distilled water was used to prepare a calibration curve. The amount of the hydroxypropyl group can be calculated by multiplying the factor 0.7763 to convert micrograms of the glycol to the hydroxyl group equivalent. The results are shown in Table 4.8 and the calibration curve is depicted in Figure 4.25.

**Table 4.8** Calibration Data for Determination of the Hydroxypropyl Equivalent Groups

Propylene glycol ( $\text{mg } 10^{-2}\text{cm}^{-3}$ )	Hydroxypropyl Equivalent Group ( $\text{mg } 10^{-2}\text{cm}^{-3}$ )	Absorbance
1.04	0.81	0.0200
1.56	1.21	0.0244
2.08	1.61	0.0435
2.60	2.02	0.0670
3.12	2.42	0.0875

**Figure 4.25** Calibration curve for determination of hydroxypropyl equivalent group

#### 4.4.3.2 Determination of Hydroxypropyl Equivalent Groups on the Modified Starch

The experimental data obtained according to Section 3.3.3.1.2 are listed in Table 4.9. Hydroxypropyl equivalent groups on the modified starch are reported as the percentage of hydroxypropyl groups.

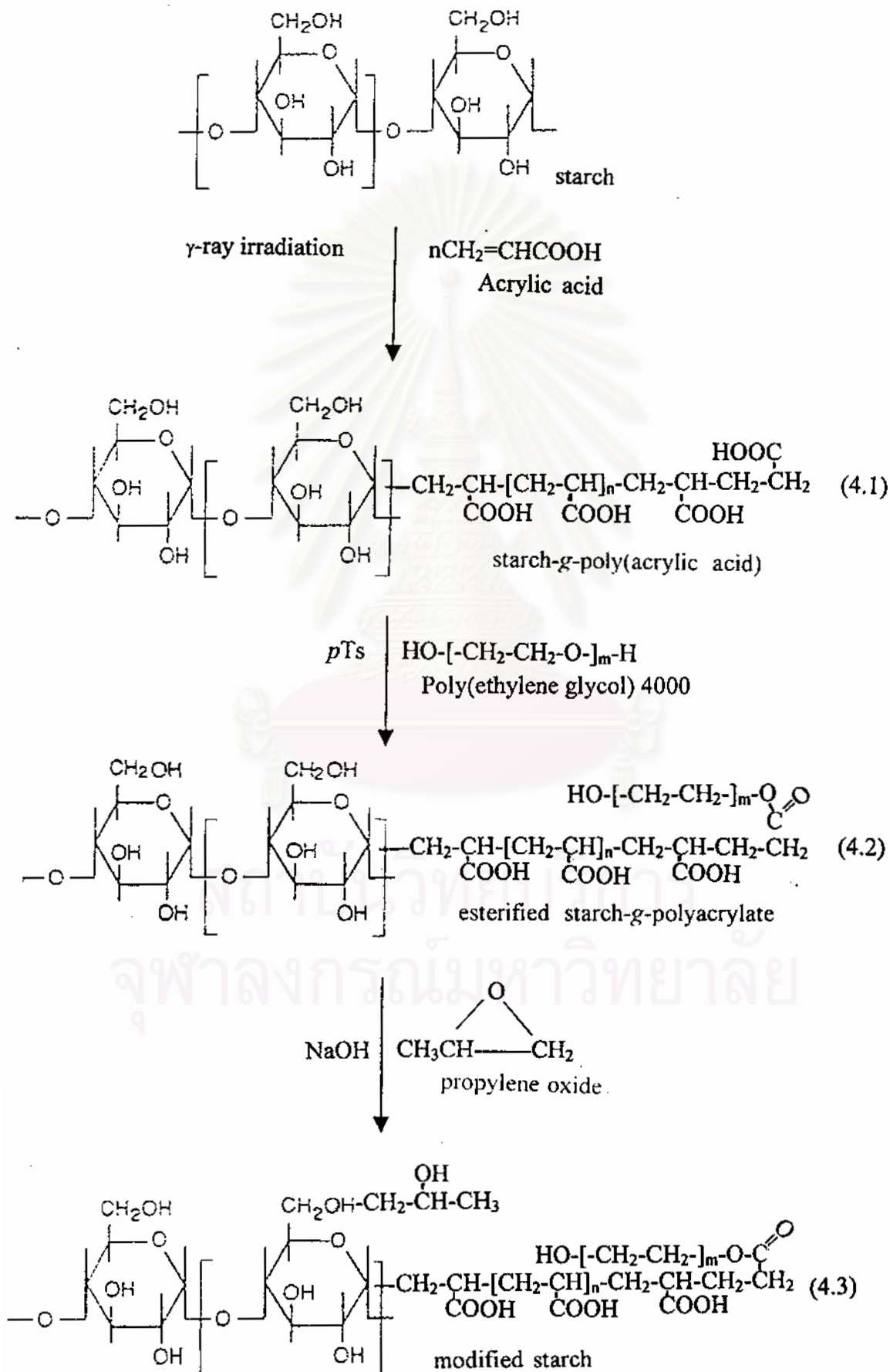
**Table 4.9** Experimental Data of Determination of the Hydroxypropyl Equivalent Groups

Sample Weight (g)	Sample Solution No.	Absorbance	Hydroxypropyl Equivalent Group (mg 10 <sup>-2</sup> cm <sup>-3</sup> )	Hydroxypropyl Equivalent Group in Sample (%)
0.0864	1	0.0221	1.08	1.25
	2	0.0244	1.12	1.30
	3	0.0261	1.16	1.34
<b>Average</b>				<b>1.30</b>

The average value of the hydroxypropyl equivalent group on the modified starch is found to be 1.30%. This relatively low value may be the result of the steric hindrance of esterified starch-g-polyacrylate, which limits the accessibility of sodium hydroxide (catalyst) and propylene oxide.

### 4.4.3 Overall Reaction Scheme

The reaction schemes of each procedure are proposed as follows:



#### 4.5 Contact Angle Measurement

The contact angle measurement of cassava starch, Esterified starch-g-polyacrylate, the etherified modified starch, EBS wax, and low density polyethylene were performed using a contact angle goniometer (FACE, Japan). The angles between water droplets on polymer film surfaces were measured. The results are presented in Table 4.10.

**Table 4.10** Contact Angles of Cassava starch, Esterified Starch-g-polyacrylate, Etherified Modified Starch, EBS wax, and Low Density Polyethylene, and the Calculated Work of Adhesion

Sample	Contact Angle (°)	$W_{ad}^a$ (mN m <sup>-1</sup> )
Cassava starch	Dissolve (0°, hydrophilic)	145.6
Esterified Starch-g-polyacrylate	80±0.3	85.4
Etherified modified starch	82±0.8	82.9
EBS wax	93±1.2	68.5
Low density polyethylene	94±1.4	68.0

<sup>a</sup> work of adhesion,  $W_{ad} = \gamma_{LV}(1 + \cos\theta)$  where  $\gamma_{LV}$  = surface tension of water (72.8 mN m<sup>-1</sup>)

It can be seen that the water droplet spread on the starch film, which indicated the hydrophilic nature of the starch. The contact angle of the modified starch was 82°. This value is comparable to that of poly(methyl methacrylate) (PMMA), which is a relatively synthetic polymer and has a contact angle of 85° [25]. The contact angles of EBS wax and LDPE are not significantly different, which are 93° and 94°, respectively. We may presumably propose that the modified starch can be mixed with LDPE without using the dispersing agent (EBS wax) or the modified starch itself may behave like the dispersing agent. In addition, the modified starch can be wetted by EBS wax, which is well dispersed in the matrix of LDPE. Since the surface of the starch is of high surface energy (high  $W_{ad}$ ), we may anticipate that the blends of LDPE/Starch can exhibit a higher value of tensile strength property in comparison to the modified starch/LDPE blends.

## **4.6 Plastic Compounding and Characterization**

### **4.6.1 Effect of Starch and Modified Starch Contents on Mechanical Properties of Low Density Polyethylene (LDPE) Composite Sheets**

The modified starch which contained 15.2% of poly(ethylene glycol) 4000 and 1.3% of hydroxypropyl group and unmodified starch was each blended with low density polyethylene (LDPE). The effects of starch and modified starch contents on mechanical properties of LDPE composite sheets are demonstrated as tensile strength and percentage of strain. The measurements of these properties were performed on an Instron mechanical tester, Model 1011, according to the ASTM D683 method. Measurements were done using a 500 mm min<sup>-1</sup> crosshead speed. Five measurements were conducted for each sample, and the results were averaged to obtain a mean value and standard deviation.

**Table 4.11** Tensile Strength and %Strain of Low Density Polyethylene (LDPE),

LDPE/ST, and LDPE/MS Blends at Various Compositions

Sample	Tensile Strength (MPa)	Strain (%)
LDPE	8.1±0.1	28.0±2.5
LDPE/ST1	7.9±0.2	25.2±2.1
LDPE/ST5	8.4±0.2	17.3±1.5
LDPE/ST10	8.6±0.3	15.8±1.0
LDPE/ST20	8.9±0.2	13.3±1.3
LDPE/MS1	7.7±0.2	21.0±3.0
LDPE/MS5	7.5±0.4	14.4±1.7
LDPE/MS10	7.8±0.3	13.0±0.7
LDPE/MS20	8.2±0.4	12.3±0.6

The effects of starch and modified starch contents in low-density polyethylene (LDPE) composite sheets on their mechanical properties are presented in Table 4.11 and Figures 4.26 - 4.27. The tensile strength and %strain of LDPE sheets were  $8.1\pm 0.1$  MPa and  $28.0\pm 1.0\%$ , respectively. The relative lines were prepared (Figure 4.27) in order to demonstrate the difference between the filled and unfilled low-density polyethylene (LDPE) sheets. The tensile strength of LDPE sheet was referenced as 100%. For starch and modified starch filled LDPE composite sheets, the same conclusion of tensile strength properties can be reached. The tensile strength of the LDPE composite sheets increased with increasing the starch and modified starch contents. But the tensile strengths of starch filled LDPE composite sheets were higher and became even higher than LDPE sheets when the contents of modified starch were higher than 1%. This may be the effect of starch phase that could enhance the strength of LDPE composite sheets. For modified starch filled LDPE composite sheets, the tensile strength was found to be lower than both unfilled and starch filled LDPE sheets, but it tended to be higher when the modified starch concentration was up to 20%. This is probably due to the fact that their blends with LDPE are still incompatible. This result may indicate that EBS wax might neither be a good dispersing agent nor an appropriate concentration was used.

In Figures 4.29 and 4.30, the percentage of strain and the relative percentage of strain values of LDPE/ST and LDPE/MS blends are presented. As observed, the percentage of strain decreased with increasing starch and modified starch contents in the blends. The addition of starch and modified starch to LDPE significantly reduced the percentage of strain, and some significant change was observed between LDPE/ST and LDPE/MS blends. This is because starch and modified starch mixed incompatibly with LDPE, leading the LDPE composite sheets to become a brittle material, which has the low tensile strength and %strain.

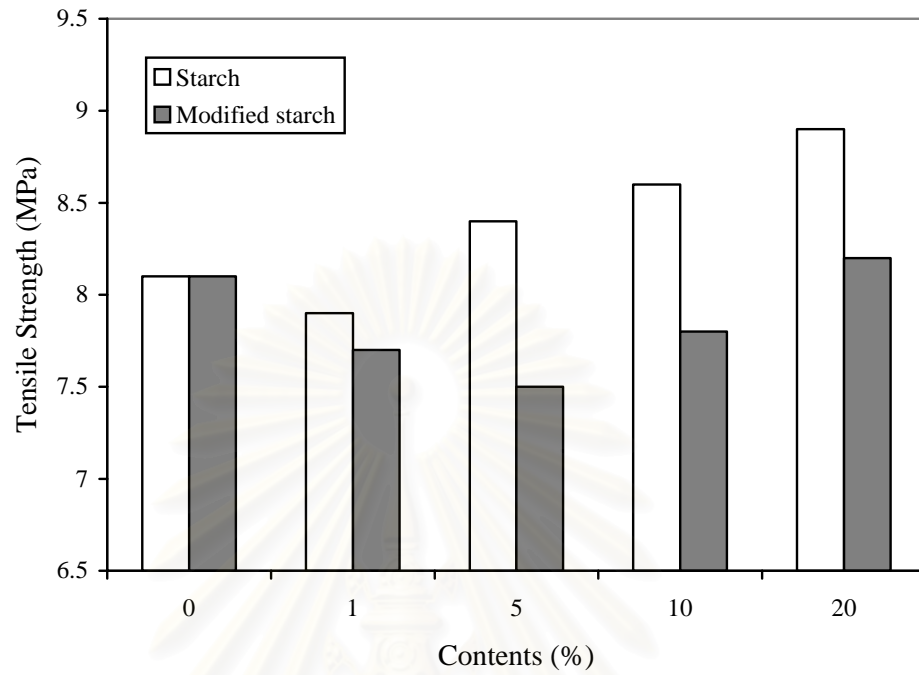


**Figure 4.26** Tensile strength of LDPE, LDPE/ST, and LDPE/MS blends at various compositions

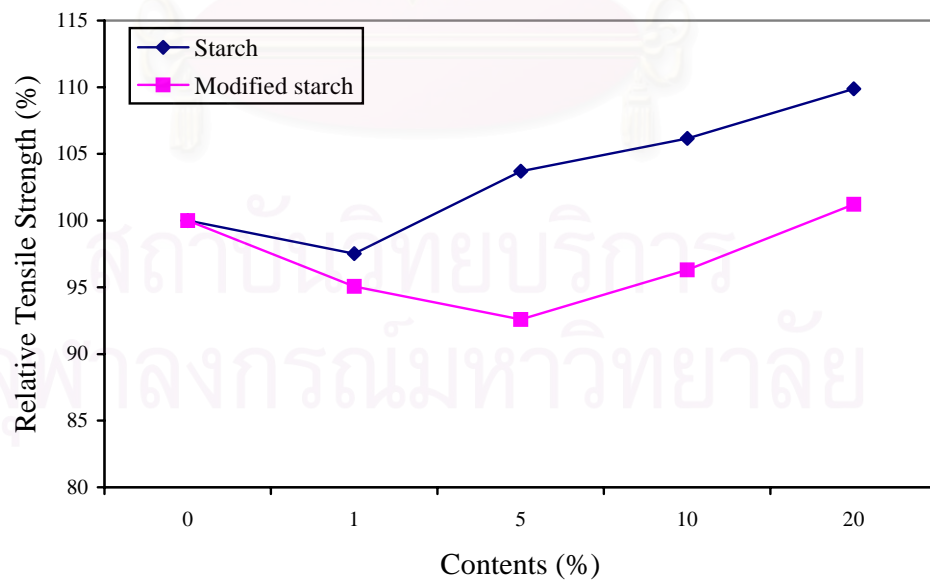


**Figure 4.27** Relative tensile strength of LDPE, LDPE/ST, and LDPE/MS blends at various compositions

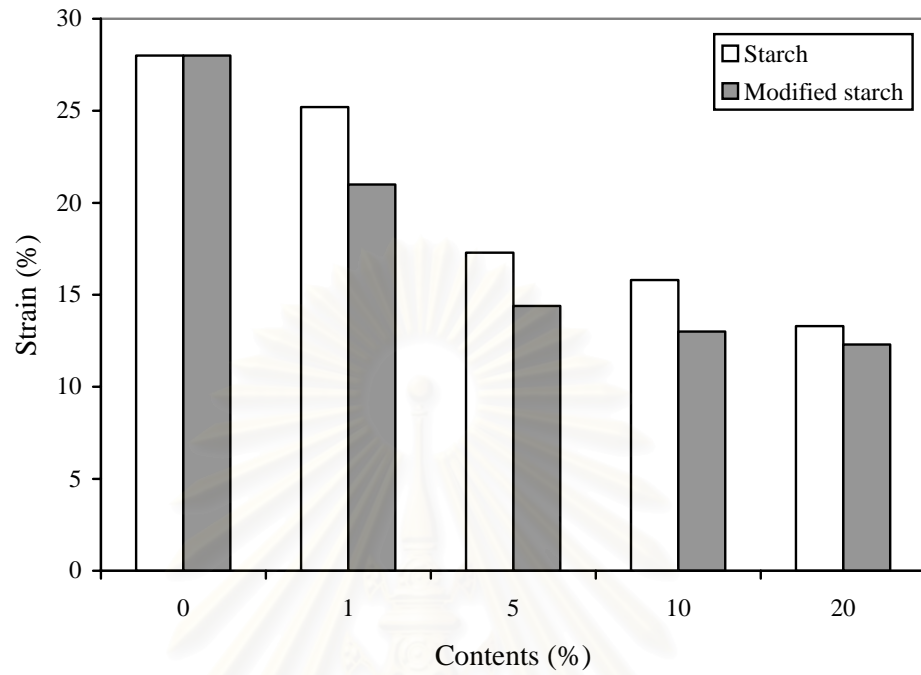


**Figure 4.28** Percentage Strain of LDPE, LDPE/ST, and LDPE/MS blends at various compositions

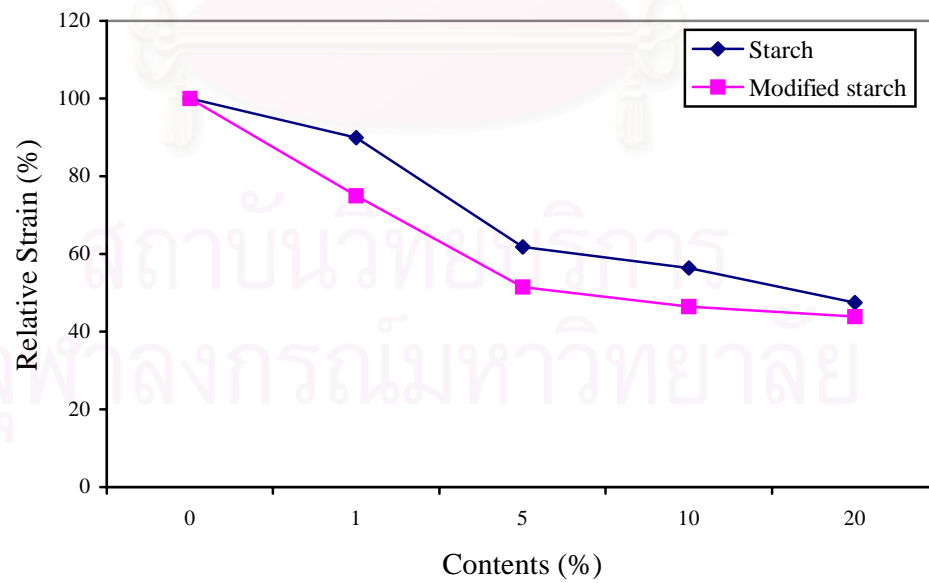


**Figure 4.29** Relatively percentage strain of LDPE, LDPE/ST, and LDPE/MS blends at various compositions

#### 4.6.2 Morphology of the Blended Samples

The plastic sheets of LDPE, LDPE/ST10, and LDPS/MS10 were selected for the observation of the fractured surface, and their morphologies were compared using scanning electron microscopy (SEM). The results are shown in Figures 4.30 - 4.32. For the starch filled polyethylene sheet, the small particles were observed. Some grains might be ruptured, which formed immiscibly with LDPE. For the modified starch filled LDPE composite sheets, less particles were observed. These results indicated that the modified starch improved the compatibility with LDPE matrix.

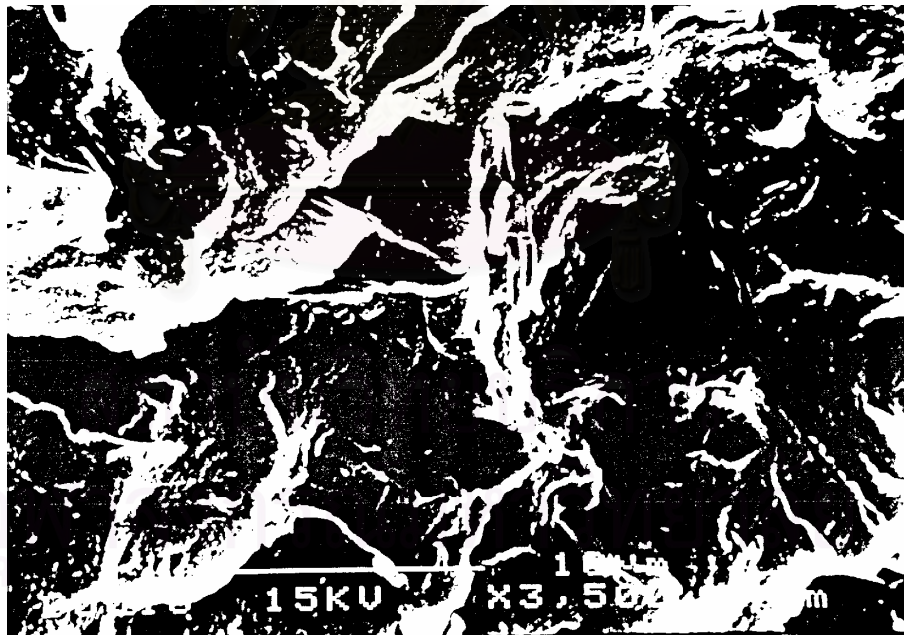


**Figure 4.30** SEM micrograph of the fractured LDPE

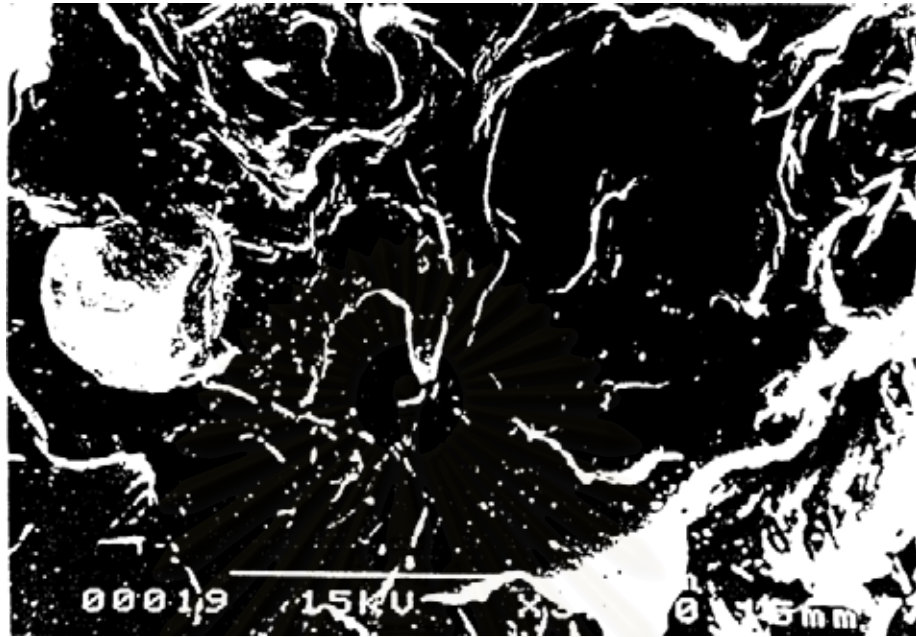


Figure 4.31 SEM micrograph of the fractured LDPE/ST10

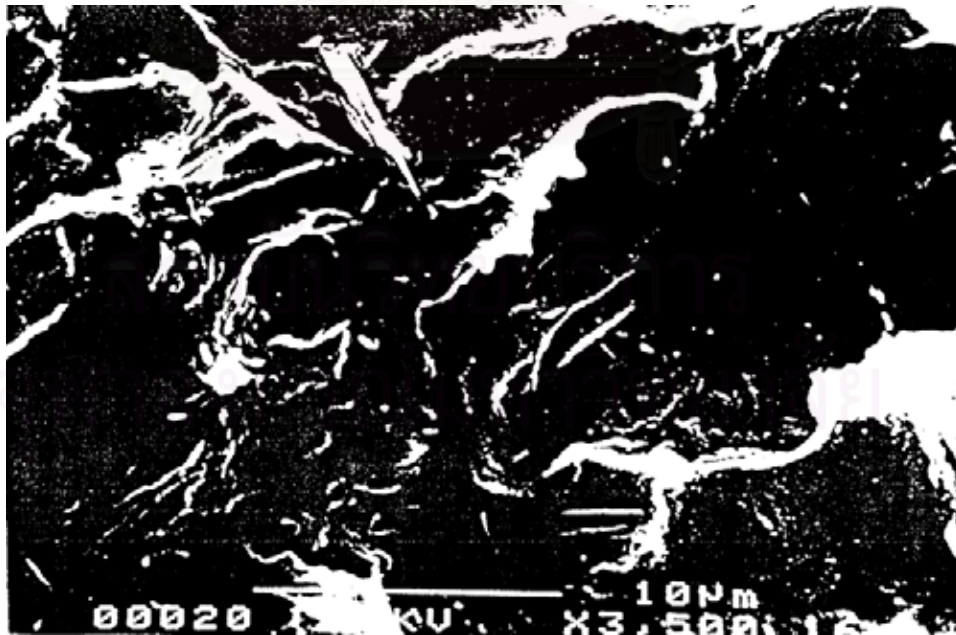


Figure 4.32 SEM micrograph of the fractured LDPE/MS10

### 4.6.3 Morphology of the Failure Samples

To elucidate the failure mechanism of these blends, the failure surface morphology of the sample subjected to tensile strength at break is used as a helpful method. The LDPE, LDPE/ST10, and LDPE/MS10 sheets were chosen to tensile properties test. The SEM micrographs of those selected plastic sheets are presented in Figures 4.33–4.35. For LDPE and LDPE/ST10 sheets, the failure surface morphology of tensile test at break seemed to be similar. The surfaces after tensile failure test showed the presence of cavities in the form of the ridges and valleys. A ridge is present on one fracture surface and a corresponding valley on the other. The failure appeared to be a shear tearing, which is an accepted mode of failure in metals and polymers [33]. The observed fibril bundles were the result of a slow crack growth. It was also found that the fibril bundle of LDPE/ST10 blend was shorter than that of LDPE sheet. For LDPE/MS10 blend, there were less valleys which indicated that materials snapped at the point of stress. The presence of the rough surface indicated that the failure surface was similar to that of a planar fracture surface. The phenomena were the evidence of no interfacial failure between starch and LDPE, resulted from a faster crack growth.

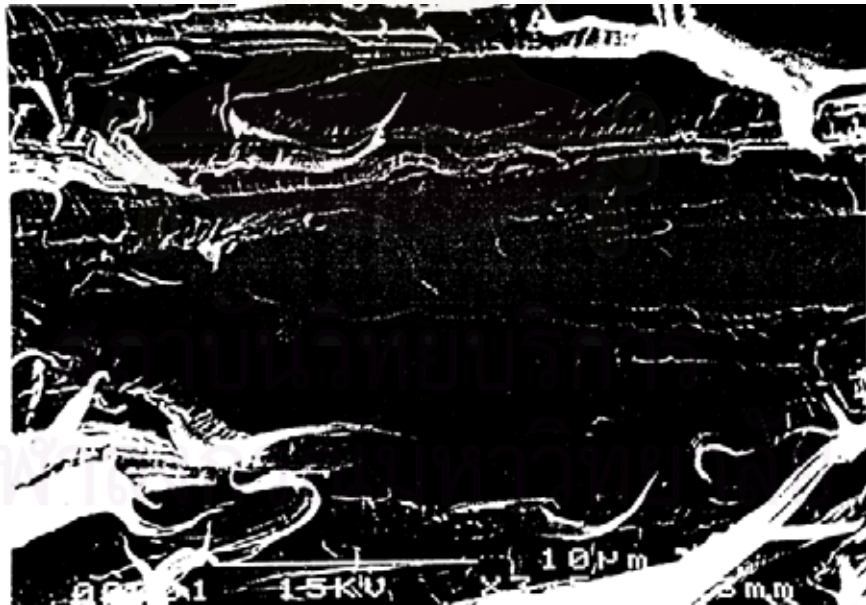
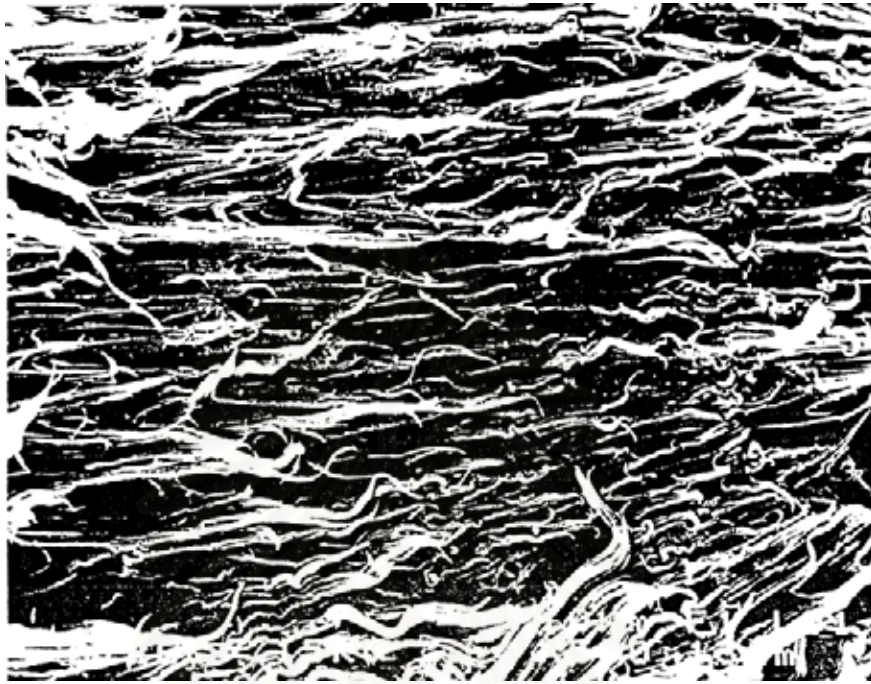


Figure 4.33 SEM micrographs of the failure surface (in a tensile test) of LDPE

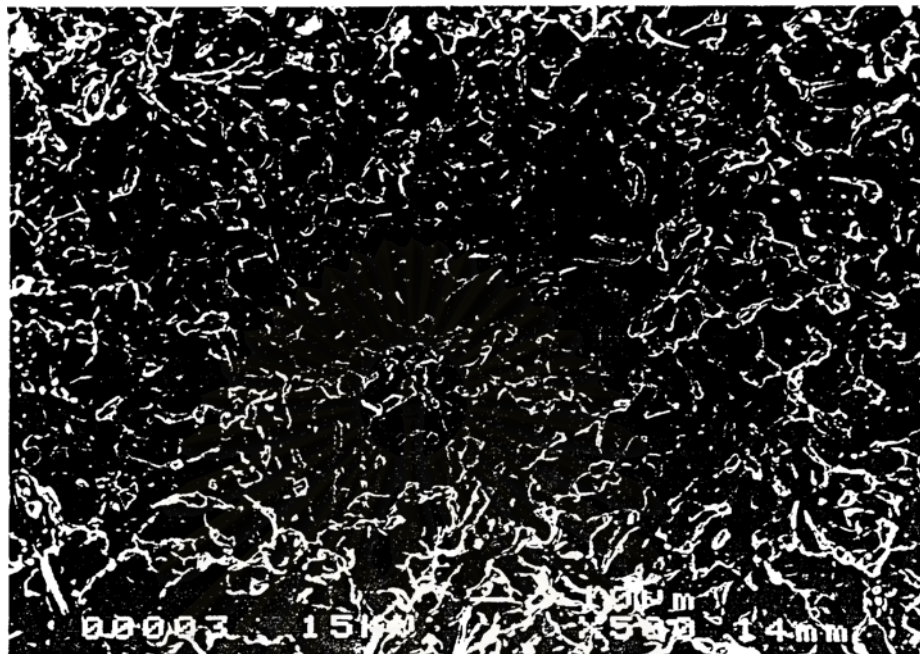


Figure 4.34 SEM micrographs of the failure surface (in a tensile test) of LDPE/MS10

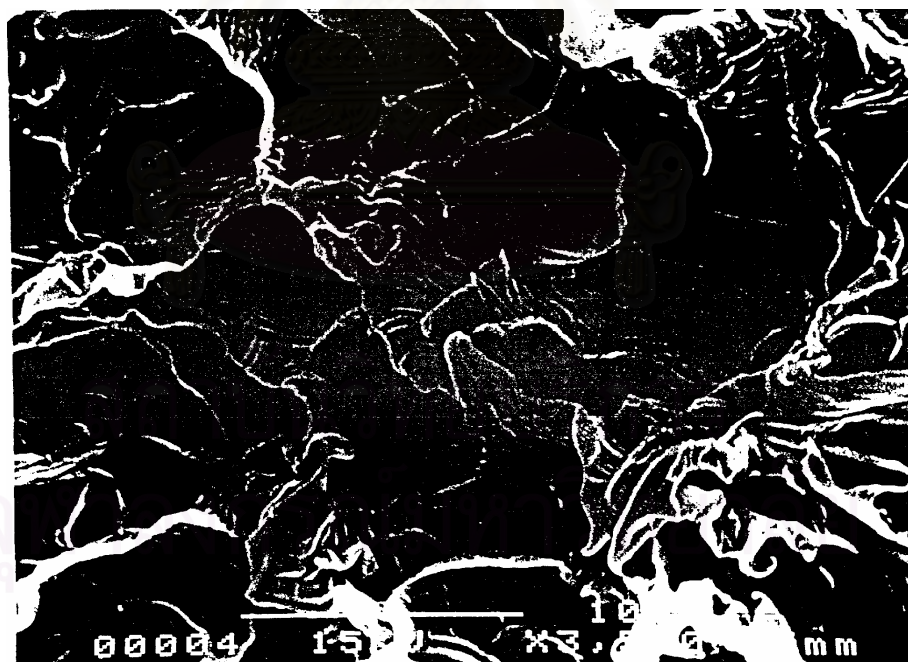
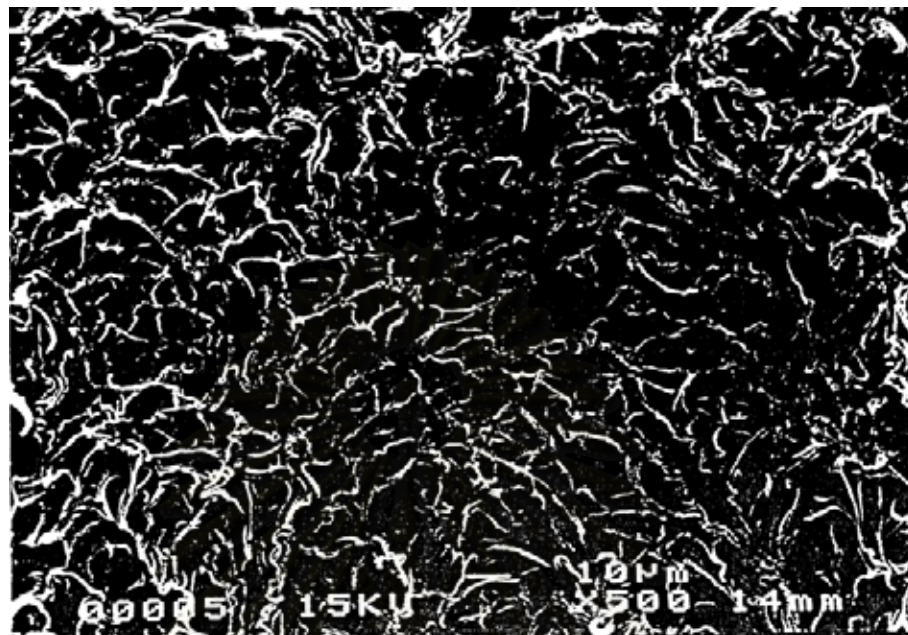


Figure 4.35 SEM micrographs of the failure surface (in a tensile test) of LDPE/ST10

#### 4.6.4 Hardness Measurement

The effects of starch and modified starch on the hardness property of LDPE composite sheets were evaluated using a digital durometer. The results are shown in Table 4.12 and Figure 4.36. The relative hardness value in Figure 4.37 shows the comparison of filled and unfilled low-density polyethylene sheets in terms of percentage. It can be observed that an increase in starch and modified starch content resulted in a slight increase in hardness. But no significant difference was observed between starch and modified starch filled LDPE composite sheets.

**Table 4.12** Hardness Values of LDPE, LDPE/ST, and LDPE/MS Blends at Various

Compositions	
Sample	Hardness Value
LDPE	41.0±1.4
LDPE/ST1	40.3±1.4
LDPE/ST5	41.2±1.2
LDPE/ST10	42.5±1.8
LDPE/ST20	44.9±0.6
LDPE/MS1	39.9±1.0
LDPE/MS5	40.7±2.1
LDPE/MS10	42.4±0.9
LDPE/MS20	43.8±0.7

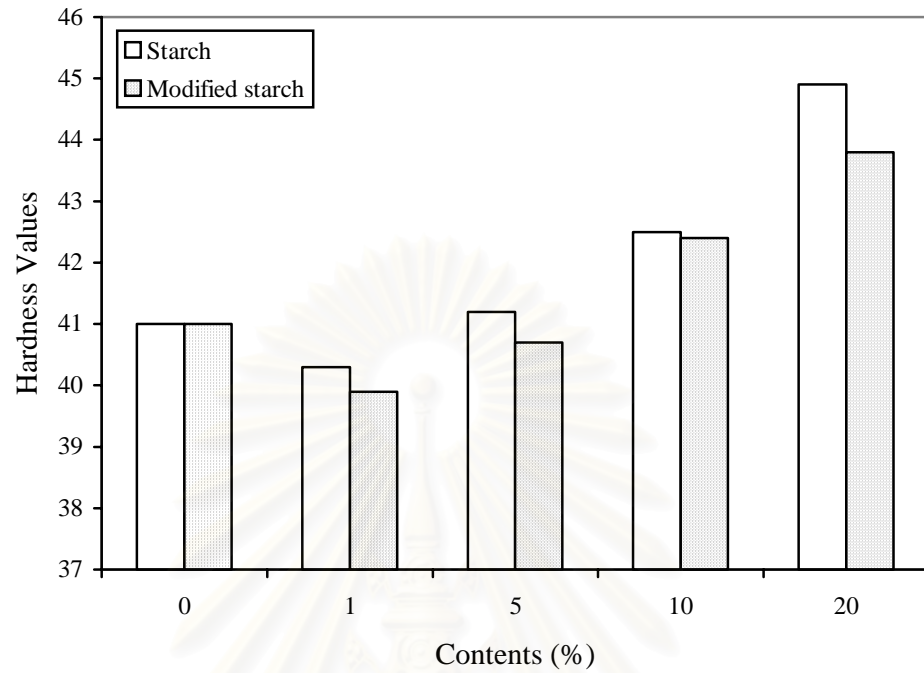


**Figure 4.36** Hardness values of LDPE, LDPE/ST, and LDPE/MS blends at various compositions

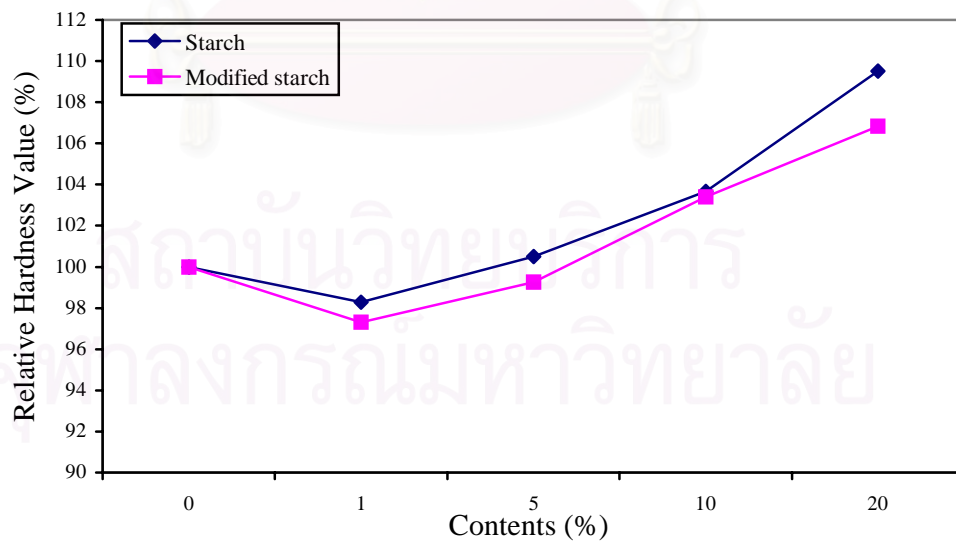


**Figure 4.37** Relative hardness value of LDPE, LDPE/ST, and LDPE/MS blends at various compositions

#### 4.6.5 Thermal Property Analysis

The thermogravimetric (TG) and differential thermogravimetric (DTG) curves of starch, starch-g-poly(acrylic acid), esterified starch-g-polyacrylate, and modified starch were shown in Figures 4.38 – 4.41, respectively. The samples were heated up to 500 °C with a heating rate of 20°C min<sup>-1</sup>. The TG and DTG curves of cassava starch in Figure 4.38 were stable up to 275°C. The maximum decomposition rate appeared at 375°C. The peak at 100°C indicated the presence of free water bound with starch molecule. For the modified cassava starch, there were 2 stages of decomposition. The first was starch moiety decomposition, and the second was poly(acrylic acid) moiety decomposition. These second decomposition stages started above 400°C and ended at about 550°C, giving an ash residue.

In Figure 4.42, LDPE was stable up to 350°C and reached the maximum decomposition at 505°C. After blending with modified starch at various contents (LDPE/MS1, LDPE/MS5, LDPE/MS10, and LDPE/MS20), the onsets of decomposition temperature of plastic composite sheets were lower than LDPE sheets, which started at about 300°C. This was attributed to the decomposition of modified starch composition. The thermogravimetric (TG) and differential thermogravimetric (DTG) curves of these blends are shown in Figures 4.42 through 4.46. The decomposition temperature and the percentage weight loss of each sample are presented in Table 4.13.

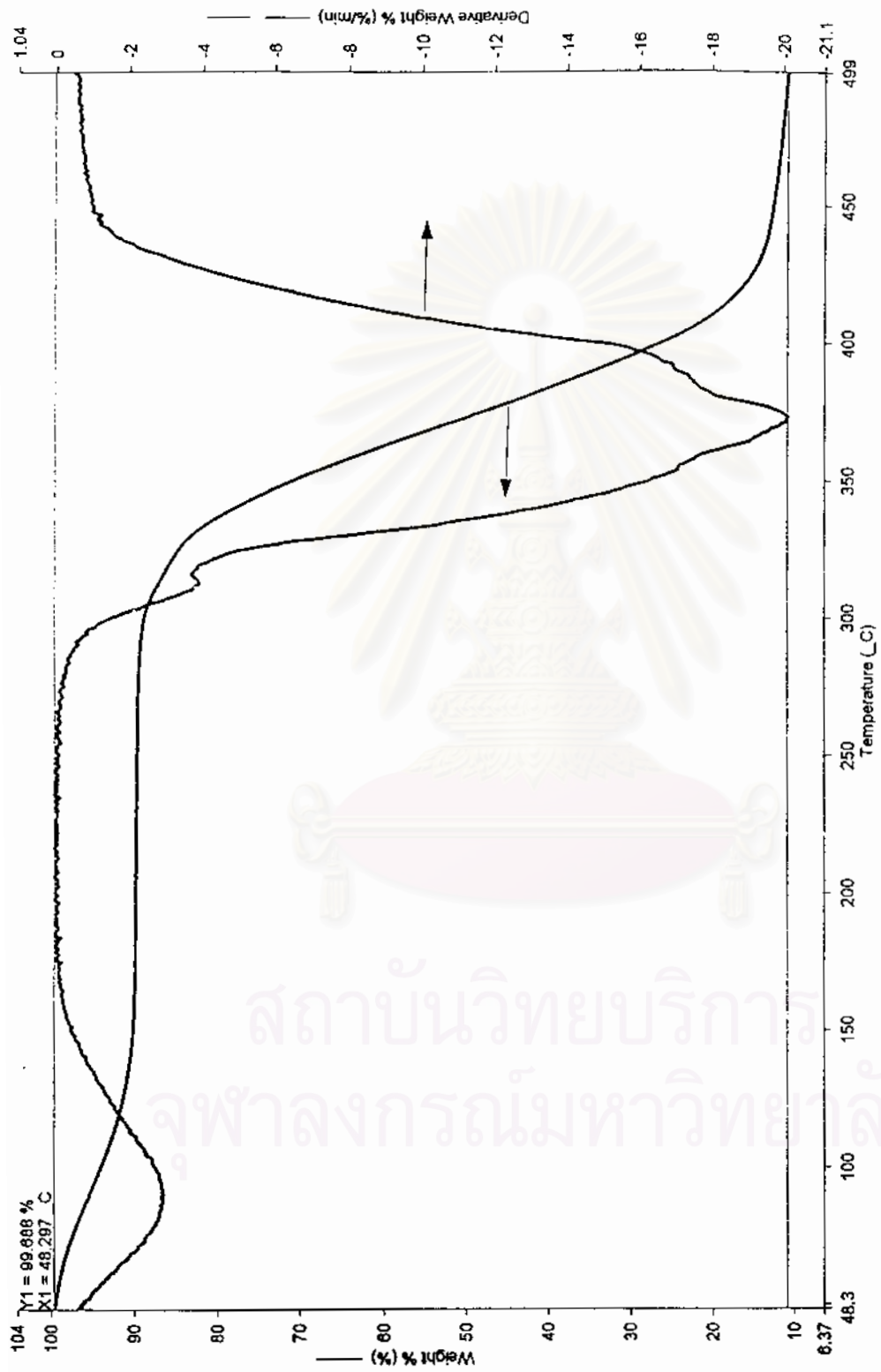
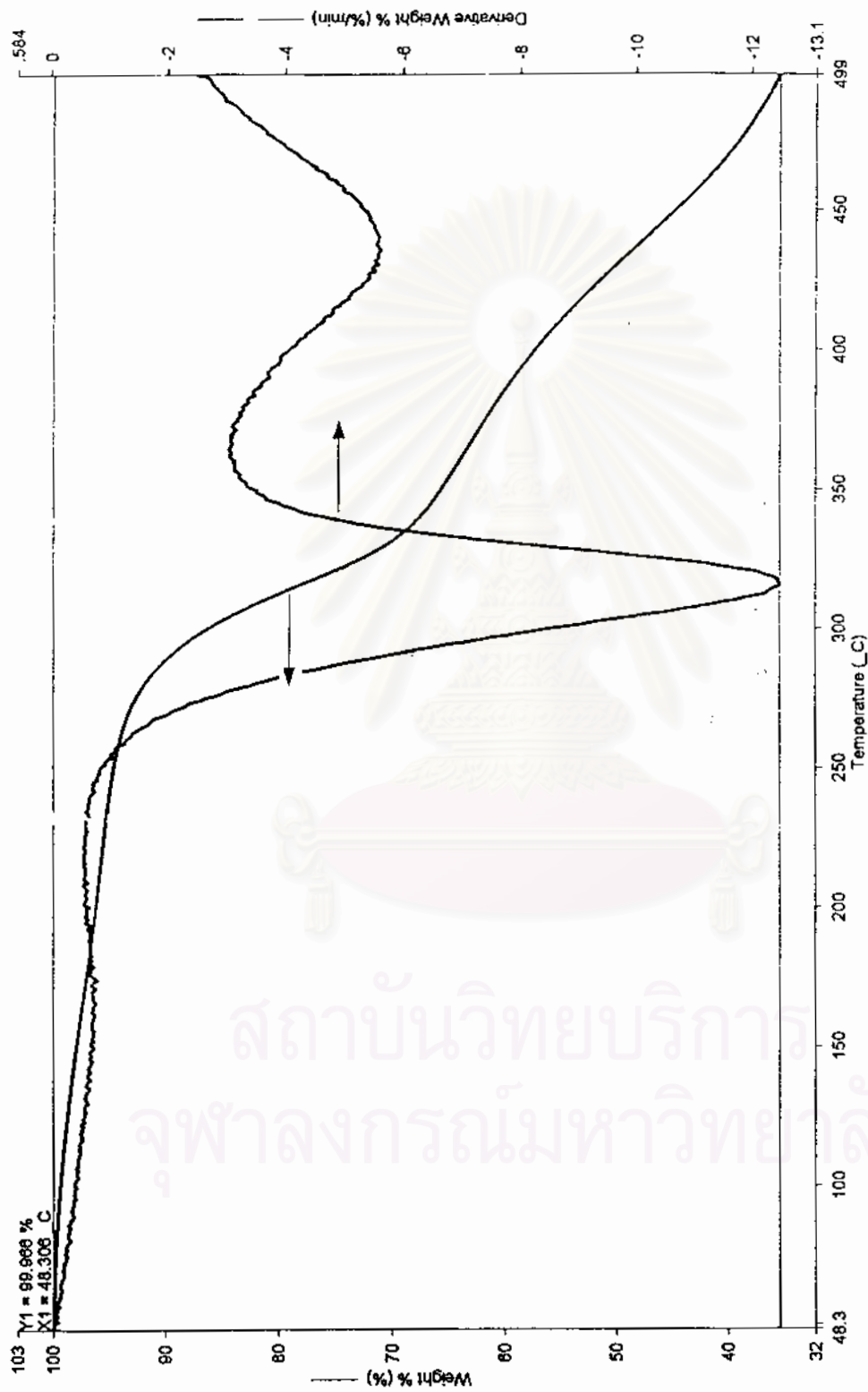


Figure 4.38 TG and DTG thermograms of cassava starch



1) Heat from 50.00\_C to 500.00\_C at 20.00\_C/min Sample Weight: 14.934 mg

Figure 4.39 TG and DTG thermograms of cassava starch-g-poly(acrylic acid)

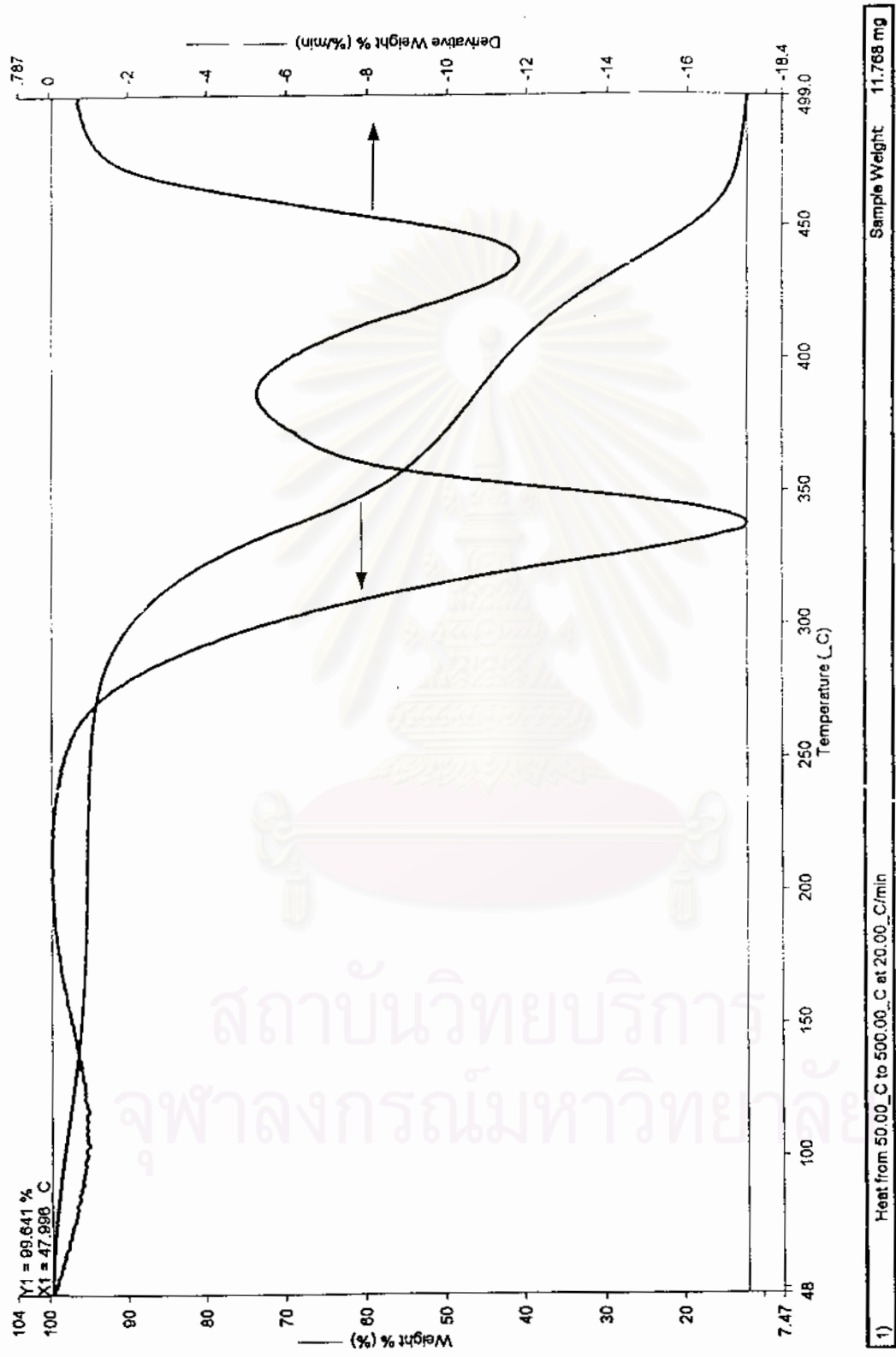


Figure 4.40 TG and DTG thermograms of esterified starch-g-polyacrylate

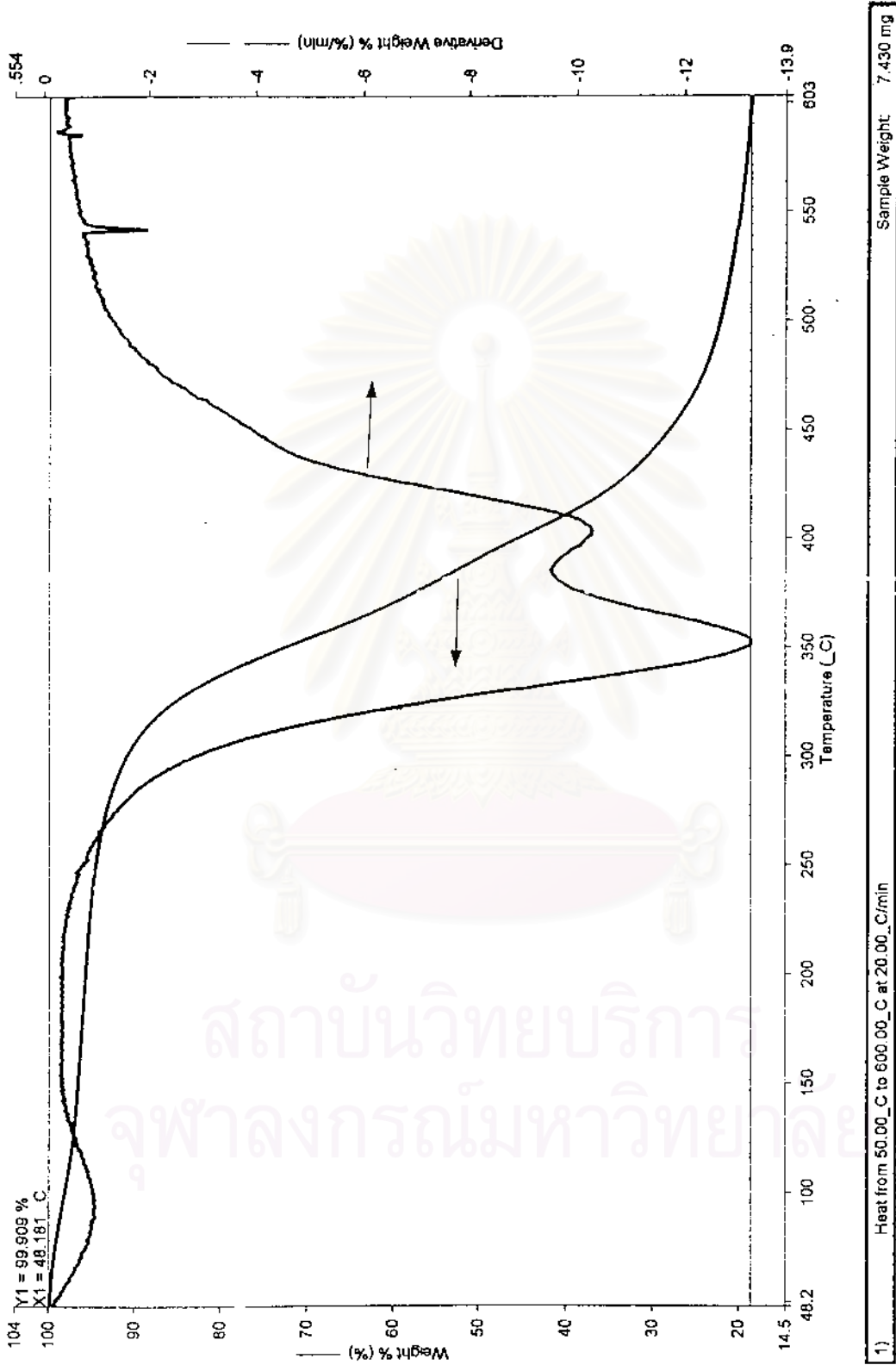


Figure 4.41 TG and DTG thermograms of modified starch

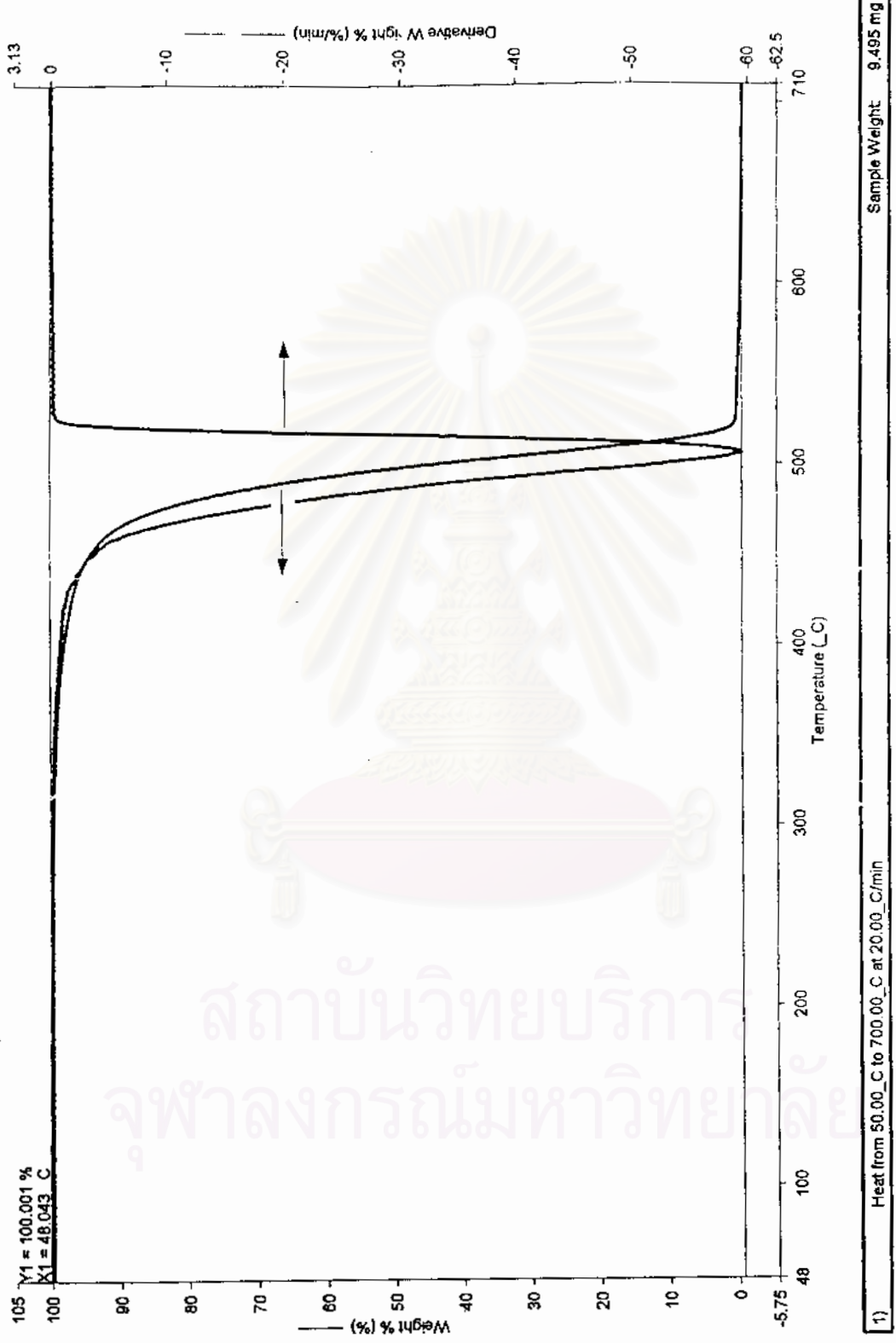


Figure 4.42 TG and DTG thermograms of LDPE

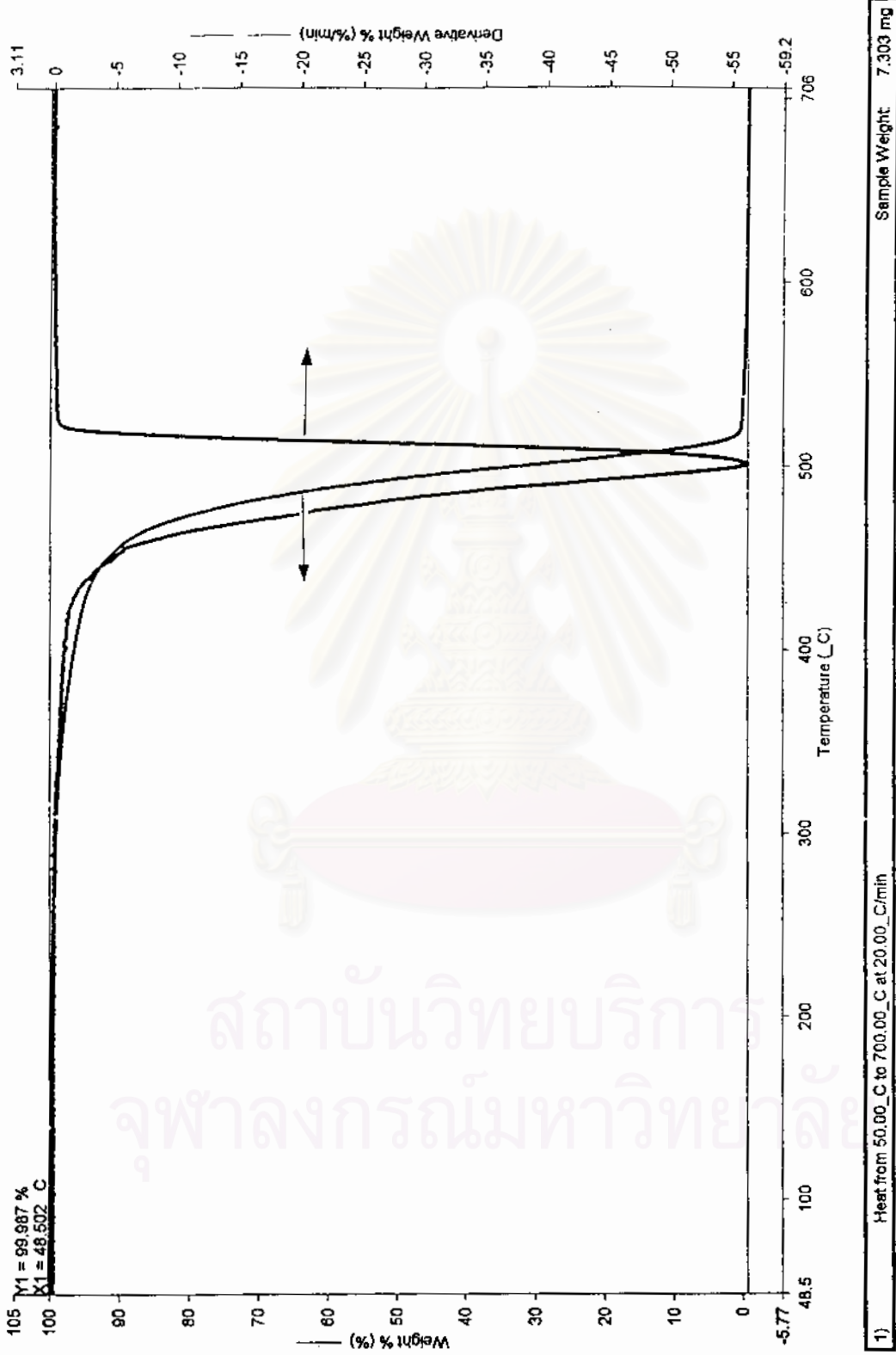
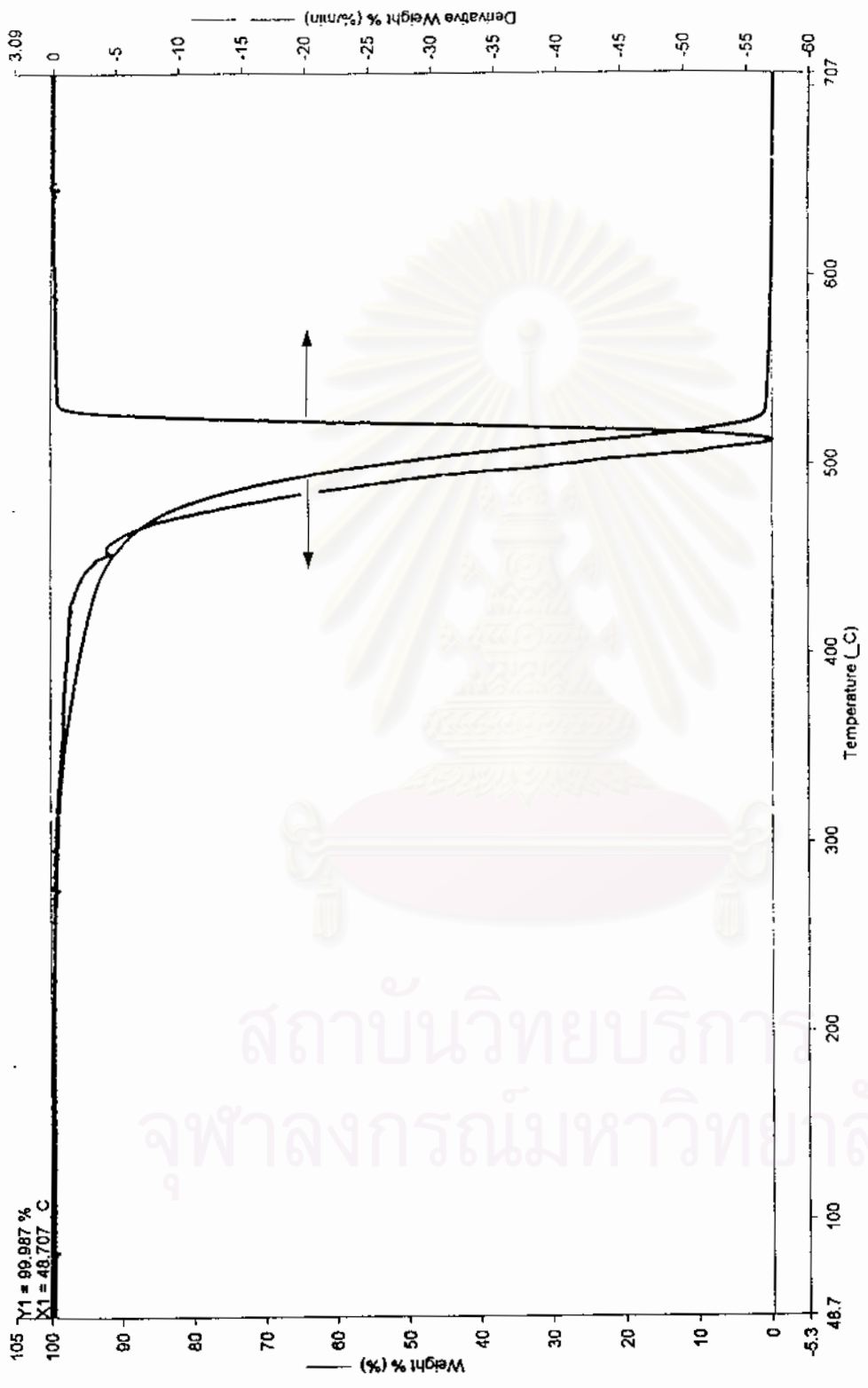


Figure 4.43 TG and DTG thermograms of LDPE/MS1 blend



1) Heat from 50.00\_C to 700.00\_C at 20.00\_C/min Sample Weight: 8.442 mg

Figure 4.44 TG and DTG thermograms of LDPE/MS5 blend

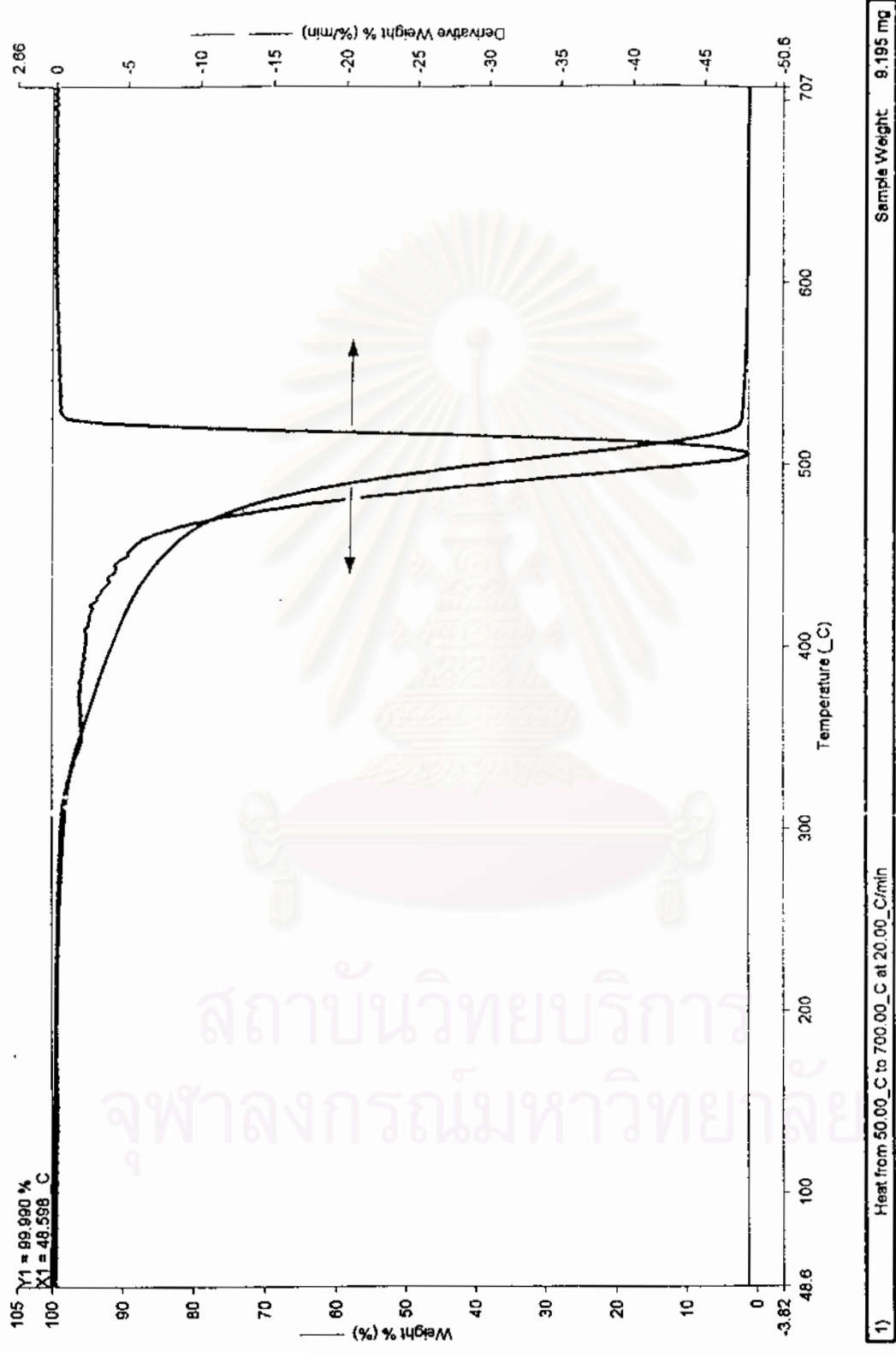


Figure 4.45 TG and DTG thermograms of LDPE/MS10 blend

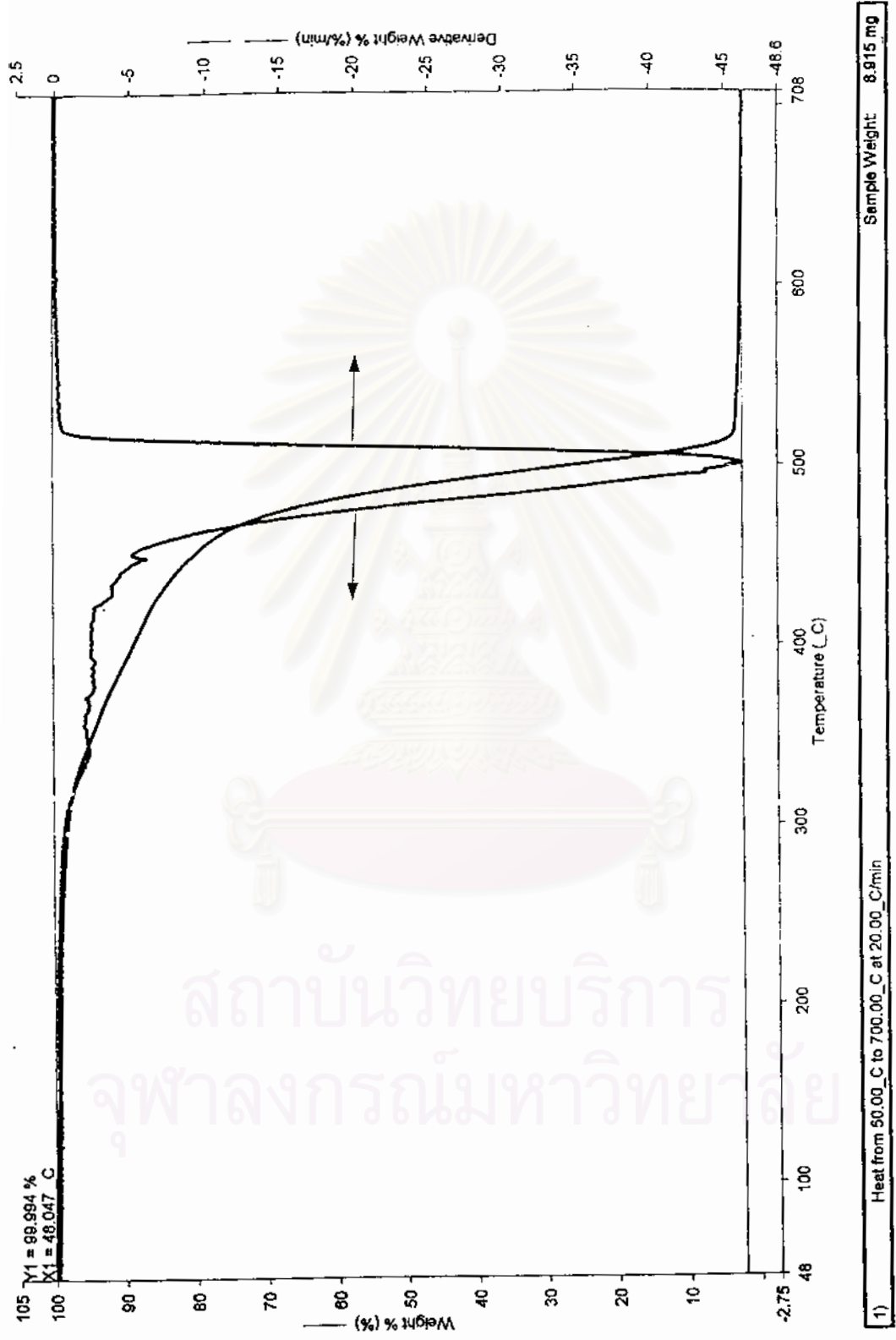


Figure 4.46 TG and DTG thermograms of LDPE/MS20 blend

**Table 4.13** Decomposition Temperature and the Percentage of Weight Loss of Starch, Modified Starch, and LDPE/MS blends at Various Composition

Sample	%Weight Loss	Decomposition Temperature (°C)
Cassava starch	99.688	375
Cassava starch-g-poly(acrylic acid)	99.966	316, 438
Esterified starch-g-polyacrylate	99.641	338, 435
Modified starch	99.909	351, 402
LDPE	100.001	505
LDPE/MS1	99.987	502
LDPE/MS5	99.987	513
LDPE/MS10	99.990	505
LDPE/MS20	99.994	500

#### **4.7 Soil Burial Test**

##### **4.7.1 Mechanical Properties Measurements**

In order to evaluate the degradation of LDPE composite sheets in a realistic environment, a soil burial experiment was carried out. The LDPE and composite LDPE sheets were buried in Saraburi soil for 2 months and removed every 2 weeks to determine the degradation in soil burial in the mechanical properties of plastic sheets. After the removal, the dark spots of mold growths on the surface of LDPE composite sheets were observed. The effects of soil burial test on the tensile strength and %strain of LDPE and LDPE composite sheets are shown in Tables 4.14 - 4.15.

**Table 4.14** Tensile Strength of LDPE, LDPE/ST, and LDPE/MS blends after the Soil

## Burial Test

Sample	Burial Time (weeks)				
	Control	2	4	6	8
LDPE	8.1±0.1	7.9±0.1	7.8±0.2	7.8±0.4	7.6±0.2
LDPE/ST1	7.9±0.2	7.7±0.1	7.5±0.2	7.4±0.3	7.3±0.1
LDPE/ST5	8.4±0.2	7.8±0.2	7.7±0.3	7.7±0.4	7.6±0.3
LDPE/ST10	8.6±0.3	7.6±0.4	7.3±0.3	7.2±0.4	7.0±0.2
LDPE/ST20	8.9±0.2	8.6±0.1	8.1±0.3	8.1±1.0	8.0±0.4
LDPE/MS1	7.7±0.2	7.6±0.1	7.3±0.4	7.2±0.3	7.1±0.2
LDPE/MS5	7.5±0.4	7.4±0.3	7.3±0.4	7.3±0.2	7.1±0.3
LDPE/MS10	7.8±0.3	7.6±0.3	7.5±0.2	7.4±0.4	7.0±0.2
LDPE/MS20	8.2±0.4	7.5±0.2	6.7±0.4	6.5±0.5	6.3±0.4

**Table 4.15** Percentage Strain of LDPE, LDPE/ST, and LDPE/MS blends after the

## Soil Burial Test

Sample	Burial Time (weeks)				
	Control	2	4	6	8
LDPE	28.0±2.5	26.5±2.2	25.1±1.7	25.0±1.2	24.8±2.3
LDPE/ST1	25.2±2.1	22.9±3.1	21.2±1.9	20.9±1.5	20.5±1.2
LDPE/ST5	17.3±1.5	16.7±0.8	15.9±2.0	15.5±1.4	14.0±1.5

**Table 4.15** Percentage Strain of LDPE, LDPE/ST, and LDPE/MS blends after the Soil Burial Test (Continued)

Sample	Burial Time (weeks)				
	Control	2	4	6	8
LDPE/ST10	15.8±1.0	13.9±1.7	13.1±2.1	13.0±1.2	12.7±1.9
LDPE/ST20	13.3±1.3	12.1±1.4	11.5±1.2	11.1±1.7	10.8±1.2
LDPE/MS1	21.0±3.0	19.7±1.3	18.8±1.0	18.5±1.3	18.0±1.2
LDPE/MS5	14.4±1.7	13.6±2.0	13.0±1.6	12.7±1.1	12.0±1.2
LDPE/MS10	13.0±0.7	12.1±1.8	11.4±1.2	11.0±1.0	10.9±1.1
LDPE/MS20	12.3±0.6	11.9±0.9	11.3±1.0	10.9±1.2	10.5±0.9

Figures 4.47 and 4.48 present the tensile strength and the percentage strain of LDPE, LDPE/ST, and LDPE/MS blends after the soil burial test, respectively. The results show that both the tensile strength and the percentage of strain decreased with a slow rate. It shows that the soil burial had a weak effect on tensile property of LDPE sheets. The decline of tensile strength and %strain was the indicator of soil burial efficiency, especially where large amounts of starch and modified starch were used. The presence of the modified moieties of ester and ether led to the decrease in mechanical properties, because they could absorb moisture in its surrounding, which could then be attacked by microorganisms, such as fungi and bacteria, and resulted in porosity and voids.

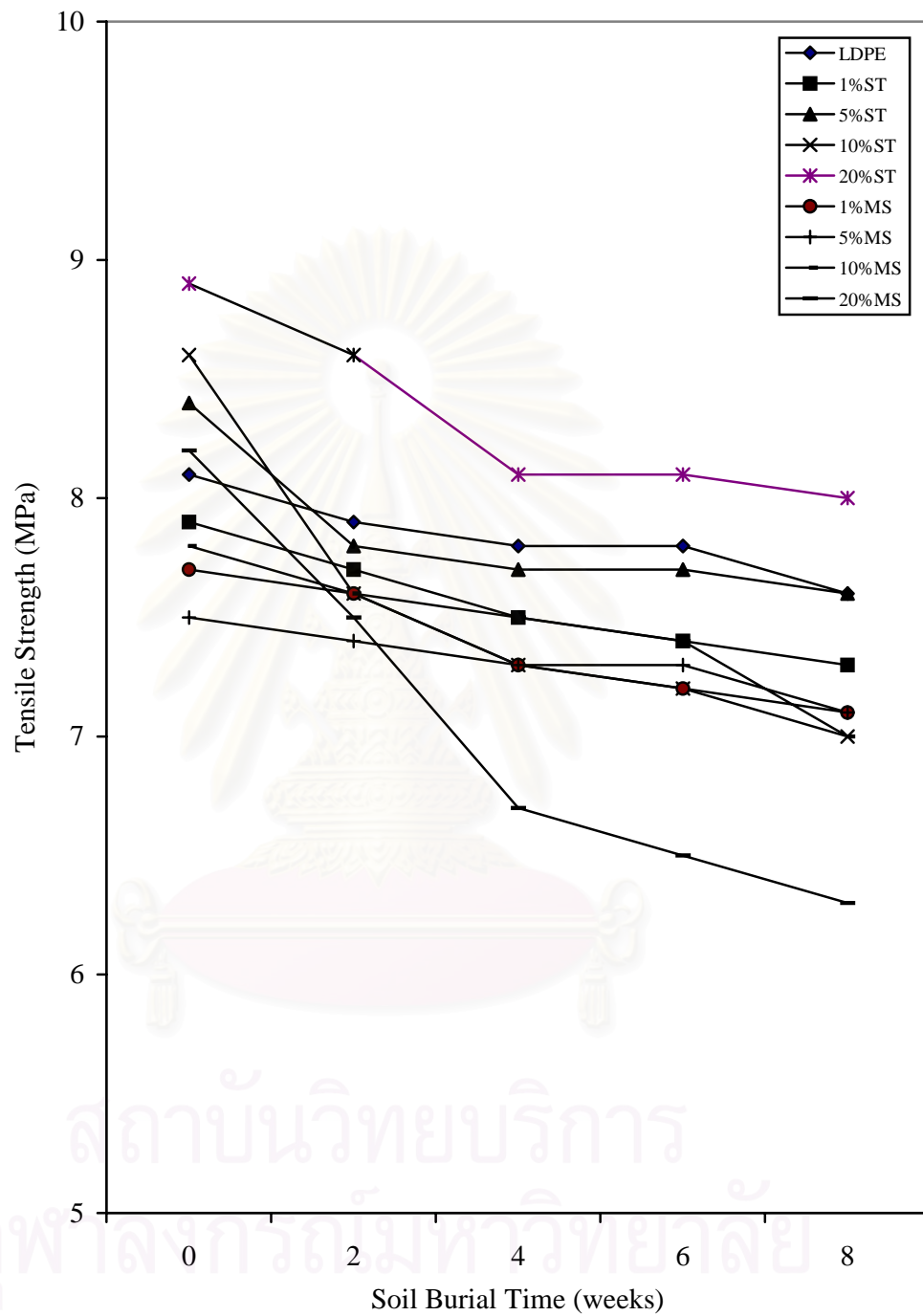


**Figure 4.47** Tensile strengths of LDPE, LDPE/ST, and LDPE/MS blends  
after the soil burial test

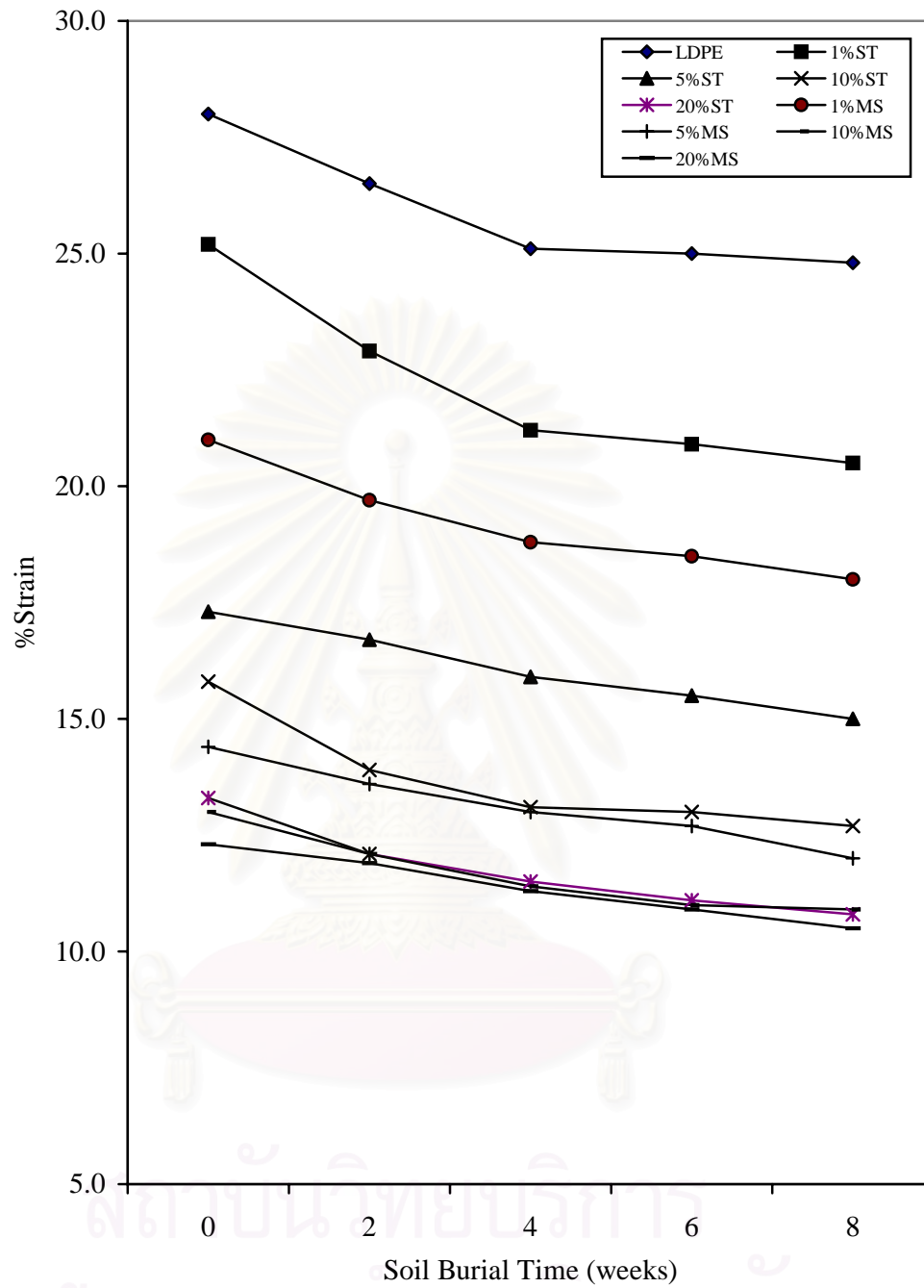


**Figure 4.48** Percentages of strain of LDPE, LDPE/ST, and LDPE/MS blends after the soil burial test

Not only the plastic sheet can be degraded by microorganisms, but it also can be degraded by chemical reaction. Scott [34] had shown the degradation mechanism as presented in Figure 4.49.

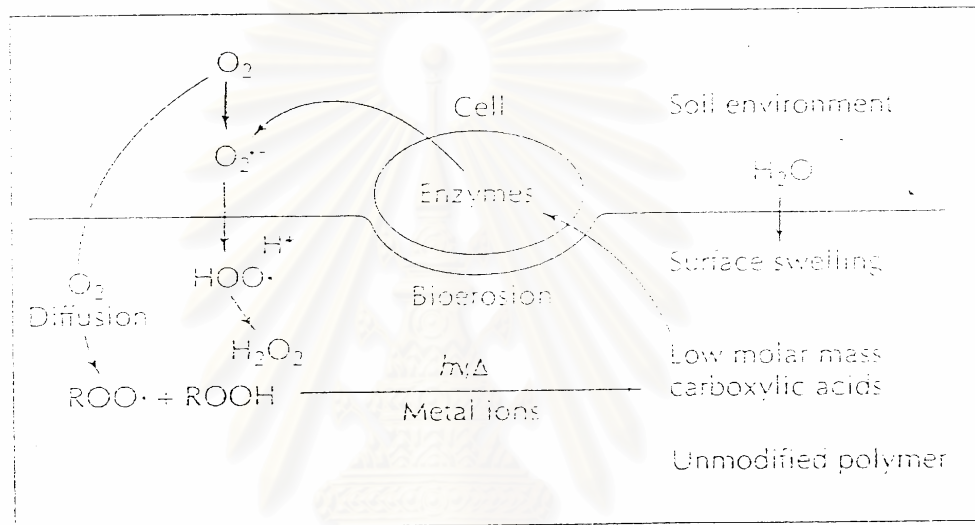


**Figure 4.49** Initiation of biodegradation in hydrocarbon polymers

#### 4.7.2 Hardness Measurement

The results of hardness measurements after the soil burial test are shown in Table 4.15 and presented in Figure 4.50. It can be seen that the hardness values of LDPE and LDPE composite sheets were slightly decreased.

**Table 4.16** Hardness Values of LDPE, LDPE/ST, and LDPE/MS blends after the Soil

## Burial Test

Sample	Soil Burial Time (Weeks)				
	Control	2	4	6	8
LDPE	41.0±1.4	40.0±0.5	39.0±0.5	38.3±1.5	38.0±0.7
LDPE/ST1	40.3±1.4	39.6±1.6	38.5±1.6	38.0±0.5	37.8±0.9
LDPE/ST5	41.2±1.2	40.6±1.0	39.3±0.4	39.0±1.0	38.9±1.2
LDPE/ST10	42.5±1.8	41.1±0.4	40.2±1.4	40.0±1.2	39.5±0.7
LDPE/ST20	44.9±0.6	43.0±1.5	42.3±1.0	41.9±1.0	41.5±0.6
LDPE/MS1	39.9±1.0	39.5±0.8	37.9±1.3	37.5±0.9	37.4±1.4
LDPE/MS5	40.7±2.1	39.9±0.4	38.9±1.0	38.2±0.9	38.0±2.1
LDPE/MS10	42.4±0.9	40.5±0.9	39.7±0.6	39.1±0.6	39.0±1.0
LDPE/MS20	43.8±0.7	41.1±0.9	40.9±0.8	40.4±0.6	40.0±0.5

สถาบันวิทยบริการ  
จุฬาลงกรณ์มหาวิทยาลัย

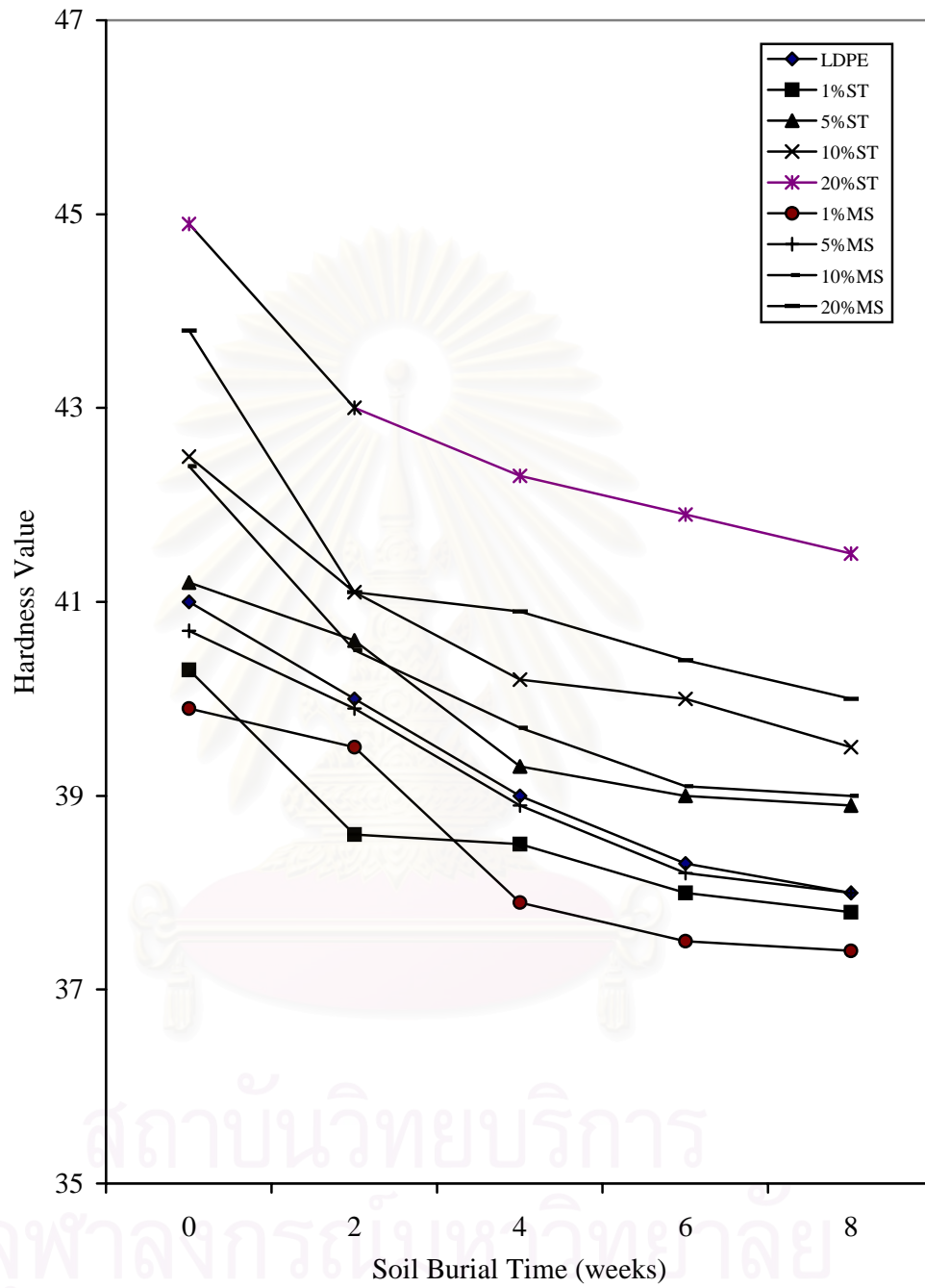


**Figure 4.50** Hardness measurements of LDPE, LDPE/ST, and

LDPE/MS blends after soil burial test

### 4.7.3 Surface Morphology of Samples

The surface morphologies of LDPE, LDPE/ST20, and LDPS/MS20 sheets were studied in order to follow the changes after the soil burial for 2 months. The SEM micrographs are shown in Figures 4.51-4.56. It can be seen that the surface of low-density polyethylene sheets after soil burial test became rougher with cavities than the control sheet. For LDPE/ST20 and LDPE/MS20 plastic sheets, many holes throughout the plastic sheets were observed. This occurrence may be caused by microorganisms in soil, which utilized the starch and modified starch as a food source or by the external influences of underground water and rainfalls leading to leaching of the destroyed surface.



Figure 4.51 SEM micrograph of the control LDPE sheet



Figure 4.52 SEM micrograph of the LDPE sheet at 2-month soil burial test

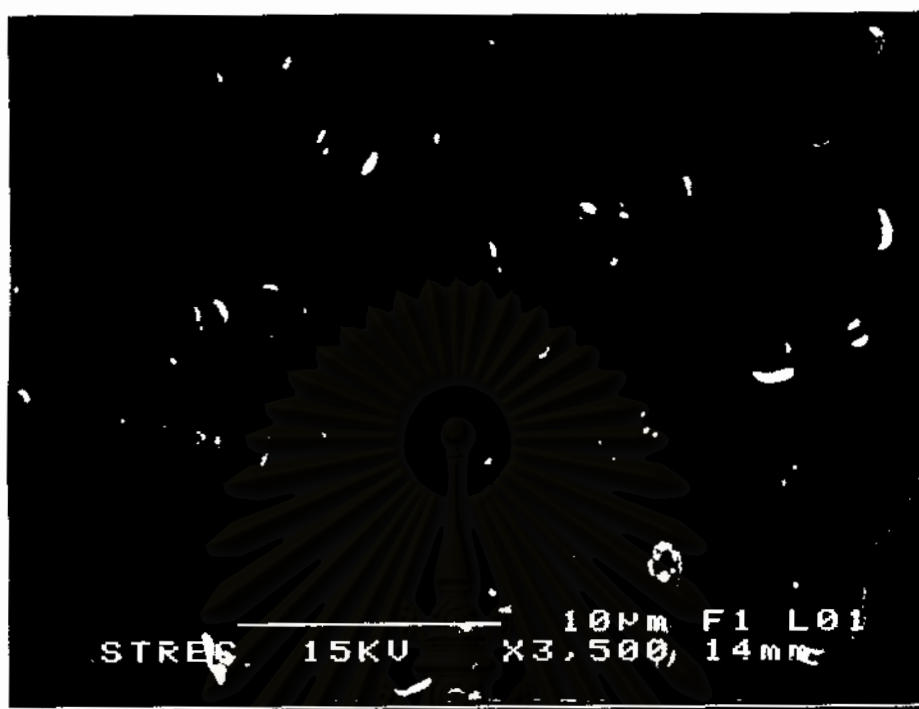


Figure 4.53 SEM micrograph of the control LDPE/ST20 sheet



Figure 4.54 SEM micrograph of the LDPE/ST20 sheet at 2-month soil burial test

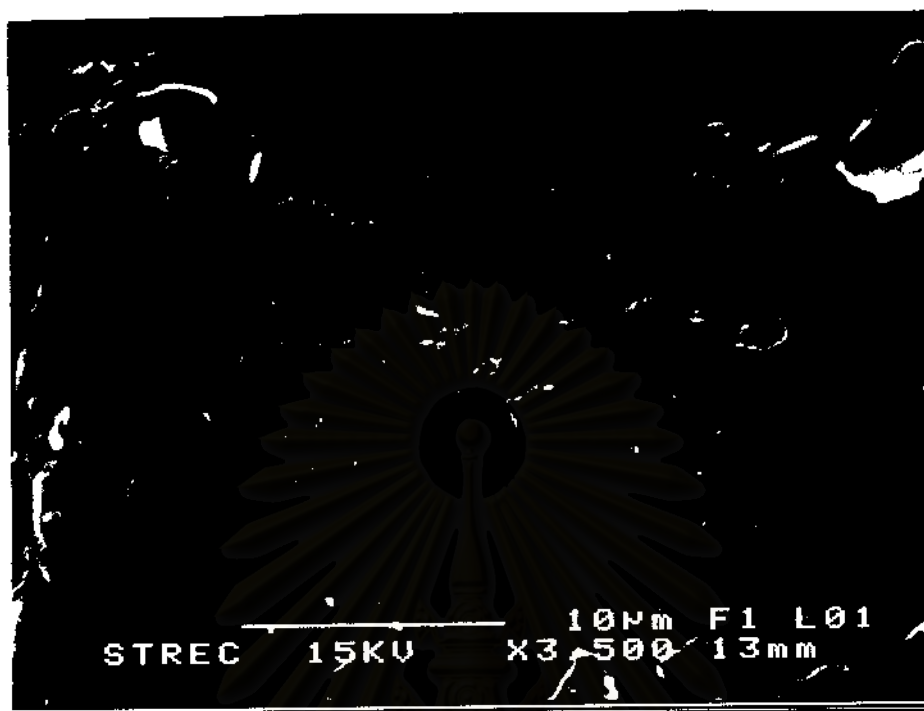


Figure 4.55 SEM micrograph of the control LDPE/MS20 sheet

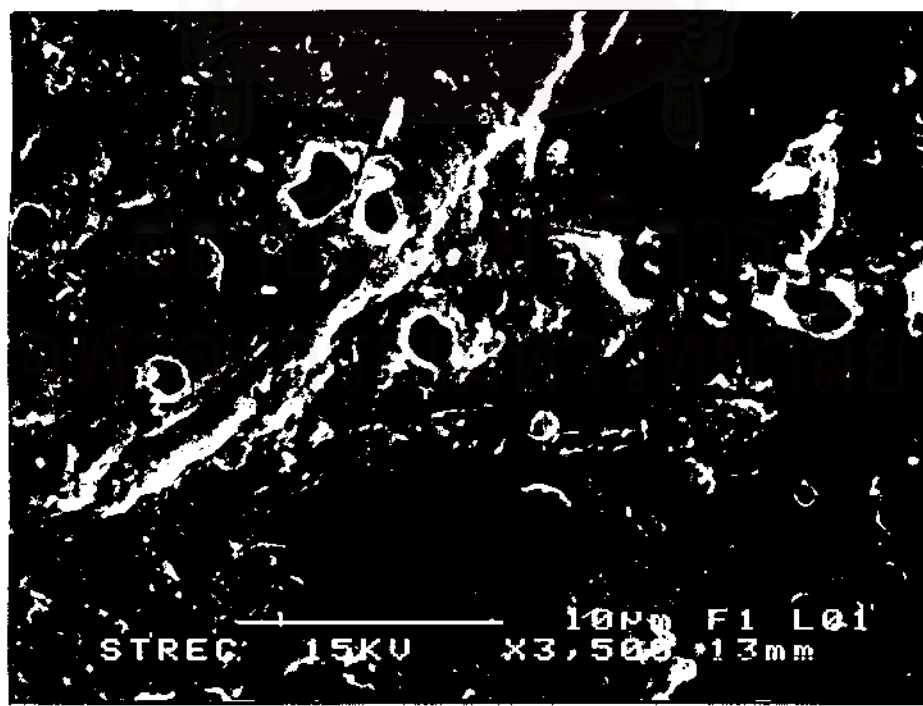


Figure 4.56 SEM micrograph of the LDPE/MS20 sheet at 2-month soil burial test

#### **4.8 Water Absorption Test**

The water permeability of modified starch is another attribution to degradation. The synthetic component appeared to be biodegraded by surface absorption of moisture and microorganism, such as fungi and bacteria, because water absorption on material triggers the microorganisms to grow and utilizes the material as a carbon source of food. The results of water absorption test are presented in Table 4.17 and in Figures 4.57-4.58.

For LDPE, the percentage of water absorption is less than 0.5%, indicating the hydrophobicity of LDPE. The water absorption of starch and modified starch filled LDPE composite sheet increased with increasing the modified moiety contents. However, the water absorption of the samples of this work is still low. It can be observed that the water absorption of the modified starch filled LDPE sheets was higher than those of the unmodified ones. This result implied that the former could absorb more water and microorganisms in soil water and thus more weight increase of water and more biodegradation of the filled LDPE sheets. The water absorption rate of the blends increased with increasing the contents of starch and modified starch. The highest water absorption rate was in the first day exposure. After that the water absorption rate decreased slowly. This result implied that the blends became saturated with water.

**Table 4.17** Water Absorption (%) and Water Absorption Rate of LDPE, LDPE/ST, and LDPE/MS blends after 4 weeks

Exposure in Distilled Water

Sample	Exposure Time (weeks)														
	24 hours			1			2			3			4		
	WA	WAR		WA	WAR		WA	WAR		WA	WAR		WA	WAR	
LDPE	0.19	1,920		0.31	439		0.37	261		0.40	189		0.43	151	
LDPE/ST1	0.33	3,072		0.59	777		0.64	430		0.67	299		0.71	238	
LDPE/ST5	0.34	3,456		0.59	868		0.88	649		0.91	442		0.98	359	
LDPE/ST10	0.54	5,312		1.04	1,472		1.32	932		1.40	664		1.60	567	
LDPE/ST20	0.54	5,952		1.07	1,682		1.40	1,097		1.90	997		2.09	823	
LDPE/MS1	0.29	2,880		0.49	695		0.52	370		0.54	256		0.63	226	
LDPE/MS5	0.48	4,736		0.88	1,307		0.92	686		1.18	582		1.26	469	
LDPE/MS10	0.68	7,168		1.20	1,801		1.76	1,321		1.78	868		1.81	681	
LDPE/MS20	0.92	10,048		1.59	2,478		2.08	1,618		2.26	1,176		2.31	901	

WA: Water Absorption, Unit: %

WAR: Water Absorption Rate, Unit:  $\text{g m}^{-3} \text{ day}^{-1}$

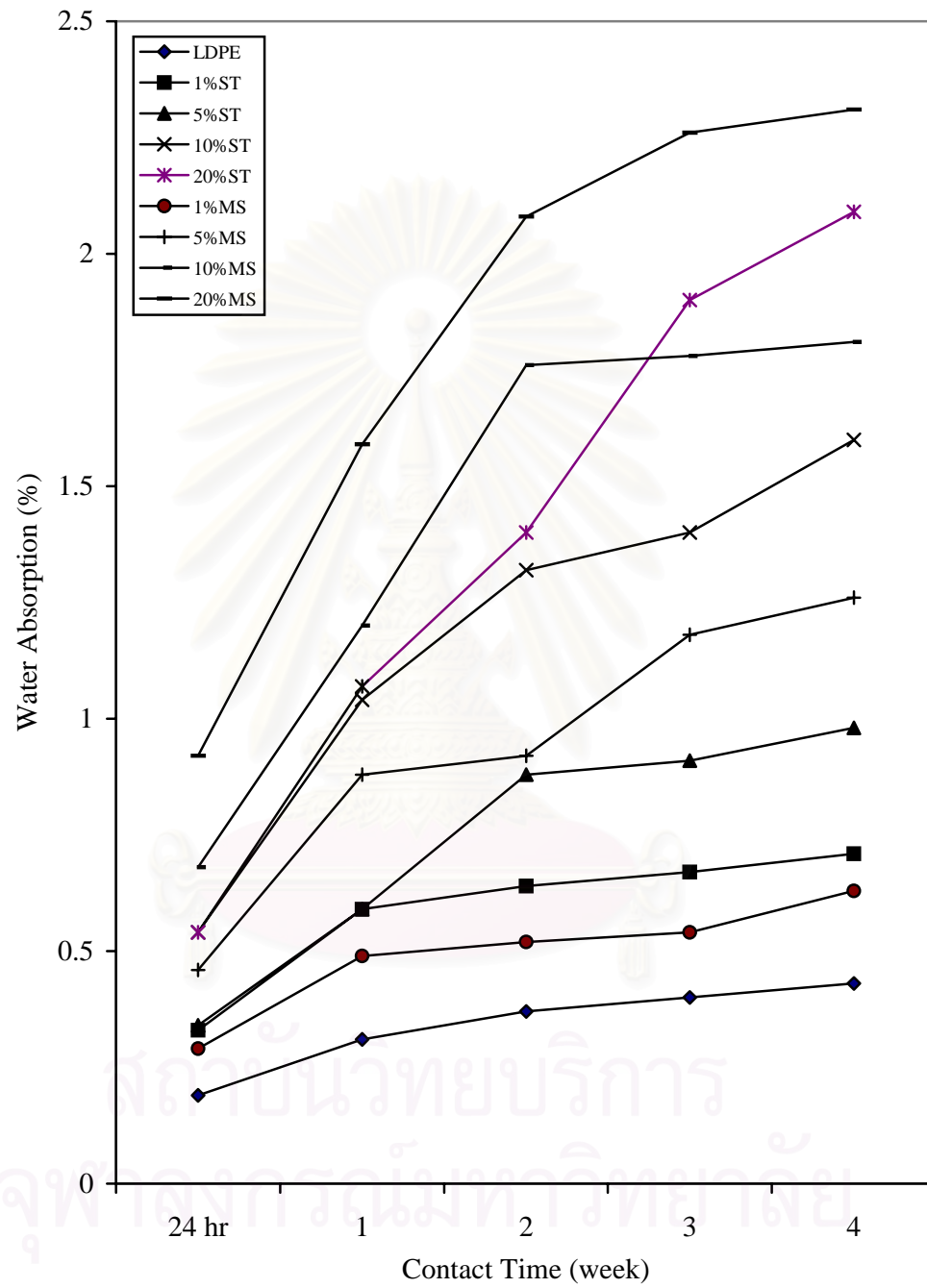


**Figure 4.57** Water Absorption of LDPE, LDPE/ST, and LDPE/MS blends after exposure to distilled water

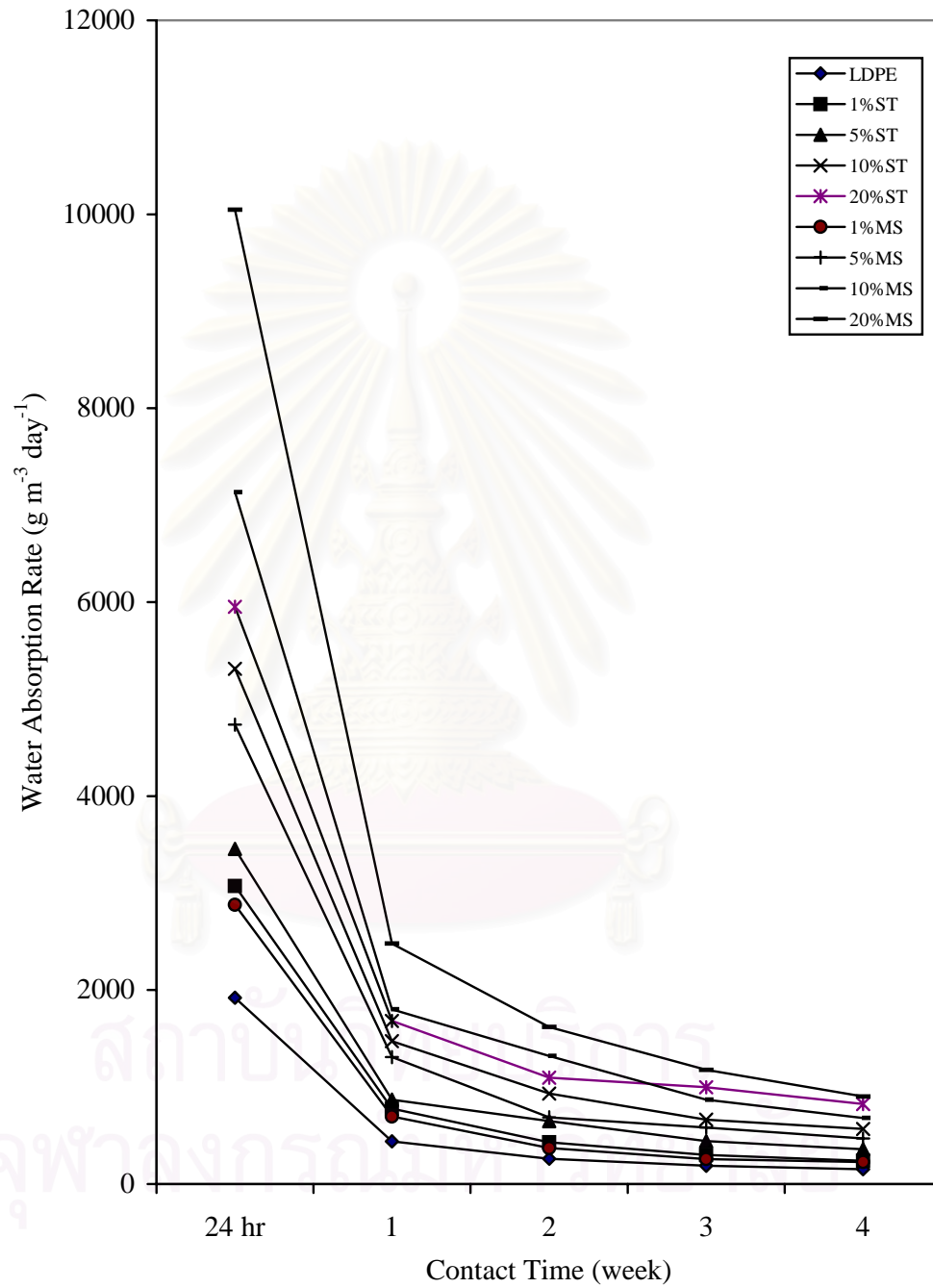


**Figure 4.58** Water Absorption Rate of LDPE, LDPE/ST, and LDPE/MS blends after exposure to distilled water

## CHAPTER 5

### CONCLUSION AND SUGGESTION

The cassava starch-g-poly(acrylic acid) was prepared via graft copolymerization by a simultaneous irradiation technique from  $^{60}\text{Co}$  source. The graft products are characterized in the terms of %homopolymer, %add-on, %conversion, %grafting efficiency, and %grafting ratio by gravimetric method of homopolymer extraction and acid hydrolysis. The grafting reaction of poly(acrylic acid) onto cassava starch was proved using Fourier transform infrared spectroscopy. After the homopolymer extraction of crude product, one can observe the strong peak at  $1727\text{ cm}^{-1}$ , which attributed to the C=O stretching of the carboxylic acid of acrylic acid.

The three values of dose rates, 2, 5, and  $12\text{ kGy h}^{-1}$ , were used to give the total doses of 2, 4, 6, 8, 10, and  $12\text{ kGy}$ . In these ranges of the dose rate and the total dose studied, we found that %homopolymer increased with the increase in the dose rate. Because the larger amount of radicals produced in the high dose rate were rapidly terminated to give homopolymer instead of graft copolymer. The controversy was found in the percentage of add-on, conversion, grafting efficiency, and grafting ratio. That is, these terms increased with the decrease in dose rate. When compared with the total dose, it can be seen that the percentage add-on, conversion, grafting efficiency, and grafting ratio were increased with increasing the total dose. Due to the fact that, the grafting sites are determined by the total dose. For the percentage of homopolymer, there were the optimum total doses of each dose rate that the least amounts of  $\text{OH}\cdot$ ,

H•, and  $e_{aq}$  to initiate homopolymer were generated. When the acrylic acid-to-cassava starch ratio was studied at the dose rate of  $2 \text{ kGy h}^{-1}$  (Total doses of 10 and 12 kGy). It was found that the percentage of add-on, conversion, grafting efficiency, and grafting ratio increased with the increase of acrylic acid-to-cassava starch ratio. This is presumably due to the fact that increase in monomer concentration enhanced the monomer accessibility. Gel effect may occur in the viscous system, leading to graft copolymerization.

The condition chosen for preparing starch-*g*-poly(acrylic acid) was the dose rate of  $2 \text{ kGy h}^{-1}$ , total dose of 10 kGy, and acrylic acid-to-cassava starch ratio of 1:1. The starch-*g*-poly(acrylic acid) obtained has 2.7% homopolymer, 24.9% add-on, 40% conversion, 90% grafting efficiency, and 33.2% grafting ratio. The esterification between starch-*g*-poly(acrylic acid) and poly(ethylene glycol) 4000 was confirmed by following the chemical shift of the function group C=O from  $1727 \text{ cm}^{-1}$  to  $1738 \text{ cm}^{-1}$ , which corresponded to the acid and ester carbonyls, respectively. Moreover, the shift of the carbonyl carbon in  $^{13}\text{C}$ -NMR spectrum from 177.9 ppm to 175.6 ppm also indicates the conversion of the carboxylic acid group into the ester group. There is an additional peak at 52 ppm, which is attributed to the -C-O- on poly(ethylene glycol) 4000 chains. After etherification, the peaks at 20 and 1.2 ppm of the  $^{13}\text{C}$ - and  $^1\text{H}$ -NMR spectra, respectively, elucidate the presence of the hydroxypropyl group on the modified starch. The amounts of poly(ethylene glycol) 4000 (PEG 4000) and the hydroxypropyl group on the modified starch were found to be 15.25% and 1.30%, determined by the gravimetric and spectrophotometric method, respectively.

The modified starch was blended with LDPE in comparison with the unmodified starch. It was found that at the same starch content, such as LDPE/ST10 and LDPE/MS10, the LDPE/ST blend series gave the higher in both tensile strength and %strain. This result may indicate that incorporation of the modified starch could possibly not be very well mixed with LDPE plastics. When increasing the modified and unmodified starch contents, the same trends are observed. That is the increase in tensile strength and the decrease in %strain. This may be the effect of the filler phase that could enhance the strength of LDPE composite sheets. The hardness of LDPE was also slightly enhanced by the incorporation of the modified starch. It was found that the hardness increased with increasing the contents.

The thermal properties of the cassava starch, the modified starch, and the blends were determined using thermogravimetric (TG) and differential thermogravimetric (DTG) method. It was found that cassava starch was decomposed at the temperature ranged from 275°C to 375°C. After the modification to modified starch the second stage of decomposition was observed. The decomposition temperature of this step ranged from 400°C to 550°C, which attributed to the moiety of poly(acrylic acid). After blending the low-density polyethylene (LDPE) with the modified starch, the onsets of the decomposition of LDPE composite sheets were decreased from 350°C to 300°C.

The degradability of the LDPE composite sheets was examined by soil burial test in the terms of tensile strength, %strain, and hardness value, and the ability in absorption of water. It can be observed that tensile strength, %strain, and hardness properties of the LDPE composite sheets were gradually decreased. The water

absorption can also be used to indicate the biodegradation of plastic sheets by microorganisms, because water absorption on the blended materials swells the material surface to trigger the microorganisms to grow and utilizes the material as a carbon food. It was found that the water absorption (%) increased with increasing the amount of the modified starch contents, but the value was not higher than 2.5%.

This work shows that incorporation of the modified starch to LDPE did not improve significantly the mechanical properties of the LDPE composite sheets. Interestingly, this modified starch did not absorb too much moisture in the air, but could absorb water in contact slightly not higher than 2.5% by weight. The inclusion of the modified starch helps enhance the biodegradability of LDPE plastic sheets.

### **Suggestions and Future Works**

1. The effect of the property of graft copolymer, such as the degree of crosslinking, should be studied by comparing the properties of the modified starch prepared from different initiation method.
2. Levels of acrylic acid concentration on the cassava starch graft copolymer should be used to esterify.
3. The effect of various amounts of the hydroxypropyl group on the modified starch in the blends should be carried out.

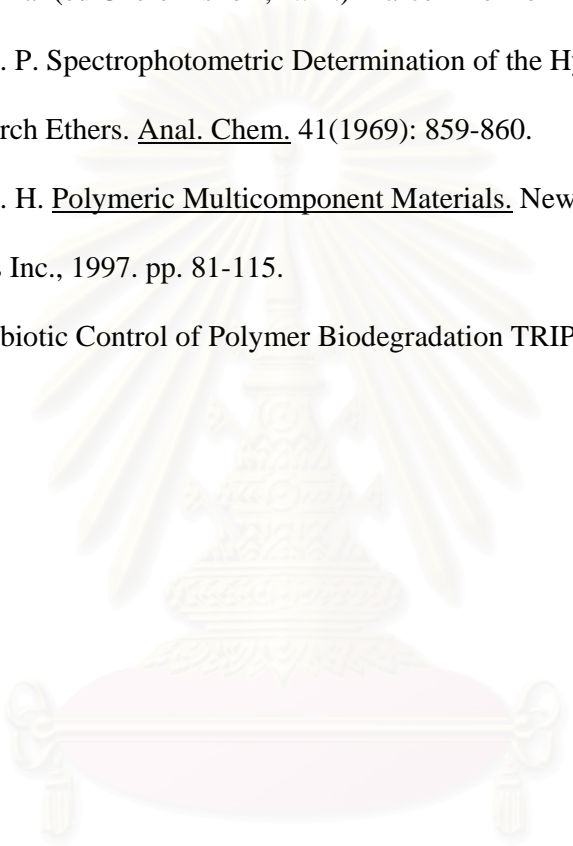
## REFERENCES

1. Scott, G. and Gilead, D. Degradable Polymers. Cambridge: Chapman & Hall, 1995. pp. 247-257.
2. Cox, M. K. Biodegradable Polymers and Plastics. (eds Vert, M., Feijen, J., Albertsson, A. et al.). Cambridge: The Royal Society of Chemistry, 1992. pp.95-100.
3. Bastioli, C. Degradable Polymers. (eds Scott, G. and Gilead, D.) Cambridge: Chapman & Hall, 1995. pp. 112-137.
4. Mark, H. F. and Gaylord, N. G. Encyclopedia of Polymer Science and Technology New York: John Wiley & Sons Inc., 1970. pp.787-853.
5. Ceresa, R. J. Block and Graft Copolymerization. London: John Wiley & Sons Inc., 1973. pp. 2-5.
6. Battaerd, H. A. J. and Tregear, G. W. Graft Copolymer. New York: John Wiley & Sons Inc., 1967. pp 54-69.
7. Schmid, G. H. Organic Chemistry. Missouri: Mosby-Year Book Inc., 1996. pp. 670-673.
8. Brown, W. H. and Foote, C. S. Organic Chemistry 2ed. New York: Saunder College Publishing, 1998. pp. 612-614.
9. Whistler, R. L. Starch: Chemistry and Technology (eds Whistler, R.L. and Paschall, E.F.). New York: Academic, 1965. pp. 460-469.
10. Nai-Hong, L. and Williams, M. C. 5<sup>th</sup> Pacific Polymer Conference. Korea, 1997. p.23
11. Reyes, Z., Syz, M. G., and Huggins, M. L. Grafting Acrylic Acid to Starch by Preirradiation. J. Polym. Sci. C. 23(1968): 401-408.

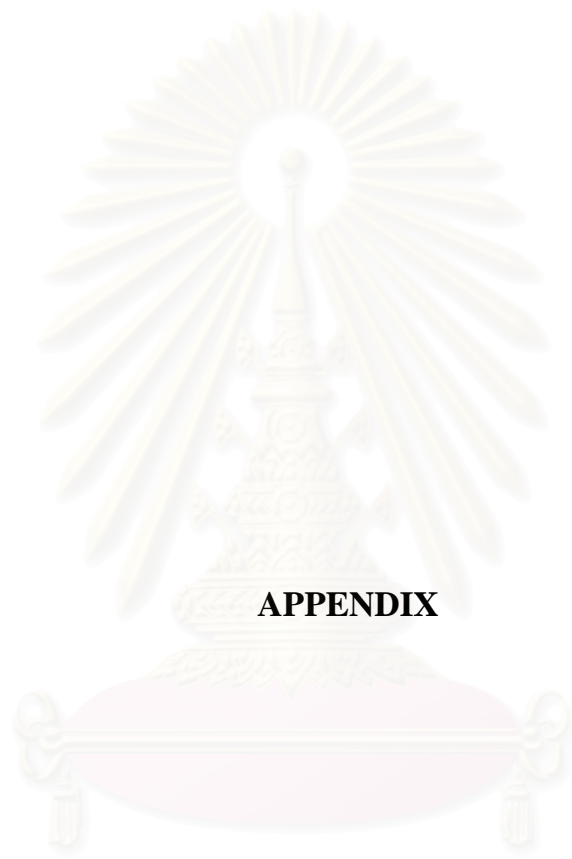
12. Zaharan, A. H., Williams, J. L., and Stannett, V. T. Radiation Grafting of Acrylic Methacrylic Acid to Cellulose Fibres to Impart High Water Sorbance. J Appl. Polym. Sci. 25(1980): 535-542.
13. Gurdag, G., Yasar, M., and Gurkaynak, M. A. Graft Copolymerization of Acrylic Acid onto Cellulose: Reaction Kinetics of Copolymerization. J Appl. Polym. Sci. 66(1997): 929-934.
14. Athawale, V. D., and Rathi, S. C. Synthesis and Characterization of Starch-Poly (methacrylic acid) Graft Copolymer. J Appl. Polym. Sci. 66(1997): 1399-1403.
15. Goni, I., Gurruchaga, M., Vazquez, B., Valero, M., and Guzman, G. M. Synthesis of Graft Copolymers of Acrylic Monomers on Amylose : Effect of Reaction Time. Eur. Polym. J. 28(1992): 976-979.
16. Liu, M., Cheng, R., and Ma, C. Graft Copolymerization of Methyl Acrylate onto Potato Starch Initiated by Ceric Ammonium Nitrate, J Appl. Polym. Sci. 31 (1993): 3181-3186.
17. Iyer, V., Varadarajan, P. V., Sawakhande, K. H., and Nachane, N. D. Preparation of Superabsorbents by Gamma-Ray Radiation. J Appl. Polym. Sci. 39 (1990): 2259-2265.
18. Hallden, A., and Wesslen, B. Preparation and Characterization of Poly(ethylene-graft-ethylene oxide). J Appl. Polym. Sci. 60(1996): 2495-2501.
19. Kiatkamjornwong, S., Pabunruang, T., Wongvisetsisrikul, N., and Prassarakich, P. Degradation of Cassava Starch-Polyethylene Blends. J. Sci. Soc. Th. 23 (1997): 135-158.
20. Goheen, S. M., and Wool, R. P. Degradation of Polyethylene-Starch Blends in Soil. J Appl. Polym. Sci. 42(1991): 2691-2701.

21. Willett, J. L. Mechanical Properties of LDPE/Granular Starch Composites. J Appl. Polym. Sci. 54(1994): 1685-1695.
22. Thiebaud, S., Aburto, J., Alric, I., Borredon, E., Bikiaris, D., Prinos, J., and Panayiotou, C. Properties of Fatty-Acid Esters of Starch and Their Blends with LDPE. J Appl. Polym. Sci. 64(1997): 705-721.
23. Arvanitoyannis, I., Psomiadou, E., Billiaderis, C. G., Ogawa, H., Kawasaki, N., and Nakayama, A. Biodegradable Films Made from Low Density Polyethylene(LDPE), Ethylene Acrylic Acid (EAA), Polycarprolactone (PCL) and Wheat Starch for Food Packaging Applications. Starch/Starke 249(1997): 306-622.
24. Sagar, A. D., and Merrill, E. W. Properties of Fatty-Acid Esters of Starch. J Appl. Polym. Sci. 58(1995): 1647-1656.
25. Aburto, J., Alric, I., Thiebaud, S., Borrendon, E., Bikiaris, D., Prinos, J., and Panayiotou, C. Synthesis, Characterization, and Biodegradability of Fatty-Acid Esters of Amylose and Starch. J Appl. Polym. Sci. 74(1999): 1440-1451.
26. Kang, B. G., Yoon, S. H., Lee, S. H., Yie, J. E., Yoon, B. S., and Suh, M. H. Studies on the Physical Properties of Modified Starch-Filled HDPE Film. J Appl. Polym. Sci. 60(1996): 1977-1984.
27. Kiatkamjornwong, S., Sonsuk, M., Wittayaphichet, S., Prasassarakich, P., and Vejjanukroh, P. Degradation of Styrene-g-cassava Starch Filled Polystyrene Plastics. Poly. Deg. Stab. 66(1999): 323-335.
28. ASTM D698-96 Standard Test Method for Tensile Properties of Plastics
29. ASTM D570-98 Standard Test Method for Water Absorption of Plastics

30. Hummel, O. D. Atlas of Polymer and Plastic Analysis 3<sup>rd</sup> ed. Munich: Carl Hanser Verlag. 1991. p. 7768.
31. Abdel-Barry, E. M., and El-Neser, E. M. Handbook of Engineer Polymeric Material (ed Cheremisnoff, N. P.) Marcell Dekker Inc., 1997. pp. 501-515.
32. Johnson, D. P. Spectrophotometric Determination of the Hydroxypropyl Group in Starch Ethers. Anal. Chem. 41(1969): 859-860.
33. Sperling, L. H. Polymeric Multicomponent Materials. New York: John Wiley & Sons Inc., 1997. pp. 81-115.
34. Scott, G. Abiotic Control of Polymer Biodegradation TRIP. 7(1997): 361-368.



สถาบันวิทยบริการ  
จุฬาลงกรณ์มหาวิทยาลัย



**APPENDIX**

สถาบันวิทยบริการ  
จุฬาลงกรณ์มหาวิทยาลัย

## APPENDIX A

### Radiation Dosimetry

Quantitative studies in radiation chemistry require a knowledge of the amount of energy transferred from the radiation field to the absorbing material.

The absorbed dose or total dose is the quantity generally sought and is the amount of energy absorbed per unit mass of irradiated material. The official unit of absorbed dose is the rad, which is defined as the energy absorption of 100 erg g<sup>-1</sup> or 10<sup>-2</sup> kg<sup>-1</sup>. The absorbed dose is a direct measure of the energy transferred to the irradiated material and capable of producing chemical or physical change in it; it is determined both by the composition of the material and characteristics of the radiation field.

The absorbed dose rate is the absorbed dose per unit time and has the unit rads, eV g<sup>-1</sup>, eV cm<sup>-3</sup>, or grays per unit time, e.g. rads min<sup>-1</sup>, grays min<sup>-1</sup>, eV g<sup>-1</sup> min<sup>-1</sup>.

Techniques for measuring ionizing radiation can be divided into absolute and secondary methods. Absolute methods involve a direct determination of exposure or absorbed dose from physical measurements of, for example, the energy absorbed (by calorimetry), the ionization produced in a gas, or the charge carried by a beam of charged particle of known energy. The absolute methods are often not suited to routine use and, in practice, secondary dosimeters (e.g. thimble ionization chambers and chemical dosimeters), whose response to radiation is known from comparison with an absolute dosimeter, are generally used.

## 1. Calorimetry

The most direct way of determining the amount of energy carried by a beam of radiation is to measure the increase in temperature of a block of material placed in the beam, the method originally used by Curie and Laborde to measure the rate of energy released by the radioactive decay of radium. The material must be such that all the absorbed energy is converted to heat, non, for example, being used to initiate chemical reaction. Good thermal conductivity is also necessary and in practice graphite or metals are generally used for this purpose. If the block is of sufficient size to completely absorb the radiation, the rate of temperature increase is related directly to the energy flux density or intensity ( $\text{erg cm}^{-2} \text{sec}^{-1}$ ) of the beam. With low intensity radiation, such as that normally available for X- and  $\gamma$ - ray sources, the temperature rise is very small and it is important as a check on other, less direct, methods, since the results are obtained directly in energy unit.

Radak and Markovic give the range of absorbed dose rate that can be measured in this way as  $10^{-7} \text{ W g}^{-1}$  ( $36 \text{ rads hr}^{-1}$ ). Absorbed dose measurements with calorimeter in which water is the absorbing material have been to calibrate the Fricky and other aqueous chemical dosimeters described later in this chapter.

## 2. Chemical Dosimetry

In chemical dosimetry, the radiation dose is determined from the chemical change produced in a suitable substrate. Calculation of the dose requires a knowledge of the G value for the reaction or product estimated, which is found by comparing the chemical system with some form of an absolute dosimeter. Chemical dosimeters are therefore secondary dosimeters and are used because of their greater convenience. In order to facilitate this conversion and to reduce errors, the dosimeter

system is usually chosen so as to have the same atomic composition and density as the sample to be irradiated, as far as this is possible. Aqueous dosimeters, for example, are used if the sample is an aqueous solution, biological material, or organic substance.

For a dosimeter in which radiation induces a chemical change, the mean absorbed dose (Dd) over the volume occupied by the dosimeter is derived as follows. For any system, by definition, G (product) is the number of molecule of product formed per 100 eV energy absorbed and 1 rad corresponds to an energy absorption of 0.01 J kg<sup>-1</sup>. Then

$$\begin{aligned}
 Dd &= \frac{\text{moles of product formed per kg (mol)}}{\text{(kg)}} \\
 &\quad \times \frac{6.02 \times 10^{23} \text{ (molecule)}}{\text{G(product) (molecule)}} \times \frac{100 \text{ (eV)}}{\text{1.602} \times 10^{-19} \text{ (J)}} \times \frac{100 \text{ (kg rad)}}{\text{(J)}} \\
 &= \frac{9.467 \times 10^8 \times \text{moles of product formed per kg rads}}{\text{G(product)}} \quad \text{(A-1)}
 \end{aligned}$$

Or

$$Dd = \frac{9.467 \times 10^8 \times \text{moles of product formed per liter rads}}{\rho \text{G(product)}} \quad \text{(A-2)}$$

where  $\rho$  is the density of the system (g cm<sup>-3</sup>). Very often the yield of product will be determined spectrophotometrically when, assuming Beer's law to be obeyed,

$$\text{moles of product formed per liter} = \frac{\Delta A}{\Delta E l} \quad (\text{A-3})$$

and

$$Dd = \frac{9.647 \times 10^8 \times \Delta A \text{ rads}}{E l \rho G(\text{product})} \quad (\text{A-4})$$

Where  $\Delta A$  is the difference in absorbance (or optical density) between the irradiated solution,  $E$  is the difference in molar extinction coefficient ( $\text{liter mol}^{-1} \text{cm}^{-1}$ ) of reactant and product at the wavelength being used, and  $l$  (cm) is the optical path length (i.e., sample thickness used when determining the absorbance).

### 2.1 Fricky (Ferrous Sulfate) Dosimetry

The reaction involved in the Fricky dosimeter is the oxidation of an acid solution of ferrous sulfate to the ferric salts, in the presence of oxygen under the influence of radiation. The standard dosimeter solution is one containing about  $10^{-3}$  M ferrous sulfate or ferrous ammonium sulfate and  $10^{-3}$  M sodium chloride in air-saturated ( $2.5 \times 10^{-4} \text{ MO}_2$ ) 0.4 M sulfuric acid (pH 0.46). The quantities required to prepare such a solution are 0.28 g  $\text{FeSO}_4 \cdot 7\text{H}_2\text{O}$  [or 0.39 g  $\text{Fe}(\text{NH}_4)_2 (\text{SO}_4)_3 \cdot 6\text{H}_2\text{O}$ ] 0.06 g NaCl and 22  $\text{cm}^3$  concentrated (95-98%)  $\text{H}_2\text{SO}_4$  per liter of solution; the solution slowly oxidized and should not be stored longer than a few days.

To determine the absorbed dose (in 0.4 M sulfuric acid) using the Fricke dosimeter, a sample of the dosimeter solution in a container thick enough to ensure electronic equilibrium is placed in the radiation field ions to be measured. To avoid under wall effects (i.e. so that practically all the secondary electrons contributing

to the energy absorption originate of at least 8 mm where  $\gamma$ -radiation is being determined; Burlin using a modified cavity theory, has calculated that with a silica cell and  $\text{Co}^{60}$ -ray, a diameter of 6 cm is needed to reduce the wall effects to below 0.1%. The most common method of measuring the ferric ions formed is by spectrophotometric analysis, comparing the absorbance at the wavelength at which ferric ions show maximum absorption (about 304  $\mu\text{m}$ ). The optical readings should be taken soon after the irradiation, so that adventitious oxidation of the solutions is minimized. The mean absorbed dose ( $D_d$ ) for the volume occupied by dosimeter solution is given by Eq. A-3.

---

#### Reference

Swallow, A. J. Radiation Chemistry. London : John Wiley & Sons Inc., 1973. pp.18-25.

สถาบันวิทยบริการ  
จุฬาลงกรณ์มหาวิทยาลัย

## VITA

Ms. Prodepran Thakeow was born on August 20, 1973 in Chiangkham District, Phayao Province. She received the Bachelor Degree of Science from Department of Chemistry, Faculty of Science, Chiang Mai University in 1996. She began her study in the Program of Petrochemistry and Polymer Science, Faculty of Science, Chulalongkorn University, in 1997 and complete the Master Degree of Petrochemistry and Polymer Science in 2000.



สถาบันวิทยบริการ  
จุฬาลงกรณ์มหาวิทยาลัย